UNIVERSITY OF CALIFORNIA
RIVERSIDE

Chemical and Molecular Genetics Approach to Study ROP1 Signaling Pathway in Pollen Tubes

A Dissertation submitted in partial satisfaction
of the requirements for the degree of

Doctor of Philosophy

in

Genetics, Genomics, and Bioinformatics

by

Augusta Viktoria Jamin

December 2011

Dissertation Committee:
Dr. Zhenbiao Yang, Chairperson
Dr. Sean Cutler
Dr. Chia-en (Angelina) Chang

The Dissertation of Augusta Viktoria Jamin is approved by:

_____

_____

_____

Committee Chairperson

University of California, Riverside

ACKNOWLEDGEMENTS

I would like to thank my major advisor, Zhenbiao Yang, and the dissertation committee members, Sean Cutler and Chia-en (Angelina) Chang for their guidance, encouragement, discussion, and help throughout my graduate studies. I also appreciate the suggestions and critical advice on my research.

My gratitude goes to Julia Bailey-Serres and Patricia Springer for being such great and wonderful mentors and professors, for giving encouragements and directions when they are needed, and for providing strength and inspiration. I thank David Carter for all of the support in confocal microscopy and Songqin Pan for all of the proteomic work done on REN1 phosphorylation study. My special thanks go to Yuxin Ma at Weill Institute, Cornell University for the internships opportunity at his lab where I was exposed to better techniques in protein expression and purification as well as preparation for generating protein crystals.

I wish to thank all of the Yang lab members for the help, discussion, and support. I would especially like to thank Yong-Jik Lee for always encouraging me to think about my research, for helping me with the technical difficulties, for being patient, and for sharing the knowledge and scientific experience. I would also like to thank Jae-Ung Hwang for being a wonderful and patient mentor. I also thank two good friends, Ornusa Khamsuk and Min Zheng, for being there, for caring, and for all of the great conversations and interesting stories that will be missed.

I am grateful for the ChemGen NSF-IGERT funding support and for the great opportunity to delve in an interdisciplinary field in broadening my scientific knowledge. I

also thank Genetics, Genomics, and Bioinformatics program for some of the financial support.

I would also like to acknowledge all of the past and current GGB and IGERT students for always supporting one another throughout these times, for all of the discussions, encouragement, and supports on being graduate students and how to make it through, and for all the entertainment and activities that we have had throughout the years.

Finally, I would like to thank my parents for always encouraging me to reach high in my education and for always wanting the best in me, and my siblings for keeping me sane. To my husband, Sergey, thank you for your continuous support, cheerful humor, positive attitude, and love during my years in graduate school.

ABSTRACT OF THE DISSERTATION

Chemical and Molecular Genetics Approach to Study ROP1 Signaling Pathway in Pollen Tubes

by

Augusta Viktoria Jamin

Doctor of Philosophy, Graduate Program in Genetics, Genomics, and Bioinformatics
University of California, Riverside, December 2011
Dr. Zhenbiao Yang, Chairperson

Polarized growth in pollen tube requires complex signaling events including ROP1 GTPase pathway and calcium signaling. The role of tip calcium in negative feedback regulation of ROP1 remains a question and potentially involves ROP1 negative regulator, REN1GAP, whose activity seems to be regulated by calcium. Calcium-dependent protein kinases (CDPKs/CPKs) are calcium sensors with known function in regulating pollen tube tip growth. As such, we hypothesized that CPK substrate(s) in pollen tube may be component of tip growth regulator such as REN1. Here we report that REN1 is phosphorylated by pollen-expressed CPK16 with a relative EC_{50} value of ~4.6 µM. MS/MS analysis revealed calcium-dependent phosphorylation sites within REN1 which include Ser_{70} and Ser_{267}. Functional analyses suggested that REN1 phosphorylation at Ser_{267} is required for its activity while at $Ser_{70,71}$ affected its localization and subsequently activity. Mutation analysis of *CPK16* loss-of-function, *cpk16-3,* revealed enhanced pollen tube growth and germination when grown in low

calcium media. Treatment of *cpk16-3* tubes with either brefeldin A or latrunculin B induced tip swelling phenotype similar to the same effects produced by chemical treatments of partially complemented *ren1-1 Lat52::GFP-REN1,* Overall, these results suggest a link between calcium and a major signaling pathway, ROP1, via calcium-dependent protein kinase and its substrate REN1.

To dissect the causal and phasal relationships between oscillations of growth, active ROP1, F-actin dynamics, and tip-focused calcium, a chemical genetics approach was utilized with the goal to identify small molecules that would specifically activate ROP1. To this end, 20000 chemicals were screened in a cell-based yeast two hybrid assay to target inhibitors of active ROP and GAP. One compound, #7, inhibited ROP-GAP interaction as confirmed by *in vitro* assays as well as slightly enhanced pollen tube tip width. Treatment of ROP1 OX severely enhanced tip swelling suggesting that it primarily targets ROP1. Docking analyses of compound 7 to the protein interaction interface of RhoA and p190RhoGAP revealed possible binding sites within the GTP-binding pockets of Rho-GAP interface in potentially disrupting protein-protein interaction. This study leads to a potential activator of ROP1 which may be useful for future ROP1 studies.

Table of Contents

List of Figures

Introduction

Chapter 1

Chapter 2

Chapter 3

Chapter 4

List of Tables

Chapter 1

Chapter 2

INTRODUCTION

Polarized growth and Rho GTPase signaling pathway

Polarized growth is a form of directed cell growth observed in many organisms such as budding yeast, fungal hyphae, moss protonemata, neurite outgrowth, plant root hair, and pollen tube (Li and Gundersen, 2008; Perez and Rincon, 2010; Menand et al., 2007; Arimura and Kaibuchi, 2005; Yang, 2008; Hepler et al., 2001). Polarized growth requires asymmetric distribution of intrinsic components such as cytoskeletal structures as well as small GTPases signaling machineries (Li and Gundersen, 2008). Cytoskeletal structures such as actin filaments and microtubules are intrinsically polar due to the head-to-tail polymerization of its subunits and are essential for the establishment and maintenance of cell polarity (Li and Gundersen, 2008). Of equal if not more important components are small GTPases, of the Rho subfamilies, which function as molecular switches in regulating various aspects of cellular processes including cytoskeleton dynamics. In addition, trafficking and recycling of signaling regulators to and from the plasma membrane are also involved in the polarization of cellular components and subsequently polar growth (Mellman and Nelson, 2008).

Rho GTPases are members of Rho family proteins that are conserved in eukaryotic organisms and play an important role in regulating cell polarity and growth (Brembu et al., 2006; Perez and Rincon, 2010; Ridley, 2006). Rho GTPases are GTP/GDP-binding protein which catalyzes its GTP to GDP hydrolysis. GTP-bound Rho proteins interact with downstream effectors which further mediate the regulation of

downstream components such as actin dynamics and vesicle trafficking. Several RhoGTPase regulatory proteins include guanine exchange factor (GEF) which functions to enhance GTP binding; GTPase activating protein (GAP) to stimulate GTP-to-GDP exchange; and guanine nucleotide dissociation inhibitor (GDI) to promote dissociation of Rho GTPases from the plasma membrane to the cytosol (Berken and Wittinghofer, 2008; Brembu et al., 2006). A class of Rho GTPases called ROP GTPases has been characterized in several plant species including Arabidopsis, rice, tobacco, and moss (Brembu et al., 2006; Chen et al., 2010; Eklund et al., 2010; Kost et al., 1999; Yang and Watson, 1993). In Arabidopsis, three ROPs, ROP1, 3, and 5 are predominantly expressed in pollen tubes with ROP1 acting as a major player in regulating pollen tube tip growth (Li et al., 1999; Lin and Yang, 1997; Yang and Watson, 1993).

Pollen tube as a model system to study polarized tip growth

As a dynamic unicellular system, pollen tube has long been a versatile tool to study the cellular mechanisms involved in tip growth. This versatility can be contributed to the accessibility of techniques available for pollen analysis and to the nature of pollen genetics itself. For example, the availability of molecular tools such as pollen-specific promoters and markers as well as molecular techniques such as transient or stable expression, facilitate the molecular analysis of pollen-expressed genes. In addition, dynamic cellular imaging can be easily performed while keeping the cellular integrity intact. Physiologically, pollen tube shapes and growth patterns are almost homogeneous in *in vitro* growth condition and thus mutation that affects polarized growth can be easily

identified. And lastly, due to its haploid nature, lethal mutations which affect pollen tube development or growth are transmissible through heterozygous plants.

Pollen tubes are essential for the successful sexual reproduction process in flowering plants by facilitating the delivery of male gametes to the egg cells (Palanivelu and Preuss, 2006; Stewman et al., 2010). Following pollination, pollen tubes grow directionally within the pistil prior to reaching the ovules. This directional pollen tube tip growth requires the delivery of new cell wall materials for the expansion of cell membrane/wall at the tip region (Castle, 1958; Cheung and Wu, 2008; Krichevsky et al., 2007; Lee and Yang, 2008; Yang, 2008). The regulation of these preceding processes involves cellular signaling which include ROP pathways (Cheung et al., 2003; Hwang et al., 2010; Kost, 2008; Yang, 2008; Zonia, 2010), actin polymerization (Cheung and Wu, 2008; Fu, 2010; Vidali et al., 2001), spatiotemporal calcium (Hepler and Winship, 2010), and lipid-dependent pathways (Krichevsky et al., 2007; Zonia, 2010).

Positive and negative feedback regulation of ROP1 pathway in pollen tube

ROP1 plays an essential role in regulating pollen tube tip growth (Li et al., 1999). Active GTP-bound ROP1 localizes to the apical plasma membrane (PM) where it defines the tip growing site (Hwang et al., 2010). Expansion of active ROP1 distribution by overexpression (OX) of wild-type ROP1 or its constitutive-active form (CA-rop1), led to depolarized growth or tip swelling phenotype (Li et al., 1999). Suppression of active ROP1 distribution by OX of dominant-negative form (DN-rop1) inhibited tube growth and produced short tubes (Li et al., 1999). ROP1 regulates tip growth by controlling actin dynamics (Fu et al., 2001; Gu et al., 2005; Gu et al., 2003), promoting cytosolic calcium

accumulation (Li et al., 1999; Yan et al., 2009), and regulating vesicular trafficking (Lee et al., 2008) (Figure 1). ROP1 activities toward these processes require downstream effectors, ROP-interactive CRIB-containing protein, RIC4 and RIC3, which consecutively regulate F-actin assembly and tip-calcium accumulation (Gu et al., 2005; Figure 1). As downstream effectors, both RIC4 and RIC3 preferentially interact with active form of ROP1 which led them to be localized to the apical PM (Hwang et al., 2005). Thus both RICs can be utilized as markers for ROP1 activity at the apical PM region.

Apical ROP1 activity is highly regulated to maintain normal pollen tube tip growth. This regulation involves both positive and negative feedback loops (Yan et al., 2009; Figure 1). The positive feedback loop involves activation of ROP1, by RopGEFs, and subsequently its downstream effectors which resulted in continuous activation of ROP1. When ROP1 activation is enhanced, for example, by RopGEF1 OX, it resulted in depolarized growth similar to CA-rop1 phenotype (Gu et al., 2006). Once activated, GTP-bound ROP1 preferentially localizes to the apical PM and recruits RIC4 to the same region (Hwang et al., 2005; Li et al., 1999). RIC4 then promotes apical F-actin assembly, as evident from the formation of dense tip F-actin network in RIC4 OX (Gu et al., 2005) which can be reversed by LatB, F-actin depolymerizing drug (Fu et al., 2001). Tip F-actin further facilitates targeting of exocytic vesicles to the apical clear zone of pollen tubes as evident from the accumulation of exocytic vesicles marker, YFP-RabA4d, to the apical cortex when tip F-actin stability was enhanced via RIC4 OX (Lee et al., 2008). Thus, exocytosis process is involved in the positive feedback of ROP1 pathway since exocytic

vesicles carry not only various cargo molecules such as cell membrane and cell wall material required for pollen tube tip elongation but also signaling molecules such as GTP-ROP1 for directed targeting of activated ROP1 to the apical PM.

Positive feedback loop is counteracted by the negative feedback loop which involves inactivation of ROP1 (Figure 1). In the negative feedback loop, inactivation of ROP1 pathway involves RopGAPs or RENGAP which promote GTP-to-GDP hydrolysis (Wu et al., 2000; Hwang et al., 2008). RopGAP1 has long been considered as the major negative regulator of ROP1 in pollen tube, especially since co-expression of RopGAP1 with ROP1 can suppress the ROP1 OX-induced tip swelling phenotype (Hwang et al., 2010; Wu et al., 2000). However, a novel class of RhoGAP proteins identified from suppressor screen of ROP1 OX named ROP1 enhancer (REN1), likely plays the major role in negatively regulating ROP1 activity since loss of function *ren1-1* resulted in severely depolarized tubes similar to CA-rop1 phenotype and expanded ROP1 localization at the apical region (Hwang et al., 2008). Interestingly, REN1 localizes to the apical region as well as the exocytic vesicles and tip-directed targeting of REN1 via exocytosis is required to restrict ROP1 activity at the tip region (Hwang et al., 2008). Although REN1 function on ROP1 is apparent, the dynamic regulation of ROP1 by REN1 requires further investigations.

In addition to GAP proteins, the negative feedback loop also involves tip-localized Ca^{2+} whose accumulation involves ROP1 downstream effector, RIC3 (Gu et al., 2005). Steep calcium gradient at the tip region is crucial for normal pollen tube growth (Holdaway-Clarke et al., 1997; Pierson et al., 1994; Pierson et al., 1996). Disruption of

such gradient by treatment with calcium chelator, calcium ionophore, caffeine, or manipulation of RIC3 levels affected pollen tube growth (Gu et al., 2005; Pierson et al., 1994; Pierson et al., 1996; Yan et al., 2009). In addition, extracellular calcium level can also have an effect on pollen tube growth. For example, RIC3 OX pollen tubes whose tip calcium level is enhanced grew well in low calcium media (0.5 mM) but displayed growth inhibition at higher calcium media (> 2.0 mM). Furthermore, these growth inhibition effects can be reversed by $LaCl_3$ treatment which blocks calcium influx (Gu et al., 2005).

Both the positive and negative feedback loops are highly interconnected as evident from the crosstalk between F-actin dynamics and tip-focused calcium (Figure 1). Tip-focused calcium has been reported to negatively affect F-actin polymerization based on the observation that RIC3 OX pollen tubes displayed loss of tip F-actin and protrusion of actin cables to the apical region; and these effects can be suppressed by treatment with calcium chelator, EGTA, or Ca^{2+} channel blocker, $LaCl_3$ (Gu et al., 2005). The effects calcium has on actin stability likely involve activation of actin disassembly factors such as profilin, though this remains a speculation (Gu et al., 2005).

Oscillatory pollen tube growth, ROP GTPase activity, and calcium

Biological oscillations have been observed in many living systems; one well-known example is circadian oscillator found in cyanobacteria (Ishiura et al., 1998) or plants (Alabadi et al., 2001). The fundamental question of how biological oscillation arises still remains and it has been speculated that biological interactions of cellular components within a cell may spontaneously produce oscillatory behaviors and

essentially a biological system with self-organizing processes (Feijo et al., 2001). Computer simulations have predicted that oscillations may be obtained based on positive feedback alone, negative feedback alone (Goldbeter, 2002), or both positive and negative loops to create a more robust and tunable frequency (Tsai et al., 2008). Regardless of these predictions, it is clear that pollen tube growth as well as the underlying signaling processes regulating tip growth have been reported to oscillate. In lily and tobacco, pollen tube growth oscillates every 30-42 sec and 80 sec respectively (Holdaway-Clarke et al., 1997; Hwang et al., 2005; Messerli and Robinson, 1997; Pierson et al., 1996). Consistently, ROP1 activation and tip F-actin oscillate with a similar period but ahead of growth oscillation, though ROP1 activation oscillates ahead of tip F-actin (Fu et al., 2001; Hwang et al., 2005; Hwang et al., 2010). In contrast, extracellular calcium influx oscillates behind growth oscillation (Holdaway-Clarke et al., 1997). Thus phase relationships seem to exist between active ROP1, tip growth, and tip-focused calcium in a way that ROP1 activation precedes RIC4-mediated tip F-actin assembly which then leads to pollen tube growth burst (Fu et al., 2001; Hwang et al., 2005). After a short time, RIC3-mediated increase in tip-focused calcium from extracellular calcium influx led to the slowing of pollen tube growth which is likely to be associated with the down regulation of ROP1 activity (Hwang et al., 2005).

Tip-focused calcium gradient is essential for normal pollen tube tip growth

In pollen tube, calcium forms a steep gradient with the highest level of calcium found at the tip region. Such calcium gradient has been observed in many plant species including Agapanthus, pea, silverworts (*Tradescantia*), tobacco, and Arabidopsis (Malho

et al., 1994; Li et al., 1998; Pierson et al., 1996; Iwano et al., 2009). It has been reported that tip region contains calcium in the range between 1 µM to > 5 µM and the subapical region (20 µM from the tip) contains around 150-300 nM of calcium (Pierson et al., 1994; Pierson et al., 1996; Holdaway-Clarke et al., 1997; Camacho et al., 2000). Dissipation of tip calcium using calcium chelator BAPTA-type buffers, caffeine, and mild thermal shock inhibited pollen tube elongation which further suggests that tip-focused calcium play an important role in regulating pollen tube growth (Pierson et al., 1994; Pierson et al., 1996).

To produce tip-localized calcium gradient, two possible mechanisms are likely involved. These are influx of extracellular calcium or release from internal calcium storage such as the ER (Holdaway-Clarke et al., 1997). Although internal calcium release remains a possibility and seems to be an attractive model in producing tip-focused calcium gradient, certain questions regarding this model still remains, one being the limited availability of ER in the apical clear zone and as such how calcium is able to move from the ER to the tip region (Holdaway-Clarke et al., 1997). Thus, based on the mathematical model and experimental observations, extracellular calcium influx seems to be the major factors involved in supplying the localized tip calcium gradient (Holdaway-Clarke et al., 1997). As such, it is conceivable that *in vitro* pollen tube growth responds differently when exposed to different calcium environment which affects the generation of tip-focused calcium. For example, WT pollen tubes grown in low calcium (0.5 mM) displayed shorter tubes with high germination inhibition while in high calcium (10-20 mM) displayed tubes bursting and some growth inhibition in comparison to those grown

in optimal condition of 2 – 5 mM calcium which produced normal tube growth (Li et al., 1999; Gu et al., 2005). The molecular mechanism underlying these different responses is still unclear. It seems likely that the growth inhibition in low calcium is due to less calcium influx at the tip region (Pierson et al., 1994; Li et al., 1999). However, growth defects in high calcium may be due to negative feedback regulation of calcium influx (Li et al., 1999) or calcium -mediated increase in cell wall rigidity caused by cross-linking of calcium to the apical pectic wall (Holdaway-Clarke et al., 1997).

The relationships between calcium, ROP1 pathway, and potentially calcium-dependent protein kinase in pollen tube

Tip-focused calcium gradient can be associated with the regulation of ROP1 activity. From the oscillations studies, it has been shown that phase relationships exist between activation of ROP1 and subsequently its downstream effectors, pollen tube growth, and calcium influx. Based on these data, calcium influx which is positively regulated by ROP1 effector, RIC3, oscillated behind growth oscillation since accumulation of tip-high calcium likely take some time once ROP1 is activated (Hwang et al., 2005). Once calcium influx takes place, pollen tube growth slows which is likely to be associated with the down regulation of ROP1 activity (Hwang et al., 2005; Yan et al., 2009). Thus we hypothesize that high tip calcium is involved in the negative regulation of ROP1 activity; however, this claim remains to be investigated. Recent identification of REN1GAP revealed a possible functional interaction between Ca^{2+} and REN1. It was observed that the pollen tubes of weak *ren1* alelle, *ren1-3*, were long and wavy with slight tip swelling when grown in optimal calcium media (2-5 mM) but became

depolarized under low calcium media (0.5 mM) (Hwang et al., 2008). This suggests that REN1 activity maybe loss or significantly reduced in pollen tubes grown under low calcium media and the resulting enhanced ROP1 led to the loss of tip polarity. Thus REN1 activity is likely regulated by calcium, although, how this regulation occurs is still a question.

Calcium perception and signal decoding involves an array of calcium sensors including Ca^{2+}-dependent protein kinases (CDPKs/CPKs) (Harper et al., 2004; Kudla et al., 2010). CPKs are involved in a multitude of biological and cellular responses in not only plants but also protozoa. Its functions have been linked to plant response to abiotic and biotic stress (Saijo et al., 2001; Sheen, 1996; Romeis et al., 2001; Boudsocq et al., 2010), regulation of ABA-responsive gene expression (Choi et al., 2005; Zhu et al., 2009), exocytosis regulation in *Toxoplasma* (Lourido et al., 2010), and regulation of normal pollen tube growth (Yoon et al., 2006; Myers et al., 2009; Zhou et al., 2009). Compared to known Ca^{2+} sensor in eukaryotes, this class of Ca^{2+} sensors is unique since its activity requires only Ca^{2+} but not calmodulin or phospholipids (Harmon et al., 1987; Harper et al., 1991). Structurally, CPKs consist of kinase domain, autoinhibitory region, and EF-fingers calmodulin-like Ca^{2+}-binding motifs (Harper et al., 1991; Huang et al., 1996). When the Ca^{2+} level is below a certain threshold, the autoinhibitory region interacts with the kinase domain and renders the protein kinase inactive. Increase in Ca^{2+} levels (above a certain threshold), which is detected by the Ca^{2+}-binding motifs, leads to the release of the kinase domain and activation of the kinase protein (Huang et al., 1996; Yoo et al., 1996; Lee et al., 1998).

Several CPK targets have been identified which include transcription factors such as Repression of Shoot Growth (RSG), ABRE binding factor 4 (ABF4), Dehydration-induced 19 (AtDi19), and CDPK Substrate Protein 1 (CSP1) (Ishida et al., 2008; Choi et al., 2005; Milla et al., 2006; Patharkar and Cushman, 2000); proteasome subunit, NtRpn3 (Lee et al., 2003); metabolism regulators such as nitrase reductase and sucrose-phosphate synthase (Bachmann et al., 1995; Bachmann et al., 1996; Douglas et al., 1998; McMichael Jr. et al., 1993); ion transports/channels such as Ca^{2+}-ATPases, ACA2, and K+ channel KAT1 (Hwang et al., 2000; Li et al., 1998); and cytoskeleton component, actin-depolymerizing factor (Allwood et al., 2001). For complete review of CDPK targets, please refer to Cheng et al., 2002 and Klimecka and Muszynska, 2007. To date, CPK targets of pollen-expressed proteins are potentially limited to those involved in ion transports or actin regulation. Nevertheless, it is clear from mutation or overexpression studies that several CPKs are involved in regulating pollen tube tip growth and guidance. For example: CPK32 OX resulted in depolarized growth phenotype (Zhou et al., 2009), double mutations of *cpk17-2cpk34-2* or *cpk17-2cpk34-2*/+ resulted in reduced seed set and defect in ovule sensing (Myers et al., 2009), and PiCDPK1 OX and DN-PiCDPK1 OX both resulted in tip swelling phenotype which mimics ROP1/CA-rop1 OX while CA-PiCDPK1 OX inhibited tube growth similar to DN-rop1 OX (Yoon et al., 2006). Thus far, the substrates of these CPKs are still unknown. Therefore, a potential CPK substrate likely includes regulator(s) of tip polarity in pollen tubes. Moreover, it is plausible that CPKs may function on ROP1 regulators or effectors.

Questions Addressed in This Dissertation

1) Is REN1 phosphorylated by pollen-expressed CPK(s)?

The phenotypic response displayed by the weak allele *ren1-3* grown in low calcium condition suggests a novel mechanism by which calcium signaling may regulate REN1. Since REN1 does not interact with calcium, it is very likely that a calcium sensor such as CPK may have a role in calcium detection and calcium response (Figure 1). CPK16 is one of the few CPKs expressed in mature pollen. Its expression correlates highly with REN1 and is linked directly to REN1 in the co-expressed gene network generated by ATTEDII gene expression database (http://atted.jp) (Obayashi et al., 2007; Obayashi et al., 2009; Obayashi et al., 2011). Thus it is critical to test whether CPK16 can indeed phosphorylate REN1. Our phosphorylation analysis *in vitro* indeed showed that CPK16 is able to phosphorylate REN1 in a calcium-dependent manner. In addition, such phosphorylation was detected in the presence of calcium level with a relative EC_{50} of ~4.6 μM which is physiologically relevant and led us to speculate that CPK16 may be involved in the regulation of REN1.

2) How does REN1 phosphorylation affect its activity?

Following the establishment of calcium-dependent phosphorylation of REN1 by CPK16, it is critical to identify REN1 phosphorylation sites to gain further insights into its functional relevance. To achieve this goal, 2D-LC/MS/MS analyses were performed on phosphopeptides which were generated using trypsin digestion. From these analyses, calcium-dependent or –independent phosphorylation sites were identified. Functional analysis was focused primarily on the residue located within the catalytic GAP domain.

In addition, other residues within the pleckstrin homology (PH) domain which is required for membrane association were also analyzed.

Since protein phosphorylation is known to affect protein activities, subcellular localization, or abundance (Schulze et al., 2010), our interests were primarily on how REN1 phosphorylation affects its activity. To this end, mutations analyses were performed. Consistent with our prediction, some phosphorylation mutations affected REN1 protein activity in transient co-expression with ROP1. Thus our analyses seem to indicate that REN1 phosphorylation within the catalytic GAP domain leads to enhanced activity while those within the PH domain affects its localization and subsequently leads to reduced activity.

3) Does *CPK16* loss-of-function mutant result in tip polarity loss in pollen tube?

If CPK16 is to be involved in regulating pollen tube growth and/or tip polarity, its loss of function may generate growth or tip polarity defect. Interestingly, CPK16 mutant displayed enhanced pollen tube growth and germination in low calcium condition with no polarity defect. However, further treatments with exocytosis inhibitor, BFA, or actin polymerization inhibitor, LatB, led to depolarized growth phenotype similar to the chemical effects on partially complemented *ren1-1 Lat52::GFP-REN1* which suggests a functional relationships between CPK16 and REN1. In the end, a model was established to explain the functional relationships between calcium sensing and response involving CPK16 in phosphorylating a major regulatory protein REN1 which controls ROP1 activation in pollen tube.

4) Chemical genetics approach to identify inhibitors of ROP-GAP interaction

Considering that factors regulating pollen tube growth such as ROP1 are tightly regulated and the growth itself is highly dynamics, studying the oscillatory pollen tube growth and its regulatory factors is a challenge when utilizing conventional mutations studies. This is because such approaches often lead to terminal phenotypes such as growth inhibition or depolarized growth phenotypes. To circumvent these issues, we have resorted to the use of reverse chemical genetics approach to investigate the causal relationships between growth, active ROP1, and tip-focused calcium in a highly dynamic, oscillatory pollen tube system. Reverse chemical genetics can be a useful tool to study known target genes or proteins by perturbing their functions using small molecules (Blackwell and Zhao, 2003; Zheng and Chan, 2002; Walsh and Chang, 2006). Our goal was to enhance ROP1 activation and as such monitor the spatial and temporal changes occurring to growth as well as other ROP1 effectors. Our attempt to obtain such chemical was focused on identifying inhibitors of ROP1 and REN1 interaction which would theoretically lead to the accumulation of active ROP1. Our cell-based yeast two hybrid screens identified putative hits in which some were confirmed in *in vitro* protein-protein interaction analysis. From these hits, one compound was identified to induce slight tip swelling in pollen tubes, enhance ROP1 OX swelling phenotype and slightly enhance weak allele *ren1-3* phenotype. Our overall analyses suggest a potential activator of ROP1 which acts by inhibiting ROP1-REN1 interaction that may potentially be useful for future ROP1 studies.

REFERENCES

Alabadi, D., Oyama, T., Yanovsky, M.J., Harmon, F.G., Mas, P., and Kay, S.A. (2001) Reciprocal regulation between TOC1 and LHY/CCA1 within the Arabidopsis circadian clock. Science **293**: 880-883

Allwood, E. G., Smertenko, A. P., Hussey, P. J. (2001) Phosphorylation of plant actin-depolymerising factor by calmodulin-like domain protein kinase. FEBS Lett **499**: 97 – 100

Arimura, N. and Kaibuchi, K. (2005) Key regulators in neuronal polarity. Neuron **48**: 881 – 884

Bachmann, M., McMichael Jr., R. W., Huber, J. L., Kaiser, W. M., and Huber, S. C. (1995) Partial purification and characterization of a calcium-dependent protein kinase and an inhibitor protein required for inactivation of spinach leaf nitrate reductase. Plant Physiol. **108**: 1083 – 1091

Bachmann, M., Shiraishi, N., Campbell, W. H., Yoo, B-C., Harmon, A. C., and Huber, S. C. (1996) Identification of Ser-543 as the major regulatory phosphorylation site in spinach leaf nitrate reductase. Plant Cell **8**: 505 – 517

Berken, A., and Wittinghofer, A. (2008) Structure and function of Rho-type molecular switches in plants. Plant Physiol. Biochem. **46**: 380-393

Blackwell, H.E., and Zhao, Y. (2003) Chemical genetic approaches to plant biology. Plant Physiol. **133**: 448-455

Boudsocq, M., Willmann, M. R., McCormack, M., Lee, H., Shan, L., He, P., Bush, J., Cheng, S-H., and Sheen, J. (2010) Differential innate immune signaling via Ca^{2+} sensor protein kinases. Nature **464**: 418 – 423

Brembu, T., Winge, P., Bones, A.M., and Yang, Z. (2006) A RHOse by any other name: a comparative analysis of animal and plant Rho GTPases. Cell Res. **16**: 435-445

Camacho, L., Parton, R., Trewavas, A. J., and Malho, R. (2000) Imaging cytosolic free-calcium distribution and oscillations in pollen tubes with confocal microscopy: a comparison of different dyes and loading methods. Protoplasma **212**: 162 – 173

Castle, E.S. (1958) The topography of tip growth in a plant cell. J. Gen. Physiol. **41**: 913-926

Chen, L., Shiotani, K., Togashi, T., Miki, D., Aoyama, M., Wong, H.L., Kawasaki, T., and Shimamoto, K. (2010) Analysis of the Rac/Rop small GTPase family in rice: expression, subcellular localization and role in disease resistance. Plant Cell Physiol. **51**: 585-595

Cheng, S-H., Willmann, M. R., Chen, H-C., and Sheen, J. (2002) Calcium signaling through protein kinases. The *Arabidopsis* calcium-dependent protein kinase gene family. Plant Physiol. **129**: 469 – 485

Cheung, A.Y., Chen, C.Y., Tao, L.Z., Andreyeva, T., Twell, D., and Wu, H.M. (2003) Regulation of pollen tube growth by Rac-like GTPases. J. Exp. Bot. **54**: 73-81

Cheung, A.Y., and Wu, H.M. (2008) Structural and signaling networks for the polar cell growth machinery in pollen tubes. Annu. Rev. Plant Biol. **59**: 547-572

Choi, H-I, Park, H-J., Park, J. H., Kim, S., Im, M-Y., Seo, H-H., Kim, Y-W., Hwang, I., and Kim, S. Y. (2005) Arabidopsis calcium-dependent protein kinase AtCPK32 interacts with ABF4, a transcriptional regulator of abscisic acid-responsive gene expression, and modulates its activity. Plant Physiol. **139**: 1750 – 1761

Douglas, P., Moorhead, G., Hong, Y., Morrice, N., and MacKintosh, C. (1998) Purification of a nitrate reductase kinase from *Spinacea oleracea* leaves, and its identification as a calmodulin-domain protein kinase. Planta **206**: 435 – 442

Eklund, D.M., Svensson, E.M., and Kost, B. (2010) *Physcomitrella patens*: a model to investigate the role of RAC/ROP GTPase signalling in tip growth. J. Exp. Bot. **61**: 1917-1937

Feijo, J.A., Sainhas, J., Holdaway-Clarke, T., Cordeiro, M.S., Kunkel, J.G., and Hepler, P.K. (2001) Cellular oscillations and the regulation of growth: the pollen tube paradigm. Bioessays **23**: 86-94

Fu, Y. (2010) The actin cytoskeleton and signaling network during pollen tube tip growth. J. Integr. Plant Biol. **52**: 131-137

Fu, Y., Wu, G., and Yang, Z. (2001) Rop GTPase-dependent dynamics of tip-localized F-actin controls tip growth in pollen tubes. J Cell Biol. **152**: 1019-1032

Goldbeter, A. (2002) Computational approaches to cellular rhythms. Nature **420**: 238-245

Gu, Y., Fu, Y., Dowd, P., Li, S., Vernoud, V., Gilroy, S., and Yang, Z. (2005) A Rho family GTPase controls actin dynamics and tip growth via two counteracting downstream pathways in pollen tubes. J. Cell Biol. **169**: 127-138

Gu, Y., Li, S., Lord, E.M., and Yang, Z. (2006) Members of a novel class of Arabidopsis Rho guanine nucleotide exchange factors control Rho GTPase-dependent polar growth. Plant Cell **18**: 366-381

Gu, Y., Vernoud, V., Fu, Y., and Yang, Z. (2003) ROP GTPase regulation of pollen tube growth through the dynamics of tip-localized F-actin. J. Exp. Bot. **54**: 93-101

Harmon, A.C., Putnam-Evans, C., and Cormier, M.J. (1987) A calcium-dependent but calmodulin-independent protein kinase from soybean. Plant Physiol. **83**: 830-837

Harper, J.F., Breton, G., and Harmon, A. (2004) Decoding Ca^{2+} signals through plant protein kinases. Annu. Rev. Plant Biol. **55**: 263-288

Harper, J.F., Sussman, M.R., Schaller, G.E., Putnam-Evans, C., Charbonneau, H., and Harmon, A.C. (1991) A calcium-dependent protein kinase with a regulatory domain similar to calmodulin. Science **252**: 951-954

Hepler, P. K., Vidali, L., and Cheung, A. Y. (2001) Polarized cell growth in higher plants. Annu. Rev. Cell Dev. Biol. **17**: 159 – 187

Hepler, P.K., and Winship, L.J. (2010) Calcium at the cell wall-cytoplast interface. J. Integr. Plant Biol. 52: 147-160

Holdaway-Clarke, T.L., Feijo, J.A., Hackett, G.R., Kunkel, J.G., and Hepler, P.K. (1997) Pollen tube growth and the intracellular cytosolic calcium gradient oscillate in phase while extracellular calcium influx is delayed. Plant Cell **9**: 1999-2010

Huang, J.F., Teyton, L., and Harper, J.F. (1996) Activation of a Ca^{2+}-dependent protein kinase involves intramolecular binding of a calmodulin-like regulatory domain. Biochem **35**: 13222-13230

Hwang, J.U., Gu, Y., Lee, Y.J., and Yang, Z. (2005) Oscillatory ROP GTPase activation leads the oscillatory polarized growth of pollen tubes. Mol. Biol. Cell **16**: 5385-5399

Hwang, I., Sze, H., and Harper, J. F. (2000) A calcium-dependent protein kinase can inhibit a calmodulin-stimulated Ca^{2+} pump (ACA2) located in the endoplasmic reticulum of Arabidopsis. Proc. Nat. Acad. Sci. **97(11)**: 6224 – 6229

Hwang, J.U., Vernoud, V., Szumlanski, A., Nielsen, E., and Yang, Z. (2008) A tip-localized RhoGAP controls cell polarity by globally inhibiting Rho GTPase at the cell apex. Curr. Biol. **18**: 1907-1916

Hwang, J.U., Wu, G., Yan, A., Lee, Y.J., Grierson, C.S., and Yang, Z. (2010) Pollen-tube tip growth requires a balance of lateral propagation and global inhibition of Rho-family GTPase activity. J. Cell Science **123**: 340-350

Ishida, S., Yuasa, T., Nakata, M., and Takahashi, Y. (2008) A tobacco calcium-dependent protein kinase, CDPK1, regulates the transcription factor Repression of Shoot Growth in response to gibberellins. Plant Cell **20**: 3273 – 3288

Ishiura, M., Kutsuna, S., Aoki, S., Iwasaki, H., Andersson, C.R., Tanabe, A., Golden, S.S., Johnson, C.H., and Kondo, T. (1998) Expression of a gene cluster kaiABC as a circadian feedback process in cyanobacteria. Science **281**: 1519-1523

Iwano, M., Entani, T., Shiba, H., Kakita, M., Nagai, T., Mizuno, H., Miyawaki, A., Shoji, T., Kubo, K., Isogai, A., and Takayama, S. (2009) Fine-tuning of the cytoplasmic Ca^{2+} concentration is essential for pollen tube growth. Plant Physiol. **150:** 1322-1334

Klimecka, M. and Muszynska, G. (2007) Structure and functions of plant calcium-dependent protein kinases. Acta Biochim. Polonica **54(2)**: 219 – 233

Kost, B. (2008) Spatial control of Rho (Rac-Rop) signaling in tip-growing plant cells. Trends Cell Biol. **18**: 119-127

Kost, B., Lemichez, E., Spielhofer, P., Hong, Y., Tolias, K., Carpenter, C., and Chua, N.H. (1999) Rac homologues and compartmentalized phosphatidylinositol 4, 5-bisphosphate act in a common pathway to regulate polar pollen tube growth. J. Cell Biol. **145:** 317-330

Krichevsky, A., Kozlovsky, S.V., Tian, G.W., Chen, M.H., Zaltsman, A., and Citovsky, V. (2007). How pollen tubes grow. Dev. Biol. **303:** 405-420

Kudla, J., Batistic, O., and Hashimoto, K. (2010) Calcium signals: the lead currency of plant information processing. Plant Cell **22**: 541 – 563

Lee, S. S., Cho, H. S., Yoon, G. M., Ahn, J-W., Kim, H-H., and Pai, H-S. (2003) Interaction of NtCDPK1 calcium-dependent protein kinase with NtRpn3 regulatory subunit of the 26S proteasome in *Nicotiana tabacum*. Plant J. **33**: 825 – 840

Lee, Y.J., Szumlanski, A., Nielsen, E., and Yang, Z. (2008) Rho-GTPase-dependent filamentous actin dynamics coordinate vesicle targeting and exocytosis during tip growth. J. Cell Biol. **181**: 1155-1168

Lee, Y.J., and Yang, Z. (2008) Tip growth: signaling in the apical dome. Curr. Op. Plant Biol. **11**: 662-671

Lee, J-Y., Yoo, B-C., and Harmon, A. C. (1998) Kinetic and calcium-binding properties of three calcium-dependent protein kinase isoenzymes from soybean. Biochemistry **37**: 6801 – 6809

Li, J., Lee, Y-R. J., and Assmann, S. M. (1998) Guard cells possess a calcium-dependent protein kinase that phosphorylates the KAT1 potassium channel. Plant Physiol. **116:** 785 – 795

Li, H., Lin, Y., Heath, R.M., Zhu, M.X., and Yang, Z. (1999) Control of pollen tube tip growth by a Rop GTPase-dependent pathway that leads to tip-localized calcium influx. Plant Cell **11**: 1731-1742

Li, R., and Gundersen, G.G. (2008) Beyond polymer polarity: how the cytoskeleton builds a polarized cell. Nature Rev. **9**: 860-873

Lin, Y., and Yang, Z. (1997) Inhibition of pollen tube elongation by microinjected anti-Rop1Ps antibodies suggests a crucial role for Rho-type GTPases in the control of tip growth. Plant Cell **9**: 1647-1659

Lourido, S., Shuman, J., Zhang, C., Shokat, K. M., Hui, R., and Sibley, L. D. (2010) Calcium-dependent protein kinase 1 is an essential regulator of exocytosis in *Toxoplasma*. Nature **465**: 359 – 363

McMichael Jr., R. W., Klein, R. R., Salvucci, M. E., and Huber, S. C. (1993) Identification of the major regulatory phosphorylation site in sucrose-phosphate synthase. Arch Biochem Biophys **307(2)**: 248 – 252

Mellman, I., and Nelson, W.J. (2008) Coordinated protein sorting, targeting and distribution in polarized cells. Nature Rev. **9**: 833-845

Menand, B., Calder, G., and Dolan, L. (2007) Both chloronemal and caulonemal cells expand by tip growth in the moss *Physcomitrella patens*. J. Exp. Bot. **58(7)**: 1843 – 1849

Mila, M. A. R., Uno, Y., Chang, I-F., Townsend, J., Maher, E. A., Quilici, D., and Cushman, J. C. (2006) A novel yeast two-hybrid approach to identify CDPK substrates: characterization of the interaction between AtCPK11 and AtDi19, a nuclear zinc finger protein. FEBS Lett. **580**: 904 – 911

Myers, C., Romanowsky, S. M., Barron, Y. D., Garg, S., Azuse, C. L., Curran, A., Davis, R. M., Hatton, J., Harmon, A. C., and Harper, J. F. (2009) Calcium-dependent protein kinases regulate polarized tip growth in pollen tubes. Plant J. **59(4)**: 528 – 539

Obayashi T, Hayashi S, Saeki M, Ohta H, Kinoshita K. (2009) ATTED-II provides coexpressed gene networks for Arabidopsis. Nucleic Acids Res. **37**: D987-D991

Obayashi T, Kinoshita K, Nakai K, Shibaoka M, Hayashi S, Saeki M, Shibata D, Saito K, Ohta H. (2007) ATTED-II: a database of co-expressed genes and cis elements for identifying co-regulated gene groups in Arabidopsis. Nucleic Acids Res. **35**: D863-D869

Obayashi T, Nishida K, Kasahara K, Kinoshita K. (2011) ATTED-II updates: condition-specific gene coexpression to extend coexpression analyses and applications to a broad range of flowering plants. Plant Cell Physiol. **52**: 213-219

Palanivelu, R., and Preuss, D. (2006) Distinct short-range ovule signals attract or repel *Arabidopsis thaliana* pollen tubes *in vitro*. BMC Plant Biol. **6**: 7-16

Patharkar, O. R. and Cushman, J. C. (2000) A stress-induced calcium-dependent protein kinase from *Mesembranthemum crystallinum* phosphorylates a two-component pseudo-response regulator. Plant J. **24(5)**: 679 – 691

Perez, P., and Rincon, S.A. (2010) Rho GTPases: regulation of cell polarity and growth in yeasts. Biochem. J. **426**: 243-253

Pierson, E.S., Miller, D.D., Callaham, D.A., Shipley, A.M., Rivers, B.A., Cresti, M., and Hepler, P.K. (1994) Pollen tube growth is coupled to the extracellular calcium ion flux and the intracellular calcium gradient: effect of BAPTA-type buffers and hypertonic media. Plant Cell **6**: 1815-1828

Pierson, E.S., Miller, D.D., Callaham, D.A., van Aken, J., Hackett, G., and Hepler, P.K. (1996) Tip-localized calcium entry fluctuates during pollen tube growth. Dev. Biol. **174**: 160-173

Ridley, A.J. (2006) Rho GTPases and actin dynamics in membrane protrusions and vesicle trafficking. Trends Cell Biol. **16**: 522-529

Romeis, T., Ludwig, A. A., Martin, R., and Jones, J. D. G. (2001) Calcium-dependent protein kinases play an essential role in a plant defense response. EMBO J. **20(20)**: 5556 – 5567

Saijo, Y., Kinoshita, N., Ishiyama, K., Hata, S., Kyozuka, J., Hayakawa, T., Nakamura, T., Shimamoto, K., Yamaya, T. and Izui, K. (2001) A Ca^{2+}-dependent protein kinase that endows rice plants with cold- and salt-stress tolerance functions in vascular bundles. Plant Cell Phys. **42(11)**: 1228 – 1233

Schulze, W. X. (2010) Proteomics approaches to understand protein phosphorylation in pathway modulation. Curr. Op. Plant Biol. **13**: 280 – 287

Sheen, J. (1996) Ca^{2+}-dependent protein kinases and stress signal transduction in plants. Science **274**: 1900 – 1902

Stewman, S.F., Jones-Rhoades, M., Bhimalapuram, P., Tchernookov, M., Preuss, D., and Dinner, A.R. (2010) Mechanistic insights from a quantitative analysis of pollen tube guidance. BMC Plant Biol. **10**: 32

Tsai, T.Y., Choi, Y.S., Ma, W., Pomerening, J.R., Tang, C., and Ferrell, J.E., Jr. (2008) Robust, tunable biological oscillations from interlinked positive and negative feedback loops. Science **321**: 126-129

Vidali, L., McKenna, S.T., and Hepler, P.K. (2001) Actin polymerization is essential for pollen tube growth. Mol. Biol. Cell **12**: 2534-2545

Walsh, D.P., and Chang, Y.T. (2006) Chemical genetics. Chem. Rev. **106**: 2476-2530

Wu, G., Li, H., and Yang, Z. (2000) Arabidopsis RopGAPs are a novel family of rho GTPase-activating proteins that require the Cdc42/Rac-interactive binding motif for rop-specific GTPase stimulation. Plant Physiol. **124**: 1625-1636

Yan, A., Xu, G., and Yang, Z.B. (2009) Calcium participates in feedback regulation of the oscillating ROP1 Rho GTPase in pollen tubes. Proc. Natl. Acad. Sci. **106**: 22002-22007

Yang, Z. (2008). Cell polarity signaling in Arabidopsis. Annu. Rev. Cell Dev. Biol. **24:** 551-575

Yang, Z., and Watson, J.C. (1993) Molecular cloning and characterization of rho, a ras-related small GTP-binding protein from the garden pea. Proc. Natl. Acad. Sci. **90**: 8732-8736

Yoo, B-C and Harmon, A. C. (1996) Intramolecular binding contributes to the activation of CDPK, a protein kinase with a calmodulin-like domain. Biochemistry **35**: 12029 – 12037

Yoon, G. M., Dowd, P. E., Gilroy, S., and McCubbin, A. G. (2006) Calcium-dependent protein kinase isoforms in *Petunia* have distinct functions in pollen tube growth, including regulating polarity. Plant Cell **18**: 867 – 878

Zheng, X. F. and Chan, T-F. (2002) Chemical genomics: a systematic approach in biological research and drug discovery. Curr. Issues Mol. Biol. **4**: 33 – 43

Zhou, L., Fu, Y., and Yang, Z. (2009) A genome-wide functional characterization of *Arabidopsis* regulatory calcium sensors in pollen tubes. J Integr. Plant Biol. **51(8)**: 751 – 761

Zhu, S-Y., Yu, X-C., Wang, X-J., Zhao, R., Li, Y., Fan, R-C., Shang, Y., Du, S-Y., Wang, X-F., Wu, F-Q., Xu, Y-H., Zhang, X-Y., and Zhang, D-P. (2007) Two calcium-dependent protein kinases, CPK4 and CPK11, regulate abscisic acid signal transduction in *Arabidopsis*. Plant Cell **19**: 3019 – 3036

Zonia, L. (2010) Spatial and temporal integration of signaling networks regulating pollen tube growth. J. Exp. Bot. **61:** 1939-1957

Figure 1. ROP1 signaling pathway in regulating pollen tube tip growth. Upon perception of activation signal, ROP1 is activated by positive regulatory protein guanine exchange factor (GEF) which promotes GDP-to-GTP exchange in ROP1. Active GTP-bound ROP1 further activates downstream effectors: ICR1/RIP1 which recruits SEC3 exocyst subunit, RIC4 which mediates F-actin assembly, and RIC3 which promotes tip calcium accumulation. These processes lead to the regulation of polar exocytosis to mediate tip-directed targeting of exocytic vesicles containing regulatory protein such as REN1GAP. The dynamic apical ROP1 activity is maintained by both positive and negative feedback loops. In the positive feedback loop, RIC4-mediated regulation of F-actin assembly is involved in further activation of ROP1 at the tip. In contrast, negative feedback loop involves RIC3-mediated accumulation of tip-localized calcium which antagonizes RIC4-mediated F-actin assembly and regulates REN1 activity.

Figure 1.

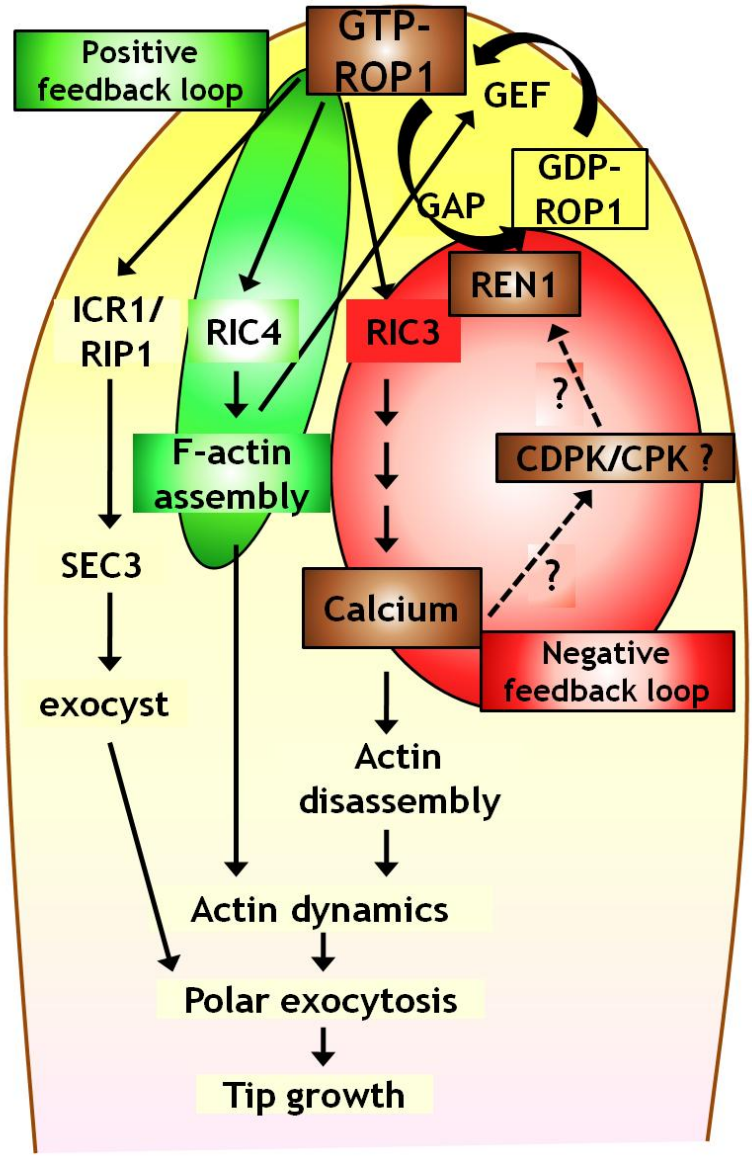
GTP-ROP1
Positive feedback loop
GEF
GAP
GDP-ROP1
REN1
ICR1/ RIP1
RIC4
RIC3
?
F-actin assembly
CDPK/CPK ?
SEC3
Calcium
?
Negative feedback loop
exocyst
Actin disassembly
Actin dynamics
Polar exocytosis
Tip growth

Chapter 1

Biochemical and mass spectrometry analysis of REN1 phosphorylation by CPK16

ABSTRACT

Calcium-dependent protein kinases (CDPKs/CPKs) are serine/threonine kinases whose functions have been attributed to many cellular processes including the regulation of pollen tube tip polarity. However, their substrate(s) involved in this process are still largely unknown. A potential calcium-regulated protein, REN1, showed enhanced depolarized growth phenotype when grown in low calcium condition. REN1 is not a calcium binding protein and is thus likely regulated by calcium sensors. Here we report that REN1 is a likely substrate for CPK16. *In vitro* kinase assays revealed that CPK16 phosphorylates REN1 in a calcium-dependent manner requiring a minimum of 2.5 μM Ca^{2+} with a relative EC_{50} value of ~4.6 μM for its activity. This calcium requirement seems to be physiologically relevant since tip-focused calcium gradient can reach to a concentration of >5 μM at the extreme tip region. Identification of REN1 phosphorylation sites by MS/MS analysis using *in vitro* kinase samples revealed many phosphorylation sites of more than 20, but only about half of those sites are calcium-dependent phosphorylation sites. In addition, most phosphorylation sites were generally found in the C-terminal region which is consistent with the NetPhos prediction. Further comparison of the phosphopeptides found in this study identified simple CPK phosphorylation motifs, particularly the presence of basic residue at P_{-3} or P_{+2} positions.

INTRODUCTION

Phosphorylation is an essential post-translational regulation of proteins which result in a change of protein activities, subcellular localizations, or abundance (Schulze, 2010). Protein phosphorylation is mediated by protein kinases, which are classified into several types depending on its substrates. CPKs are calcium-dependent Ser/Thr protein kinases that are unique in plants and protists (Cheng et al., 2002; Harper et al., 2004; Hrabak et al., 2003; Klimecka and Muszynska, 2007). Under basal calcium level, CPKs are inactive due to the binding of its autoinhibitory region to the kinase domain (Yoo and Harmon, 1996; Harper et al., 2004). Calcium binding to the calmodulin-like calcium binding domain of CPKs leads to conformational changes of the proteins which further release the interaction between autoinhibitory region and the kinase domain (Yoo and Harmon, 1996; Harper et al., 2004). This activation of CPKs requires a certain calcium threshold which can vary depending on the kinases. For example, the amount of Ca^{2+} required for CPKs half maximal activation ($K_{0.5}$) was reported to be ~600 nM for PiCDPK1 (Yoon et al., 2006); ~2 μM for soybean CDPK (Harmon et al., 1987); 0.06 μM for soybean CDPKα isoform, 0.4 μM for soybean CDPKβ isoform, and 1 μM for soybean CDPKγ isoform (Lee et al., 1998).

Calcium, as a ubiquitous element, plays a significant role in plant developmental and cellular processes (Kudla et al., 2010; Dodd et al., 2010; Cheng et al., 2002). Calcium response to a certain developmental or environmental stimulus results in an increase of tip-focused cytosolic calcium in terms of spatial distribution, timing, frequency, and amplitude, producing a unique "calcium signatures" (Kudla et al., 2010). Calcium

sensors, including CPKs, decode these calcium signatures and transduce the signals by phosphorylating downstream targets. In plants, CPKs consist of a large family member: 34 in Arabidopsis (Cheng et al., 2002), 31 in rice (Ye et al., 2009, Ray et al., 2007, Asano et al., 2005), and 20 members in wheat (Li et al., 2008). Each CPK displays a certain tissues/subcellular expression pattern, protein abundance, calcium stimulation, activity, and substrate specificity in response to internal or external stimuli (Damman et al., 2003; Lu and Hrabak, 2002; Li et al., 1998; Yoo and Harmon, 1996; Ito et al., 2010). Thus each or a subset of kinase is most likely involved in regulating distinct signaling pathways as evident from the roles of various CPKs in diverse biological processes.

The role of CPKs in regulating an array of biological events involves its downstream target(s) and subsequently the cascading pathway(s). Targets of CPKs include transcription factors, metabolic enzymes, cytoskeletal proteins, ion transport/channels, and others. Some of the known targets and CPK pairs are: Repression of Shoot Growth (RSG) which is phosphorylated by NtCDPK1 at Ser_{114} in feedback regulation of giberrelin (GA) (Ishida et al., 2008); ABF4 which is phosphorylated by AtCPK32 at Ser_{110} (Choi et al., 2005), Dehydration-induced 19 (AtDi19) which is phosphorylated by AtCPK11 at Thr_{105} and Ser_{107} (Milla et al., 2006); CDPK Substrate Protein 1 (CSP1) which belongs to the two-component pseudo-response regulator class of transcription factors is phosphorylated by CDPK1 from *Mesembryanthemum crystallinum* (Patharkar and Cushman, 2000); regulatory subunit of 26S proteasome, NtRpn3, which is also phosphorylated by NtCDPK1 (Lee et al., 2003); *Spinacea oleracea* CDPK (and its orthologue AtCDPK6/ AtCPK3) phosphorylates nitrase

reductase at Ser_{543} and sucrose-phosphate synthase (Bachmann et al., 1995; Bachmann et al., 1996; Douglas et al., 1998; McMichael Jr. et al., 1993); Ca^{2+}-ATPases, ACA2, is phosphorylated by AtCPK1 at Ser_{45} within its N-terminal calmodulin-binding domain (Hwang et al., 2000); K^+ channel KAT1 is phosphorylated by *Vicia faba* CDPK in the guard cell (Li et al., 1998). More CPK targets are listed in Cheng et al., 2002 and Klimecka and Muszynska, 2007.

Here we report a potential substrate for CPK16, REN1 which is a negative regulatory protein of ROP1. CPK16 phosphorylates REN1 *in vitro* in a calcium-dependent manner suggesting a potential regulation of REN1 activity via phosphorylation. MS/MS analysis of REN1 phosphopeptides revealed phosphorylated residues that are calcium dependent as well as calcium independent. This study will provide new direction into investigating the involvement of CDPK in regulating a key signaling pathway in pollen tube.

MATERIALS AND METHODS

Molecular cloning

CPK16 cDNA was amplified from *Ler* wild-type flower tissues using gene-specific primers containing attB sequence for Gateway cloning. CPK32 cDNA was amplified from *Col-0* wild-type plants using gene-specific primers also containing attB sequence for Gateway cloning. REN1 cDNA was also amplified similar as above from *Col-0* wild-type flowers. Entry clones were subcloned into destination vectors for protein

expression containing His-tag (pDEST17) (Invitrogen Corporation, Carlsbad, CA). MBP-tagged proteins were obtained by subcloning the constructs into pMAL-c2x vector.

Protein overexpression and purification

All recombinant protein was expressed in E. coli BL21 cells. CPK16/CPK32 fused to 6xHIS and REN1 fused to MBP were expressed at 30^{o}C for 4-6 h after induction with 1 mM isopropyl-b-D-thiogalactopyranoside (Wu et al., 2000). Cells were pelleted by centrifugation at 5000 rpm for 10 min and resuspended in HIS-lysis buffer (50 mM HEPES, 10 mM imidazole, pH 7.4) or MBP-binding buffer(50 mM HEPES, 1 mM EDTA, pH 7.4). Following sonication, cell lysate was collected after centrifugation at 10,000 rpm for 15 min and incubated with cobalt resins (Clontech Laboratories Inc., Mountainview, CA) for HIS-fusion protein or amylose resin (New England Biolabs, Ipswich, MA) for MBP-fusion protein using batch affinity purification method. After 1-2 h of incubation, beads were washed with HIS-wash buffer (50 mM HEPES, 250 mM NaCl, and 30 mM imidazole, pH 7.4) or MBP-binding buffer. Proteins were eluted with His- elution buffer (50 mM HEPES, 300 mM imidazole, pH 7.4) or MBP-elution buffer (50 mM HEPES, 10 mM maltose, pH 7.4).

In vitro kinase assays

Kinase assay reaction mixture was performed as described in Lee et al. (1998) with some modification as followed: 50 mM HEPES, pH 7.2, 10 mM $MgCl_2$, 1 mM EGTA, 2 mM $CaCl_2$, 66.7 µM [γ-^{32}P]ATP, approximately 0.5 – 1 µg of kinase enzyme, and 1 – 2 µg of REN1 substrate (with the exception of the use around 2 – 5 µg of REN1 substrate for MS/MS analysis). Kinase reaction mixture was incubated at room

temperature for 1 hour. Following incubation, SDS loading buffer was added to the reaction mixture and 15 µL of reaction mixture was loaded to the 10% SDS-PAGE gel. The gel was then used to exposed phosphorimager screen for 45 min to 2 hr, after which the screen was scanned using Typhoon 9410 scanner (GE Healthcare, Piscataway, NJ).

Mass spectrometry analysis

Proteins were precipitated from kinase reaction solution using cold acetone treatment (final concentration of 80%) and overnight precipitation at -20^{o}C. Protein pellet was digested with trypsin prior to running on 2D-LC/MS/MS. For in-gel digestion, kinase assay mixture was run on SDS-PAGE until the protein dye reached approximately 1 cm passed the resolving gel. Protein gel containing the protein bands was cut right above the dye front and right below the stacking gel. Proteins were digested in gel, after which the phosphopeptides generated were run on 2D-LC/MS/MS.

Image analysis

Quantification of band intensity and area from SDS-PAGE gel or phosphoscreen was performed using ImageJ software (Abramoff et al., 2004; Rasband, 1997) particularly for gel analysis.

RESULTS

REN1 contains putative phosphorylation motifs

Plant Protein Phosphorylation Database (P^{3}DB) and the Arabidopsis Protein Phosphorylation Site Database (PhosphPhAt 3.0) were searched for the presence of REN1 in their collections of experimentally-derived phosphorylated proteins. The search

produced zero hit suggesting that REN1 phosphopeptides have not been identified in other studies to date. To identify putative phosphorylation sites within REN1, two predictors were utilized. NetPhosK 1.0 (http://www.cbs.dtu.dk/services/NetPhosK/) predicts kinase-specific phosphorylation sites while NetPhos 2.0 (http://www.cbs.dtu.dk/services/NetPhos/) predicts general phosphorylation sites within serine, threonine, and tyrosine in eukaryotic proteins (Blom et al., 1999). NetPhosK 1.0 predicted 52 sites to be phosphorylated by different kinases. These kinases include: protein kinase A (PKA), C (PKC), G (PKG), casein kinase II (CKII), cyclin-dependent kinase 2 (CDCII), ataxia telangiectasia mutated (ATM), DNA-dependent protein kinase (DNAPK), cyclin-dependent kinase 5 (cdk5), p38 mitogen-activated protein kinase (p38MAPK), glycogen synthase kinase 3 (GSKIII), casein kinase I (CKI), and ribosomal S6 kinase (RSK). NetPhos 2.0 predicted 95 phosphorylated sites at Ser residues and 15 at Thr residues. These potential phosphorylation sites were mapped on REN1 protein which seems to generally indicate more phosphorylations toward the C-terminal region (Figure 1.1A, B). Although both tools predicted many potential phosphorylation sites based on the current knowledge of eukaryotic kinomes, some of the eukaryotic kinases listed above are not yet identified in *Arabidopsis*, and thus, the predicted phosphorylation sites may not be relevant. In addition, these predictors did not predict potential phosphorylation sites by plant-specific CPKs since they are lacking in other eukaryotic genomes.

CPK16 is one of pollen-specific CDPKs/CPKs

The search of gene expression browser Bio-Array Resource (BAR) (Toufighi et al., 2005) resulted in the identification of 5 CPKs (out of 26) which displayed pollen-specific expression, in order of the highest to the lowest expression are CPK24, CPK14, CPK17, CPK16, and CDPK34 (Figure 1.2A). CPK17 and CPK34 are homologous and their roles in pollen tube growth have been presented in Myers et al., 2009. CPK14 and CPK32 are homologous and its overexpression in pollen tubes has resulted in tip swelling phenotype (Zhou et al., 2009). The functions of both CPK24 and CPK16 are currently unknown and since both are expressed specifically in mature pollen, they are likely to play some roles in regulating pollen tube growth. CPK24 belongs to group III of CPKs which consists of 8 members that includes CPK14 and CPK32 (Cheng et al., 2002). It is likely that CPK24 may function redundantly with other CPKs in this group. In contrast, CPK16 belongs to the smallest group IV along with its homologs, CPK18 and CPK28 (Cheng et al., 2002), making it an interesting kinase to focus on. In addition, CPK16 expression correlates highly with REN1 and is linked directly to REN1 in the coexpressed gene network generated by ATTEDII gene expression database (http://atted.jp) which is an indicator that the two proteins may be involved in the same pathway (Figure 1.2B).

CPK16 phosphorylates REN1 in the presence of calcium in *in vitro* condition

Since REN1 is predicted to be phosphorylated based on known kinases in the database, we are interested in determining whether CPK16 can phosphorylate REN1 *in vitro*. *In vitro* kinase assays were performed using E. coli-purified recombinant proteins

and radiolabelled ATP. Coommassie staining of the kinase reactions showed a shift in CPK16 protein band from high to lower molecular weight of about 3 kDa when calcium (Ca^{2+}) was present regardless of the presence of REN1 substrate (Figure 1.3A). This is consistent with previously reported change in protein mobility in SDS-PAGE when CDPK was treated with Ca^{2+} (Harmon et al., 1987; Li et al., 1998). This suggests that Ca^{2+} may induce conformational change in CPK16 protein that leads to its reduced size.

With regards to REN1 phosphorylation, in the absence of Ca^{2+} which was achieved by treatment with Ca^{2+} chelator, EGTA, CPK16 autophosphorylation and REN1 phosphorylation was not observed (Figure 1.3B). However, in the presence of 1.1 mM Ca^{2+}, CPK16 autophosphorylation and REN1 phosphorylation can be observed (Figure 1.3B). These data show that CPK16 can phosphorylate REN1 *in vitro* and that its activity requires Ca^{2+}. To further test whether other CPKs can phosphorylate REN1, *in vitro* kinase assays were also performed using CPK32. We found that CPK32 can autophosphorylate as well as phosphorylate REN1 substrate; however, its Ca^{2+}-dependency is quite unclear (Figure 1.3C). We found that in both Ca^{2+}-free or Ca^{2+}-containing assays, either CPK32 or REN1 phosphorylation can be detected (Figure 1.3C). Even in the presence of up to 10 mM EGTA, CPK32 autophosphorylation was still be observed (data not shown). We cannot rule out the possibility of REN1 as a substrate for CPK32; however we cannot establish in certainty the Ca^{2+}-dependency nature of CPK32 phosphorylation of REN1. Based on these analyses, we focused our attention to characterizing REN1 phosphorylation by CPK16.

CPK16 phosphorylation of REN1 requires submicromolar calcium level *in vitro*

To test the minimal amount of Ca^{2+} required for CPK16 phosphorylation of REN1, Ca^{2+} dose responses were performed with varying EGTA concentration: 10 µM (Figure 1.4A), 100 µM (Figure 1.4C, D), and 1 mM (Figure 1.4B). By manipulating the EGTA concentration and free Ca^{2+} level, the minimal amount of Ca^{2+} required for REN1 phosphorylation can be determined. The lowest EGTA level of 10 µM was insufficient in chelating free Ca^{2+} trace since background phosphorylation can be detected (Figure 1.4A). In contrast, 1 mM EGTA was more than sufficient in chelating free Ca^{2+} trace and at least 1.1 mM Ca^{2+} (relative free Ca^{2+} of 0.1 mM) led to REN1 phosphorylation (Figure 1.4B). In the presence of 100 µM EGTA, significant REN1 phosphorylation was still detectable and seemed an appropriate concentration to generate dose-dependent phosphorylation curve (Figure 1.4C). Detailed analysis of Ca^{2+}–dependent phosphorylation using smaller changes in the Ca^{2+} level showed that approximately 2.5 µM of free Ca^{2+} was sufficient to produce an increase in REN1 phosphorylation (for example: between 65 to 67.5 µM Ca^{2+}; Figure 1.4D – F). In addition, phosphorylation increased as Ca^{2+} concentration increases with maximal phosphorylation observed at ~75 µM Ca^{2+} (in the presence of 100 µM EGTA). To further determine the relative EC_{50}, nonlinear regression curve was plotted (Figure 2E, F). The relative free Ca^{2+} was determined by subtracting [Ca^{2+}] to the arbitrary 65 µM Ca^{2+} as the relative 0 µM Ca^{2+}, whose value was comparable to basal REN1 phosphorylation response. Using this method, the relative EC_{50} was determined to be ≈ 4.6 µM. This relative EC_{50} seems to be between 4- to 70-fold higher than previously reported EC_{50} for different CDPKs (Lee et

al., 1998; Yoon et al., 2006). However, those values were obtained using general substrate syntide-2 and may not reflect the true EC_{50} value for their specific substrates. In addition, many CPKs respond to distinct Ca^{2+} level and as such, CPK16 may require higher Ca^{2+} concentration compared to others. Nevertheless, our relative EC_{50} value seems to be physiologically relevant since tip-focused cytosolic Ca^{2+} concentration at the apex of pollen tubes range from ≈ 1 to >5 μM (Pierson et al., 1994; Pierson et al., 1996; Holdaway-Clarke et al., 1997; Camacho et al., 2000).

MS/MS analysis reveals REN1 phosphorylation sites by CPK16 and CDPK32

To identify REN1 phosphorylation sites by CPKs, 2D-LC MS/MS analysis was performed on *in vitro* kinase reaction samples, as mentioned previously, using either CPK16 or CPK32, in the presence or absence of Ca^{2+} (Figure 1.5B). Samples were prepared two ways: one was protein precipitation of *in vitro* kinase reaction followed by protease digestion, while another was quick separation of *in vitro* kinase assay in SDS-PAGE gel followed by protease digestion in gel (Figure 1.5). Trypsin which cleaves lysine or arginine, except when either was followed by proline, was used to generate REN1 phosphopeptides. MS/MS analysis revealed that phosphorylations were detected throughout REN1 protein; some are specific for certain assay condition while others are detected in all assay conditions (Table 1.1). Most phosphorylations seem to be localized to the C-terminal region where coiled coil regions important for REN1 localization to the exocytic vesicles can be found (Table 1.1) which seems to be consistent with the predicted phosphorylation sites using general predictors NetPhosK 1.0 or NetPhos 2.0. Within the catalytic GAP domain, one phosphopeptide was identified at Ser_{267} residue

(Figure 1.6) which would be interesting to characterize further since phosphorylation at the catalytic domain is known to affect protein activity (Minoshima et al., 2003). Meanwhile, within the PH domain, two calcium-dependent phosphorylation sites were also identified at Ser_{70} and Thr_{151} (Figure 1.7 and 1.8). REN1 phosphorylation within the PH domain may likely affect its subcellular localization due to the role of PH domain in interacting with PM-localized phospholipids (Harlan et al., 1994; Lemmon et al., 1995; Ma et al., 1997). Finally, the effect of REN1 phosphorylation on the coiled coil (CC) region is not known. The CC region is known to be involved in REN1 localization to the exocytic vesicles (Hwang et al., 2008) and thus phosphorylation at this region may possibly affect REN1 association with these vesicles.

DISCUSSION

Here we report the identification of a new CPK16 substrate, REN1. REN1 is a negative regulator of ROP1 which is important for tip growth in pollen tubes (Hwang et al., 2008). To date, a collection of CPKs substrates have been identified, however CPK substrates in pollen tube have not been reported thus far. Since CPKs function in regulating pollen tube growth and tip polarity have been demonstrated, it is likely that CPKs target a regulator of tip polarity in pollen tube. Thus REN1 may be the first example of a key regulator of pollen tube tip polarity protein to be phosphorylated by CPK16 in response to elevated Ca^{2+} level. The EC_{50} of REN1 phosphorylation is calculated to be ≈ 4.6 μM which is much higher than the reported EC_{50} for other CDPKs, e.g. 0.06 μM for soybean CDPKα, 0.4 μM for soybean CDPKβ, 1 μM for soybean

CDPKγ, and 0.6 μM for PiCDPK1 (Lee et al., 1998; Yoon et al., 2006). However, the EC_{50} for these CDPKs were obtained by using general substrate, syntide-2, and thus may not represent the true EC_{50} for a more specific substrate(s). In addition, different CPKs respond to calcium level differently which provides additional level of regulation in CPKs activity. The apical region of pollen tube has been reported to contain cytosolic free Ca^{2+} ranging from 0.6 μM (Malho et al., 1994), 1 – 2 μM (Camacho et al., 2000; Franklin-Tong et al., 1997), to ≥ 3 μM (Holdaway-Clarke et al., 1997; Pierson et al., 1996; Pierson et al., 1994). Thus EC_{50} of 4.6 μM for CPK16 seems to be physiologically relevant which suggests that REN1 phosphorylation by CPK16 occurs when the tip cytosolic Ca^{2+} level is relatively high. Interestingly, accumulation of tip-localized Ca^{2+} is promoted by ROP1 effector, RIC3 (Gu et al., 2005), and thus indicates a mechanism to inactivate ROP1 pathway once high tip-localized Ca^{2+} is detected by CPKs, such as CPK16.

Thus far, CPK phosphorylation motif predictors are few. Several motifs have been generated based on known CPK substrates and synthetic peptide studies (for review: Klimecka and Muszynska, 2007; Cheng et al., 2002). The simplest motifs were identified based on spinach nitrate reductase phosphorylation which was ϕ_{-5}-X_{-4}-$Basic_{-3}$-X_{-2}-X_{-1}-**S/T** (where ϕ represents hydrophobic residue and X any residues) (Bachmann et al., 1996) or based on potato carboxypeptidase inhibitor phosphorylation which was either **S**-X_{+1}-X_{+2}-$Basic_{+3}$ or **S**-X_{+1}-$Basic_{+2}$ (Neumann et al., 1996). Another study based on phosphorylation of spinach sucrose-phosphate synthase concluded a consensus sequence for CDPK substrate to be: $Basic_{-6}$-X_{-5}-X_{-4}-$Basic_{-3}$-X_{-2}-X_{-1}-**S/T** (McMichael Jr. et al.,

1995). Further refinement of the basic phosphorylation motif based on that of ACA2 and aquporin PM28A led to another motif containing Basic$_{-9}$-Basic$_{-8}$-X$_{-7}$-Basic$_{-6}$-ϕ$_{-5}$-X$_{-4}$-X$_{-3}$-X$_{-2}$-X$_{-1}$-**S/T**-X$_{+1}$-Basic$_{+2}$ (Huang et al., 2001). Finally, the motif required for maximal phosphorylation was reported to be: Basic$_{-6}$-ϕ$_{-5}$-X$_{-4}$-Basic$_{-3}$-X$_{-2}$-X$_{-1}$-**S/T**-X$_{+1}$-X$_{+2}$-X$_{+3}$-ϕ$_{-4}$-Basic$_{-5}$ (Huang and Huber, 2001). Interestingly, the phosphopeptides identified in our REN1 study only seem to contain the simple phosphorylation motif such as the presence of basic residue at P$_{-3}$. For example: Thr^{151} (GRAFTLKAD**T**MEDL displays X-Basic-X-ϕ-X-ϕ-Basic-ϕ-Acid-**T**-X-Acid-Acid-ϕ), Ser^{267} (EYEKGKNEF**S**PEED displays Acid-ϕ-Acid-Basic-X-Basic-X-Acid-ϕ-**S**-X-Acid-Acid-Acid), and Ser^{604} (GRTPGKKNL**S**MESI displays X-Basic-X-X-X-Basic-Basic-X-ϕ-**S**-X-Acid-X-ϕ). Meanwhile, some others seem to display another simple motif with the presence of a basic residue at P$_{+2}$ position: Ser^{70} (VFKSGPLSI**S**SKGI displays ϕ-ϕ-Basic-X-X-X-ϕ-X-ϕ-**S**-X-Basic-X-ϕ) and Ser^{819} (RGSSKLVGL**S**KRSG displays Basic-X-X-X-Basic-ϕ-ϕ-X-ϕ-**S**-Basic-Basic-X-X). The presence of simple CPK phosphorylation motifs in the REN1 phosphorylated residues identified in our studies suggests that these residues may be truly phosphorylated by CPK16, although their functional significance remains to be investigated.

REFERENCES

Abramoff, M. D., Magalhaes, P. J., and Ram, S. J. (2004) Image processing with ImageJ. Biophotonics Int. **11(7)**: 36 – 42

Asano, T., Tanaka, N., Yang, G., Hayashi. N., and Komatsu, S. (2005) Genome-wide identification of the rice calcium-dependent protein kinase and its closely related kinase gene families: comprehensive analysis of the CDPKs gene family in rice. Plant Cell Physiol. **46(2)**: 356 – 366

Bachmann, M., McMichael Jr., R. W., Huber, J. L., Kaiser, W. M., and Huber, S. C. (1995) Partial purification and characterization of a calcium-dependent protein kinase and an inhibitor protein required for inactivation of spinach leaf nitrate reductase. Plant Physiol. **108**: 1083 – 1091

Bachmann, M., Shiraishi, N., Campbell, W. H., Yoo, B-C., Harmon, A. C., and Huber, S. C. (1996) Identification of Ser-543 as the major regulatory phosphorylation site in spinach leaf nitrate reductase. Plant Cell **8**: 505 – 517

Blom, N. Gammeltoft, S., and Brunak, S. (1999) Sequence- and structure-based prediction of eukaryotic protein phosphorylation sites. J. Mol. Biol. **294(5)**: 1351 – 1362

Camacho, L., Parton, R., Trewavas, A. J., and Malho, R. (2000) Imaging cytosolic free-calcium distribution and oscillations in pollen tubes with confocal microscopy: a comparison of different dyes and loading methods. Protoplasma **212**: 162 – 173

Cheng, S-H., Willmann, M. R., Chen, H-C., and Sheen, J. (2002) Calcium signaling through protein kinases. The *Arabidopsis* calcium-dependent protein kinase gene family. Plant Physiol. **129**: 469 – 485

Choi, H-I, Park, H-J., Park, J. H., Kim, S., Im, M-Y., Seo, H-H., Kim, Y-W., Hwang, I., and Kim, S. Y. (2005) Arabidopsis calcium-dependent protein kinase AtCPK32 interacts with ABF4, a transcriptional regulator of abscisic acid-responsive gene expression, and modulates its activity. Plant Physiol. **139**: 1750 – 1761

Dammann, C., Ichida, A., Hong, B., Romanowsky, S. M., Hrabak, E. M., Harmon, A. C., Pickard, B. G., and Harper, J. F (2003) Subcellular targeting of nine calcium-dependent protein kinase isoforms from Arabidopsis. Plant Physiol. **132**: 1840 – 1848.

Dodd, A. N., Kudla, J., and Sanders, D. (2010) The language of calcium signaling. Annu. Rev. Plant Biol. **61**: 593 – 620

Douglas, P., Moorhead, G., Hong, Y., Morrice, N., and MacKintosh, C. (1998) Purification of a nitrate reductase kinase from *Spinacea oleracea* leaves, and its identification as a calmodulin-domain protein kinase. Planta **206**: 435 – 442

Franklin-Tong, V. E., Hackett, G., and Hepler, P. K. (1997) Ratio-imaging of Ca^{2+}_i in the self-incompatibility response in pollen tubes of *Papaver rhoeas*. Plant J. **12(6)**: 1375 – 1386

Gu, Y., Fu, Y., Dowd, P., Li, S., Vernoud, V., Gilroy, S., and Yang, Z. (2005) A Rho family GTPase controls actin dynamics and tip growth via two counteracting downstream pathways in pollen tubes. J. Cell Biol. **169**: 127-138

Harlan, J. E., Hadjuk, P. J., Yoon, H. S., and Fesik, S. W. (1994) Pleckstrin homology domains bind to phasphatidylinositol-4,5-biphosphate. Nature **371**: 168 – 170

Harmon, A.C., Putnam-Evans, C., and Cormier, M.J. (1987) A calcium-dependent but calmodulin-independent protein kinase from soybean. Plant Physiol. **83**: 830-837

Harper, J.F., Breton, G., and Harmon, A. (2004) Decoding Ca^{2+} signals through plant protein kinases. Annu. Rev. Plant Biol. **55**: 263-288

Holdaway-Clarke, T.L., Feijo, J.A., Hackett, G.R., Kunkel, J.G., and Hepler, P.K. (1997) Pollen tube growth and the intracellular cytosolic calcium gradient oscillate in phase while extracellular calcium influx is delayed. Plant Cell **9**: 1999-2010

Hrabak, E. M., Chan, C. W. M., Gribskov, M., Harper, J. F., Choi, J. H., Halford, N., Kudla, J., Luan, S., Nimmo, H. G., Sussman, M. R., Thomas, M., Walker-Simmons, K., Zhu, J-K., and Harmon, A. C. (2003) The Arabidopsis CDPK-SnRK superfamily of protein kinases. Plant Physiol. **132**: 666 – 680

Huang, J-Z., Hardin, S., C., and Huber, S. C. (2001) Identification of a novel phosphorylation motif for CDPKs: phosphorylation of synthetic peptides lacking basic residues at P-3/P-4. Arch. Biochem. Biophys. **393(1)**: 61 – 66

Huang, J-Z. and Huber, S. C. (2001) Phosphorylation of synthetic peptides by a CDPK and Plant SNF1-related protein kinase. Influence of proline and basic amino acid residues at selected positions. Plant Cell Physiol. **42(10)**: 1079 – 1087

Hwang, I., Sze, H., and Harper, J. F. (2000) A calcium-dependent protein kinase can inhibit a calmodulin-stimulated Ca^{2+} pump (ACA2) located in the endoplasmic reticulum of Arabidopsis. Proc. Nat. Acad. Sci. **97(11)**: 6224 – 6229

Hwang, J.U., Vernoud, V., Szumlanski, A., Nielsen, E., and Yang, Z. (2008) A tip-localized RhoGAP controls cell polarity by globally inhibiting Rho GTPase at the cell apex. Curr. Biol. **18**: 1907-1916

Ishida, S., Yuasa, T., Nakata, M., and Takahashi, Y. (2008) A tobacco calcium-dependent protein kinase, CDPK1, regulates the transcription factor Repression of Shoot Growth in response to gibberellins. Plant Cell **20**: 3273 – 3288

Ito, T., Nakata, M., Fukazawa, J., Ishida, S., and Takahashi, Y. (2010) Alteration of substrate specificity: the variable N-terminal domain of tobacco Ca^{2+}-dependent protein kinase is important for substrate recognition. Plant Cell **22**: 1592 – 1604

Klimecka, M. and Muszynska, G. (2007) Structure and functions of plant calcium-dependent protein kinases. Acta Biochim. Polonica **54(2)**: 219 – 233

Kudla, J., Batistic, O., and Hashimoto, K. (2010) Calcium signals: the lead currency of plant information processing. Plant Cell **22**: 541 – 563

Lee, J-Y., Yoo, B-C., and Harmon, A. C. (1998) Kinetic and calcium-binding properties of three calcium-dependent protein kinase isoenzymes from soybean. Biochemistry **37**: 6801 – 6809

Lee, S. S., Cho, H. S., Yoon, G. M., Ahn, J-W., Kim, H-H., and Pai, H-S. (2003) Interaction of NtCDPK1 calcium-dependent protein kinase with NtRpn3 regulatory subunit of the 26S proteasome in *Nicotiana tabacum*. Plant J. **33**: 825 – 840

Lemmon, M. A., Ferguson, K. M., O'Brien, R., Sigler, P. B., and Schlessinger, J. (1995) Specific and high-affinity binding of inositol phosphates to an isolated pleckstrin homology domain. Proc. Natl. Acad. Sci. **92**: 10472 – 10476

Li, J., Lee, Y-R. J., and Assmann, S. M. (1998) Guard cells possess a calcium-dependent protein kinase that phosphorylates the KAT1 potassium channel. Plant Physiol. **116:** 785 – 795

Li, A-L., Zhu, Y-F., Tan, X-M., Wang, X., Wei, B., Guo, H-Z., Zhang, Z-L., Chen, X-B., Zhao, G-Y., Kong, X-Y., Jia, J-Z., and Mao, L. (2008) Evolutionary and functional study of the CDPK gene family in wheat (*Triticum aestivum L.*). Plant Mol. Biol. **66**: 429 – 443

Lu, S. X. and Hrabak, E. M. (2002) An Arabidopsis calcium-dependent protein kinase is associated with the endoplasmic reticulum. Plant Physiol. **128**: 1008 – 1021

Ma, A. D., Brass, L. F., and Abrams, C. S. (1997) Pleckstrin associates with plasma membranes and induces the formation of membrane projections: requirements for phosphorylation and the NH_2-terminal PH domain. J. Cell Biol. **136(5)**: 1071– 1079

Malho, R., Read, N. D., Pais, M. S., and Trewavas, A. J. (1994) Role of cytosolic free calcium in the reorientation of pollen tube growth. Plant J. **5(3)**: 331 – 341

McMichael Jr., R. W., Klein, R. R., Salvucci, M. E., and Huber, S. C. (1993) Identification of the major regulatory phosphorylation site in sucrose-phosphate synthase. Arch Biochem Biophys **307(2)**: 248 – 252

McMichael Jr., R. W., Kochansky, J., Klein, R. R., and Huber, S. C. (1995) Characterization of the substrate specificity of sucrose-phosphate synthase protein kinase. Arch. Biochem. Biophys. **321(1)**: 71 – 75

Mila, M. A. R., Uno, Y., Chang, I-F., Townsend, J., Maher, E. A., Quilici, D., and Cushman, J. C. (2006) A novel yeast two-hybrid approach to identify CDPK substrates: characterization of the interaction between AtCPK11 and AtDi19, a nuclear zinc finger protein. FEBS Lett. **580**: 904 – 911

Minoshima, Y., Kawashima, T., Hirose, K., Tonozuka, Y., Kawajiri, A., Bao, Y. C., Deng, X., Tatsuka, M., Narumiya, S., May Jr., W. S., Nosaka, T., Semba, K., Inoue, T., Satoh, T., Inagaki, M., and Kitamura, T. (2003) Phosphorylation by Aurora B converts MgcRacGAP to a RhoGAP during cytokinesis. Dev. Cell **4**: 549 – 560

Myers, C., Romanowsky, S. M., Barron, Y. D., Garg, S., Azuse, C. L., Curran, A., Davis, R. M., Hatton, J., Harmon, A. C., and Harper, J. F. (2009) Calcium-dependent protein kinases regulate polarized tip growth in pollen tubes. Plant J. **59(4)**: 528 – 539

Neumann, G. M., Thomas, I., and Polya, G. M. (1996) Identification of the site on potato carboxypeptidase inhibitor that is phosphorylated by plant calcium-dependent protein kinase. Plant Sci. **114**: 45 – 51

Patharkar, O. R. and Cushman, J. C. (2000) A stress-induced calcium-dependent protein kinase from *Mesembranthemum crystallinum* phosphorylates a two-component pseudo-response regulator. Plant J. **24(5)**: 679 – 691

Pierson, E.S., Miller, D.D., Callaham, D.A., Shipley, A.M., Rivers, B.A., Cresti, M., and Hepler, P.K. (1994) Pollen tube growth is coupled to the extracellular calcium ion flux and the intracellular calcium gradient: effect of BAPTA-type buffers and hypertonic media. Plant Cell **6**: 1815-1828

Pierson, E.S., Miller, D.D., Callaham, D.A., van Aken, J., Hackett, G., and Hepler, P.K. (1996) Tip-localized calcium entry fluctuates during pollen tube growth. Dev. Biol. **174**: 160-173

Rasband, W. S. ImageJ, US National Institute of Health, Bethesda, Maryland, USA. http://imagej.nih.gov/ij/ 1997 – 2011

Ray, S., Agarwal, P., Arora, R., Kapoor, S., and Tyagi, A. K. (2007) Expression analysis of calcium-dependent protein kinase gene family during reproductive development and abiotic stress conditions in rice (*Oryza sativa* L. ssp. *indica*). Mol. Genet. Genomics **278**: 493 – 505

Schulze, W. X. (2010) Proteomics approaches to understand protein phosphorylation in pathway modulation. Curr. Op. Plant Biol. **13**: 280 – 287

Toufighi, K., Brady, S. M., Austin, R., Ly, E., and Provart, N. J. (2005) The Botany Array Resource: e-Northerns, Expression Angling, and promoter analysis. Plant J. **43**: 153 – 163.

Wu, G., Li, H., and Yang, Z. (2000) Arabidopsis RopGAPs are a novel family of rho GTPase-activating proteins that require the Cdc42/Rac-interactive binding motif for rop-specific GTPase stimulation. Plant Physiol. **124**: 1625-1636

Ye, S., Wang, L., Xie, W., Wan, B., Li, X., and Lin, Y. (2009) Expression profile of calcium-dependent protein kinase (CDPKs) genes during the whole lifespan and under phytohormone treatment conditions in rice (*Oryza sativa L. ssp. Indica*). Plant Mol. Biol. **70(3)**: 311 – 325

Yoo, B-C. and Harmon, A. C. (1996) Intramolecular binding contributes to the activation of CDPK, a protein kinase with a calmodulin-like domain. Biochemistry **35**: 12029 – 12037

Yoon, G. M., Dowd, P. E., Gilroy, S., and McCubbin, A. G. (2006) Calcium-dependent protein kinase isoforms in *Petunia* have distinct functions in pollen tube growth, including regulating polarity. Plant Cell **18**: 867 – 878

Zhou, L., Fu, Y., and Yang, Z. (2009) A genome-wide functional characterization of *Arabidopsis* regulatory calcium sensors in pollen tubes. J Integr. Plant Biol. **51(8)**: 751 – 761

Figure 1.1. REN1 phosphorylation prediction. A) Structure of REN1 protein. PH, Pleckstrin Homology domain; GAP, GTPase Activating Domain; and CC, coiled coil region. B) NetPhos 2.0 prediction of phosphorylation sites within REN1 according to the position within amino acid sequence.

Figure 1.1.

A

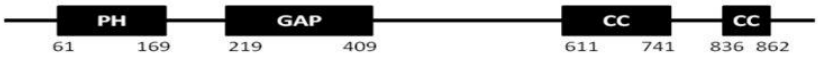
PH
GAP
CC
CC
61
169
219
409
611
741
836
862

B

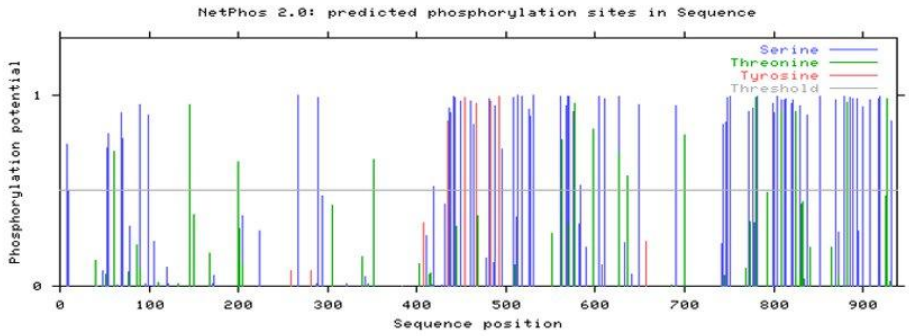
NetPhos 2.0: predicted phosphorylation sites in Sequence
Serine
Threonine
Tyrosine
Threshold
Phosphorylation potential
1
0
0
100
200
300
400
500
600
700
800
900
Sequence position

Figure 1.2. Gene expression analysis of pollen-expressed Arabidopsis calcium-dependent protein kinase. A) Gene expression obtained from the Bio-Array Resource (BAR) Expression Browser using the dataset of the AtGenExpress_Plus – Extended Tissue Series from flower and mature pollen tissue types. B) Gene network generated by Atted II gene expression database (http://atted.jp) linking CPK16 (At2g17890) to REN1 (At4g24580; RhoGAP).

Figure 1.2.

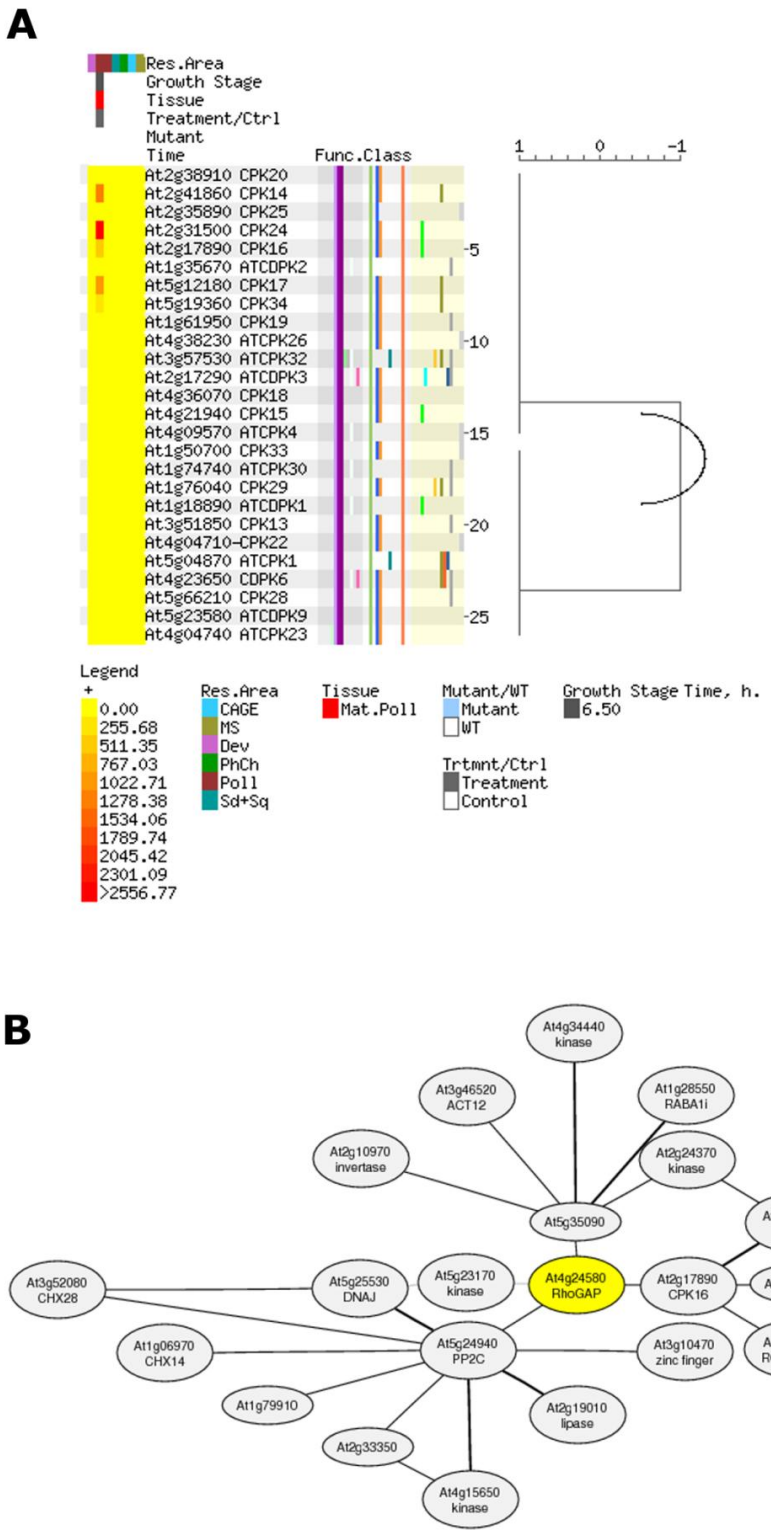
A
Res.Area
Growth Stage
Tissue
Treatment/Ctrl
Mutant
Time
Func.Class
1
0
-1
At2g38910 CPK20
At2g41860 CPK14
At2g35890 CPK25
At2g31500 CPK24
At2g17890 CPK16
At1g35670 ATCDPK2
At5g12180 CPK17
At5g19360 CPK34
At1g61950 CPK19
At4g38230 ATCPK26
At3g57530 ATCPK32
At2g17290 ATCDPK3
At4g36070 CPK18
At4g21940 CPK15
At4g09570 ATCPK4
At1g50700 CPK33
At1g74740 ATCPK30
At1g76040 CPK29
At1g18890 ATCDPK1
At3g51850 CPK13
At4g04710-CPK22
At5g04870 ATCPK1
At4g23650 CDPK6
At5g66210 CPK28
At5g23580 ATCDPK9
At4g04740 ATCPK23
-5
-10
-15
-20
-25
Legend
+
0.00
255.68
511.35
767.03
1022.71
1278.38
1534.06
1789.74
2045.42
2301.09
>2556.77
Res.Area
CAGE
MS
Dev
PhCh
Poll
Sd+Sq
Tissue
Mat.Poll
Mutant/WT
Mutant
WT
Trtmnt/Ctrl
Treatment
Control
Growth Stage Time, h.
6.50
B
At4g34440 kinase
At3g46520 ACT12
At1g28550 RABA1i
At2g10970 invertase
At2g24370 kinase
At5g35090
At2g25600 SPIK
At3g52080 CHX28
At5g25530 DNAJ
At5g23170 kinase
At4g24580 RhoGAP
At2g17890 CPK16
At5g46770
At1g06970 CHX14
At5g24940 PP2C
At3g10470 zinc finger
At1g79860 ROPGEF12
At1g79910
At2g19010 lipase
At2g33350
At4g15650 kinase

Figure 1.3. In vitro phosphorylation assay of REN1 by CPK16 or CPK32. A) Coomassie staining of phosphorylation assays. Calcium induces molecular shift of CPK16 protein band from higher MW to lower MW band (lane 3 and 6). B) CPK16 is autophosphorylated and can phosphorylate REN1 substrate only in the presence of calcium. C) CPK32 constitutively autophosphorylates itself and slight enhancement of REN1 phosphorylation can be detected in the presence of calcium.

Figure 1.3.

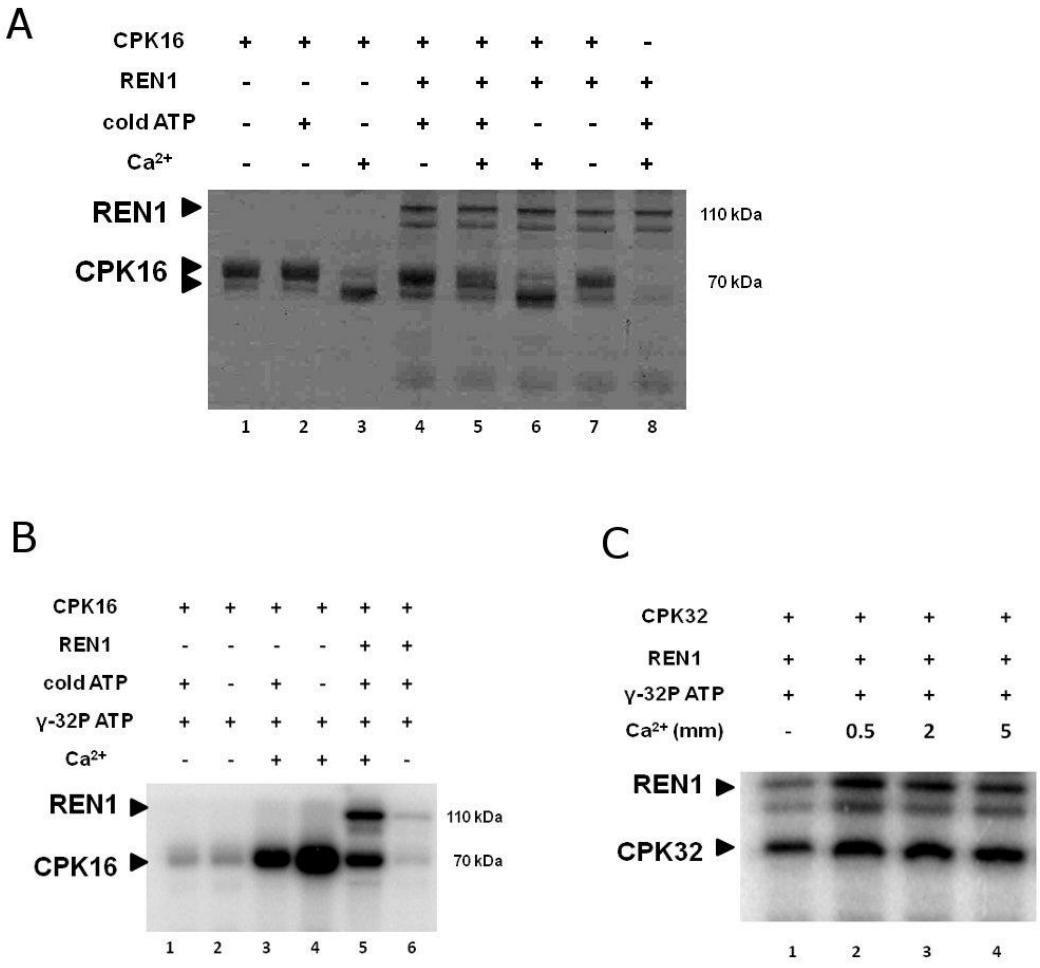
A
CPK16 + + + + + + + -
REN1 - - - + + + + +
cold ATP - + - + + - - +
Ca2+ - - + - + + - +
REN1
CPK16
110 kDa
70 kDa
1 2 3 4 5 6 7 8
B
CPK16 + + + + + +
REN1 - - - - + +
cold ATP + - + - + +
γ-32P ATP + + + + + +
Ca2+ - - + + + -
REN1
CPK16
110 kDa
70 kDa
1 2 3 4 5 6
C
CPK32 + + + +
REN1 + + + +
γ-32P ATP + + + +
Ca2+ (mm) - 0.5 2 5
REN1
CPK32
1 2 3 4

Figure 1.4. Dose-dependent calcium response of REN1 phosphorylation by CPK16. A) *In vitro* kinase assays contained 10 µM calcium chelator, EGTA. Calcium-dependent phosphorylation was not detected at this condition. B) The same kinase assays containing 1 mM EGTA. Calcium-dependent phosphorylation was detected and at least 0.1 mM free calcium was sufficient for REN1 phosphorylation. C and D) 100 µM calcium chelator, EGTA, was present in the assay. Calcium-dependent phosphorylation was detected and at least 2.5 µM calcium was sufficient for REN1 phosphorylation. E) Dose-dependent phosphorylation curve of REN1 by CPK16 showing basal phosphorylation at ~65 µM and maximal phosphorylation at ~75 µM. F) Relative curve generated from figure E where basal phosphorylation at 65 µM was used as a relative 0 free calcium concentration. From this curve, EC_{50} can be determined to be ~4.6 µM.

Figure 1.4.

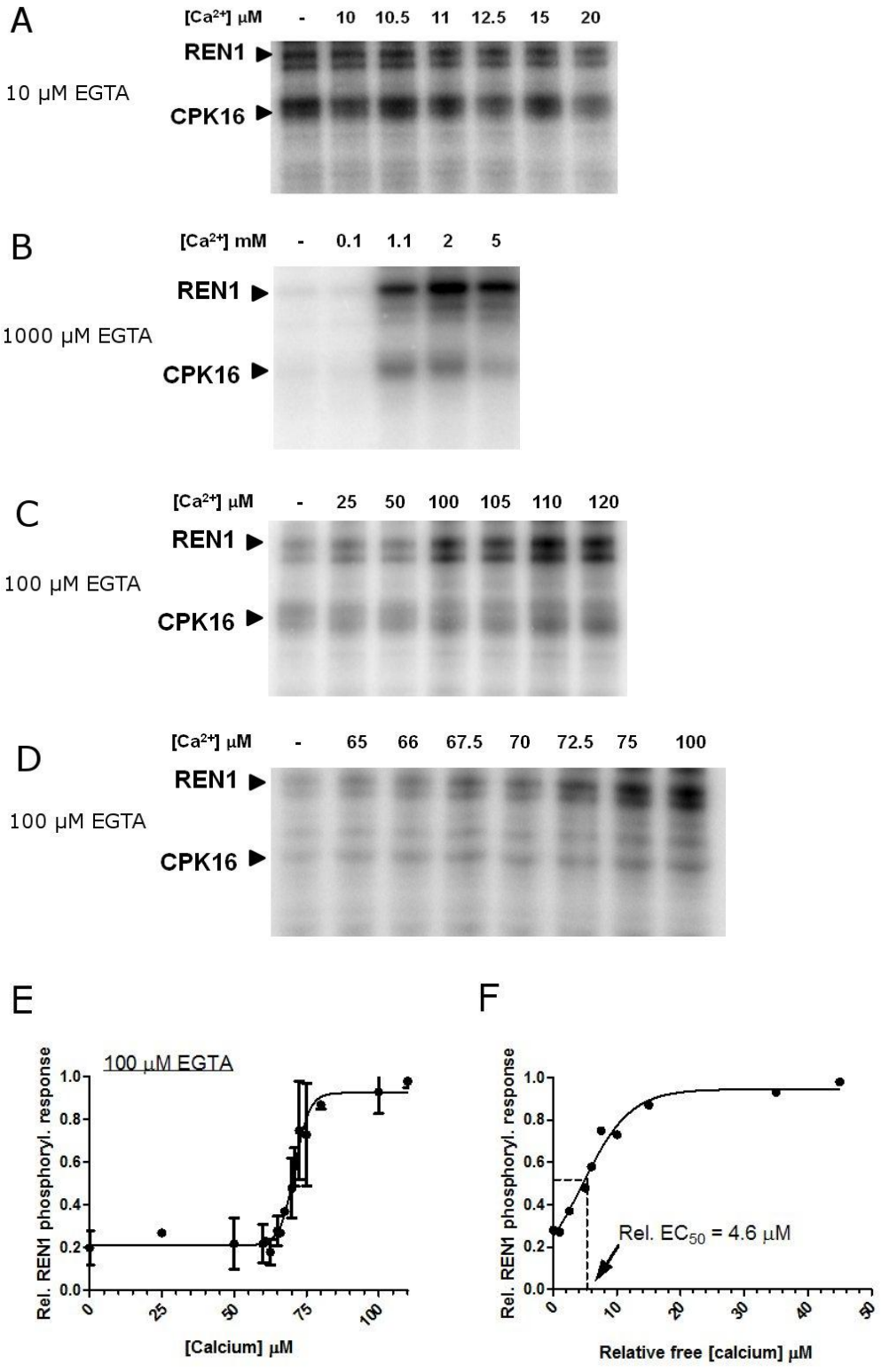
A
[Ca2+] µM - 10 10.5 11 12.5 15 20
REN1
10 µM EGTA
CPK16
B
[Ca2+] mM - 0.1 1.1 2 5
REN1
1000 µM EGTA
CPK16
C
[Ca2+] µM - 25 50 100 105 110 120
REN1
100 µM EGTA
CPK16
D
[Ca2+] µM - 65 66 67.5 70 72.5 75 100
REN1
100 µM EGTA
CPK16
E
100 µM EGTA
Rel. REN1 phosphoryl. response
[Calcium] µM
F
Rel. REN1 phosphoryl. response
Rel. EC50 = 4.6 µM
Relative free [calcium] µM

Figure 1.5. Outline of sample preparation for 2D-LC/MS/MS analysis. A) Phosphopeptide samples were generated two different ways. Following *in vitro* kinase reactions, proteins were either precipitated using acetone (final concentration of 80%) or separated with SDS-PAGE gel. Precipitated proteins were directly digested with trypsin while SDS-PAGE separated proteins were digested in-gel with trypsin. Following MS/MS run, quantitative analyses were performed by comparing the spectral intensities between different treatments. B) An example of four different treatments for MS/MS analysis. *In vitro* kinase assays were loaded onto 10% SDS-PAGE gel and run for short time (~ 30 min). The portion of gel cut for trypsin digestion is indicated.

Figure 1.5.

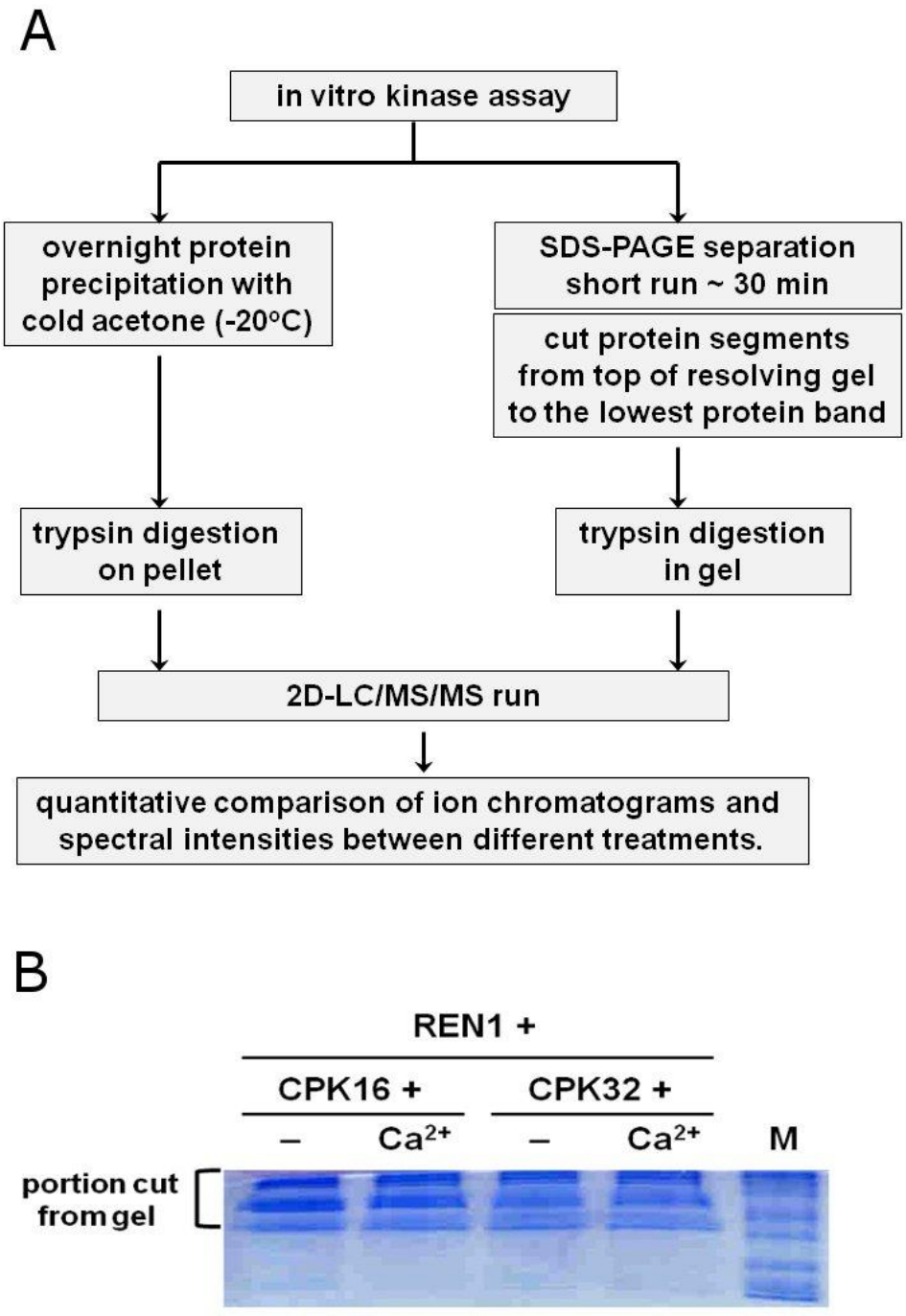
A
in vitro kinase assay
overnight protein precipitation with cold acetone (-20°C)
SDS-PAGE separation short run ~ 30 min
cut protein segments from top of resolving gel to the lowest protein band
trypsin digestion on pellet
trypsin digestion in gel
2D-LC/MS/MS run
quantitative comparison of ion chromatograms and spectral intensities between different treatments.
B
REN1 +
CPK16 +
CPK32 +
–
Ca2+
–
Ca2+
M
portion cut from gel

Figure 1.6. MS/MS spectra of Ca^{2+}-dependent REN1 phosphorylated residue, Ser_{267}. Inset indicates the spectra of Ca^{2+}-containing samples compared to Ca^{2+}-free samples.

Figure 1.6.

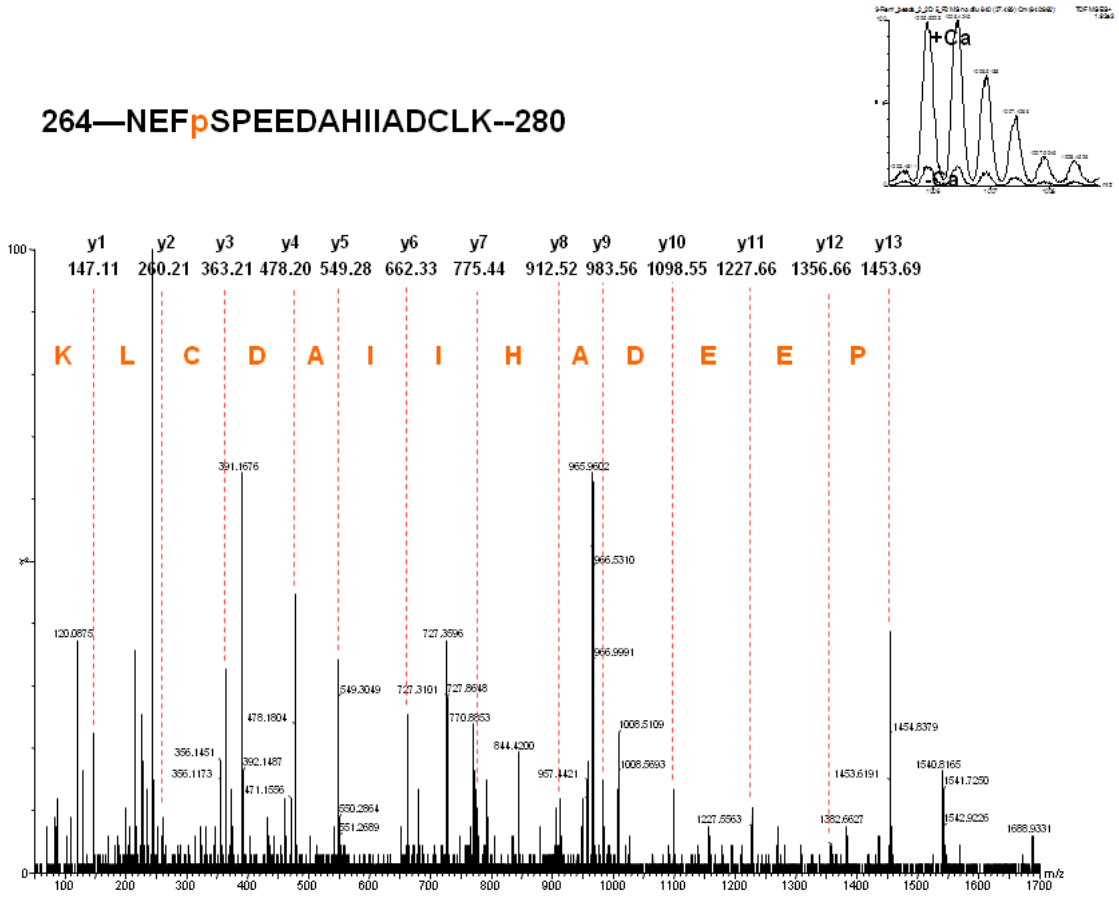
264—NEFpSPEEDAHIIADCLK--280
+Ca
-Ca
y1 y2 y3 y4 y5 y6 y7 y8 y9 y10 y11 y12 y13
147.11 260.21 363.21 478.20 549.28 662.33 775.44 912.52 983.56 1098.55 1227.66 1356.66 1453.69
K L C D A I I H A D E E P
391.1676
965.9602
966.5310
120.0875
727.3696
966.9991
549.3049
727.3101
727.8648
770.8653
478.1804
1008.5109
844.4200
356.1451
356.1173
392.1487
957.4421
1008.5693
1454.8379
1453.6191
1540.8165
1541.7250
471.1556
1227.5563
1382.6627
1542.9226
550.2864
551.2689
1688.9331
m/z

Figure 1.7. MS/MS spectra of Ca^{2+}-dependent REN1 phosphorylated residue, Ser_{70}. Inset indicates the spectra of Ca^{2+}-containing samples compared to Ca^{2+}-free samples.

Figure 1.7.

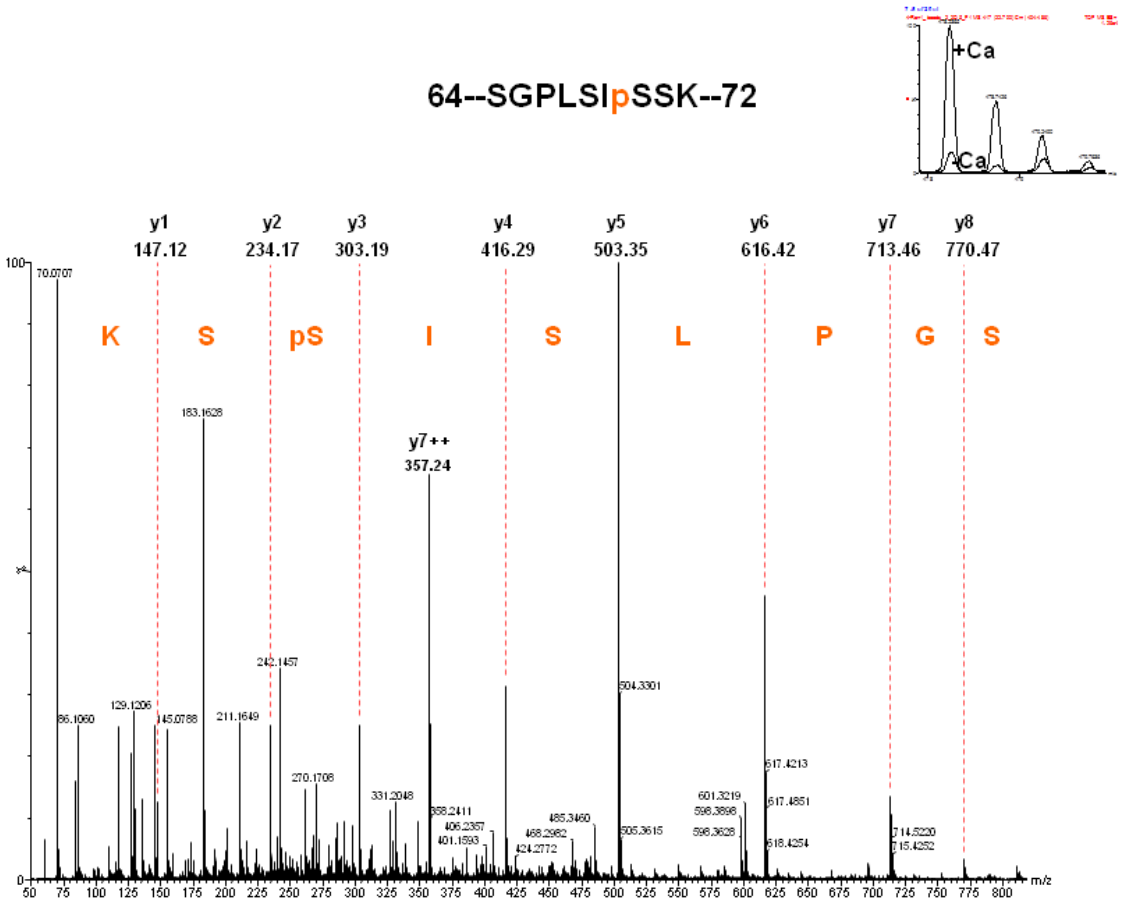
64--SGPLSIpSSK--72
+Ca
-Ca
y1
147.12
y2
234.17
y3
303.19
y4
416.29
y5
503.35
y6
616.42
y7
713.46
y8
770.47
K
S
pS
I
S
L
P
G
S
y7++
357.24
m/z

Figure 1.8. MS/MS spectra of Ca^{2+}-dependent REN1 phosphorylated residue, Thr_{151}. Inset indicates the spectra of Ca^{2+}-containing samples compared to Ca^{2+}-lacking samples.

Figure 1.8.

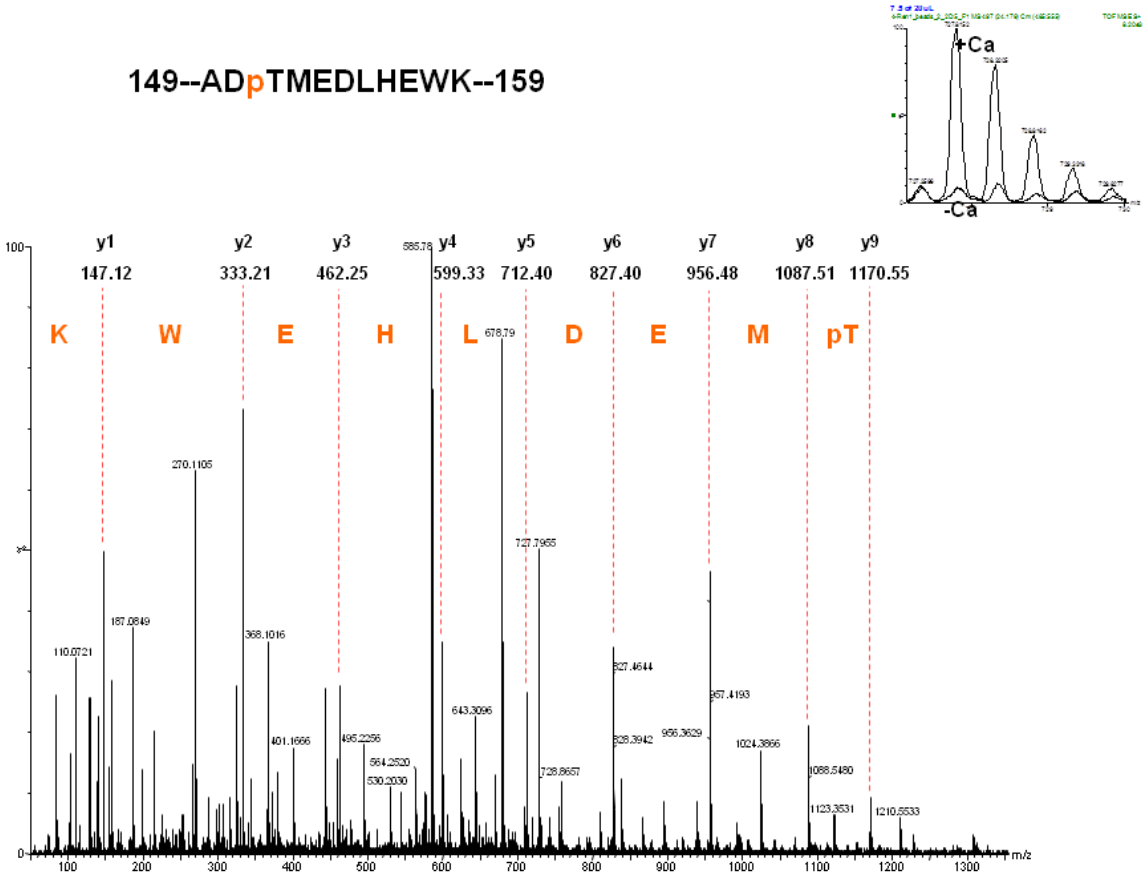
149--ADpTMEDLHEWK--159
+Ca
-Ca
y1
147.12
y2
333.21
y3
462.25
y4
599.33
y5
712.40
y6
827.40
y7
956.48
y8
1087.51
y9
1170.55
K
W
E
H
L
D
E
M
pT
678.79
270.1105
727.7955
187.0849
368.1016
110.0721
827.4644
957.4193
643.3096
401.1666
495.2256
564.2520
530.2030
828.3942
956.3629
1024.3866
728.8657
1088.5480
1123.3531
1210.5533
100
%
0
100
200
300
400
500
600
700
800
900
1000
1100
1200
1300
m/z

Table 1.1. REN1 phosphopeptides associated with CPK16 or CP3K32 generated by 2D-LC/MS/MS analysis. Phosphopeptides identified were assigned on whether they were present in the Ca^{2+}-free or Ca^{2+}–containing samples of either CPK16, CPK32, or both kinases. The position of phosphopeptides in relations to REN1 full length proteins was included. In addition, the numbers of phosphorylated residues in the phosphopeptides were also included.

Table 1.1.

Assay	Position	Peptides	#	Domain
CPK16 + Ca^{2+}	57 - 72	R.GGNTVFKSGPLSISSK.G	2	PH
	149 - 159	K.AD<u>T</u>MELDLHEWK.A	1	PH
	160 - 183	K.AALENALTQAPSASHVMGQNGIFR.N	1	PH
	204 - 227	K.STVLGRPYLLALEDVDGAPSFLEK.A	1	
	262 - 280	K.GKNEF<u>S</u>PEEDAHIIADCLK.Y	1	GAP
	492 - 502	K.YAD<u>S</u>IPDDHK.I	1	
	567 - 582	K.NSSTSDVASDTQKPSK.L	1	
	602 - 623	K.NLSMESIDFSVEVDEDNADIER.L	1	CC
	624 - 634	R.LESTKLELQSR.I	1	
	811 - 821	R.GSSKLVGLSKR.S	2	
	815 - 821	K.LVGL<u>S</u>KR.S	1	
	878 - 896	R.VSEETEKGSGSNQDPDSSK.L	1	
CPK16 – Ca^{2+}	66 - 72	G.PLSISSK.G	1	PH
	144 - 159	R.AFTLKADTMEDLHEWK.A	1	PH
	210 - 227	R.PVLLALEDVDGAP<u>S</u>FLEK.A	1	GAP
	556 - 582	K.AVVEVSTSEDKNSSTSDVASDTQKPSK.L	2	
CDPK32 + Ca^{2+}	262 - 280	K.GKNEF<u>S</u>PEEDAHIIADCLK.Y	1	GAP
	624 - 634	R.LESTKLELQSR.I	1	
All 4 assays	522 - 529	K.KLLSGSRR.S	1	
	529 - 534	R.RSSLPR.H	1	
	583 - 592	K.LSDAPGGSKR.H	1	
	765 - 778	K.QKDTEAASTHISER.S	1	

Chapter 2

Functional analysis of REN1 phosphorylation by CPK16

ABSTRACT

The regulation of protein activity through phosphorylation is common in proteins that are involved in signaling pathway. Previous 2D-LC/MS/MS analysis revealed that, in response to Ca^{2+}, CPK16 phosphorylated REN1 at several residues spanning the pleckstrin homology (PH), GAP, and coiled coil domains. Functional analyses of these different residues show that phosphorylation affects either protein activity or subcellular localization. Phosphorylation of REN1 residue, Ser_{267}, within the GAP domain is required for REN1 activity. This is evident from the inability of nonphosphorylation mutant REN1 ($S_{267}A$) to suppress ROP1 OX-induced tip swelling phenotypes in tobacco pollen tubes which was resulted from enhanced ROP1 activity and expanded ROP1 apical domain. Unlike REN_{267} phosphorylation, phosphorylation of REN1 residues, Ser_{70} and Ser_{71}, within the PH domain affected the REN1 protein localization as evident from the presence of cytosolic fluorescence patches which indirectly resulted in reduced REN1 activity and enhanced ROP1 activity. However, phosphorylation of other residues Thr_{146} and Thr_{151} in the PH domain may not be significant for REN1 function since either phosphorylation mutants led to reduced REN1 activity. The evidence for functional significance of REN1 phosphorylation within the PH and GAP domain are presented in this study. To explain the REN1 multiple phosphorylation sites and its contrasting functions, a model incorporating what is currently known about PH and GAP domain is presented.

INTRODUCTION

Phosphorylation is a common mechanism in which components within signaling pathways are regulated. Calcium-dependent protein kinases (CDPKs/CPKs) are a class of kinases which are activated by calcium and subsequently transduce the calcium signal to its downstream targets in response to extracellular or intracellular stimuli (for review: Harper and Harmon, 2005; Harper et al., 2004). CPKs are involved in variety of signaling events including plant response to cold and salinity/drought (Saijo et al., 2000; Saijo et al., 2001; Sheen, 1996), plant defense response to biotic stress (Romeis et al., 2000; Romeis et al., 2001; Boudsocq et al., 2010), regulation of ABA-responsive gene expression (Choi et al., 2005; Zhu et al., 2007), exocytosis regulation in *Toxoplasma* (Lourido et al., 2010), and pollen tube tip growth (Yoon et al., 2006; Myers et al., 2009; Zhou et al., 2009). The involvement of CPKs in diverse cellular signaling events is attributable to its phosphorylating a variety of substrates which range from components of cytoskeletal proteins, transcription factors, to plasma membrane channels and pumps. Furthermore, phosphorylations of target substrates have been shown to result in increased/decreased substrates activity, enhanced protein-protein interaction, and a change in substrates localization. For example: *Vicia faba* CDPK phosphorylation of novel vacuolar chloride (VCL) led to its activation (Pei et al., 1996), soybean CDPK phosphorylation of barley slow-vacuolar ion channels inhibited its activity (Bethke and Jones, 1997), phosphorylation of beet root H^+-ATPase by CDPK from the same species reduced its activity (Lino et al., 1998), AtCPK1 phosphorylation of Ca^{2+}-ATPases, ACA2, within the N-terminal calmodulin-binding domain at Ser_{45} inhibited ACA2 basal

activity and calmodulin activation (Hwang et al., 2000), AtCPK32 phosphorylation of ABF4 at Ser_{110} residue was important for its ABA-dependent transcriptional activity as well as interaction with AtCPK32 (Choi et al., 2005), and NtCDPK1 phosphorylation of transcription factor Repression of Shoot Growth (RSG) promoted intracellular localization of RSG due to enhanced binding of phosphorylated RSG to 14-3-3 protein in response to giberrelin (GA) (Ishida et al., 2008).

Previous 2D-LC/MS/MS analysis revealed that calcium-dependent REN1 phosphorylation by CPK16 *in vitro* occurred at several residues including Ser^{267} (GAP domain), Ser^{70} (PH domain), and Thr^{151} (PH domain). To understand the impact of phosphorylation on REN1 function, phosphorylation mutations were generated and analyzed. Here we presented evidence of the functional significance of REN1 phosphorylation by CPK16.

MATERIALS AND METHODS

Molecular cloning

CPK16 cDNA was amplified from *Ler* wild-type flower tissues using gene-specific primers containing attB sequence for Gateway cloning. CPK32 cDNA was amplified from *Col-0* wild-type plants using gene-specific primers also containing attB sequence for Gateway cloning. REN1 cDNA was also amplified similar as above from *Col-0* wild-type flowers. Entry clones were subcloned into destination vectors for protein expression containing His-tag (pDEST17) or GST-tag (pDEST15) (Invitrogen

Corporation, Carlsbad, CA). MBP-tagged proteins were obtained by subcloning the constructs into pMAL-c2x vector.

Plant materials and growth condition

Arabidopsis plants were grown at 22^{o}C growth room under 16 h light and 8 h dark. Tobacco plants were grown at 28^{o}C growth room under natural light.

Particle bombardment-mediated transient expression in tobacco pollen tubes

Mature tobacco (*Nicotiana tabacum*) pollen grains were collected in tobacco germination media (Fu et al., 2001). Approximately 0.3 – 0.7 mg of plasmids were used to coat 0.5 mg gold (1.0 mm in diameter). Freshly collected pollen grains were bombarded by the plasmid-coated gold using a PDS-1000/He particle delivery system (Bio-Rad Laboratories, Hercules, CA) as described previously (Fu et al., 2001). Following bombardment, pollen tubes were allowed to germinate in room temperature.

Protein overexpression and purification

All recombinant protein was expressed in E. coli BL21 cells. CPK16 fused to 6xHIS and REN1 fused to MBP were expressed at 30^{o}C for 4-6 h after induction with 1 mM isopropyl-b-D-thiogalactopyranoside (Wu et al., 2000). Cells were pelleted by centrifugation at 5000 rpm for 10 min and resuspended in HIS-lysis buffer (50 mM HEPES, 10 mM imidazole, pH 7.4) or MBP-binding buffer(50 mM HEPES, 1 mM EDTA, pH 7.4). Following sonication, cell lysate was collected after centrifugation at 10,000 rpm for 15 min and incubated with cobalt resins (Clontech Laboratories Inc., Mountainview, CA) for HIS-fusion protein or amylose resin (New England Biolabs, Ipswich, MA) for MBP-fusion protein for batch affinity purification method. After 1-2 h

of incubation, beads were washed with HIS-wash buffer (50 mM HEPES, 250 mM NaCl, and 30 mM imidazole, pH 7.4) or MBP-binding buffer. Proteins were eluted with His-elution buffer (50 mM HEPES, 300 mM imidazole, pH 7.4) or MBP-elution buffer (50 mM HEPES, 10 mM maltose, pH 7.4).

In vitro kinase assay

Kinase assay reaction mixture was performed as described in Lee et al. (1998) with some modification as followed: 50 mM HEPES, pH 7.2, 10 mM $MgCl_2$, 1 mM EGTA, 2 mM $CaCl_2$, 66.7 μM [γ-^{32}P]ATP, approximately 0.5 – 1 μg of kinase enzyme, and 1 – 2 μg of REN1 substrate (with the exception of the use around 2 – 5 μg of REN1 substrate for MS/MS analysis). Kinase reaction mixture was incubated at room temperature for 1 hour. Following incubation, SDS loading buffer was added to the reaction mixture and 15 μL of reaction mixture was loaded to the 10% SDS-PAGE gel. The gel was then used to exposed phosphorimager screen for 45 min to 2 hr, after which the screen was scanned using Typhoon 9410 scanner (GE Healthcare, Piscataway, NJ).

Microscopy

For fluorescence observations, confocal microscope Leica SP2 (Leica, Wetzlar, Germany) was used. Most images were obtained using either a 20x or a 63x water-immersion lens, zoomed 4x to 8x with 524 x 524 frame and 400-Hz scanning speed. Time-lapse images were obtained at 1 – 3 sec intervals.

Image Analysis

Image analysis such as pollen tube length and tip width measurements were performed using Metamorph software (Molecular Devices, Sunnyvale, CA). Pollen tube

growth oscillation analyses were performed using ImageJ 1.43u software as available from http://rsbweb.nih.gov/ij/ (Abramoff et al., 2004; Rasband, 1997).

RESULTS

2D-LC-MS/MS revealed REN1 phosphorylation sites by CPK16

Previous MS/MS analysis led to the identification of calcium-dependent REN1 phosphorylation sites by CPK16 *in vitro* (please refer to chapter 1). Some of these sites are Ser_{70}, Thr_{151}, and Ser_{267} (Table 2.1). In order to investigate the functional relevance of phosphorylation, each site was mutated to either Glu to mimic the negatively-charged phosphorylated states (phosphomimic mutant) or Ala to mimic the nonphosphorylated states (Figure 2.1; Witte et al., 2010; Choi et al., 2005).

REN1 phosphorylation within the GAP domain is important for its activity

GAP domain of RhoGAP proteins is known to be crucial for the RhoGAPs activity (Ohta et al., 2006; Klahre and Kost, 2006; Lancaster et al., 1994). The GAP domain is known to interact with its target Rho GTPase proteins such as ROPs and enhances the GTPase activity of ROP proteins. The activities of REN1 mutants were tested on tobacco pollen tubes by measuring the effects on protein sub-cellular distribution and pollen tube tip width. Nonphosphorylated REN1 mutant, $S_{267}A$, displayed cytosolic localization pattern similar to WT REN1 (Figure 2.2A). However, phosphomimic mutant, $S_{267}E$, was localized to both the cytosol and vegetative nucleus (Figure 2.2A). With respect to pollen tube tip width, overexpression of REN1 $S_{267}E$ resulted in reduced tip width compared to overexpression of WT REN1 (Figure 2.2B; $p <$

0.0001). Meanwhile, REN1 $S_{267}A$ had comparable tip width to WT REN1. Since ROP1 regulates pollen tube polarity and growth, as evident from swollen and short tubes phenotype in ROP1 OX and narrow and short tubes phenotype in DNROP1 OX (Li et al., 1999; Hwang et al., 2010), and REN1 negatively regulates ROP1 activity, then REN1 OX indirectly affects pollen tube growth as well. As a result, pollen tube tip width (or tube length) can serve as indirect outputs of ROP1 activity. Thus, the reduced tip width resulted in the REN1 $S_{267}E$ OX suggests a reduced ROP1 activity caused by an increase in REN1 activity.

To further confirm the effect of phosphorylation on REN1 activity, REN1 activity assay was performed. In this assay, the ability of REN1 mutants to suppress ROP1 OX – induced swelling was measured in a transient expression system in tobacco pollen tubes. ROP1 OX in pollen tubes resulted in swollen tip and relatively short tubes (Li et al., 1999) which can be suppressed when co-expressed with RopGAP1 (Hwang et al., 2010). Similar to RopGAP1, co-expression of ROP1 with WT REN1 or REN1 $S_{267}E$ also suppressed ROP1 OX-induced tip swelling (Figure 2.3A, B; $p < 0.0001$). In contrast, co-expression of ROP1 with REN1 $S_{267}A$ did not suppress ROP1 OX-induced tip swelling, as compared to ROP1 OX alone (Figure 2.3B). Overall, these results suggest that REN1 phosphorylation at Ser_{267} is required for its activity toward ROP1 as evident from no activity observed when it is nonphosphorylated.

REN1 phosphorylation within the GAP domain is essential to suppress ROP1 activity

To further confirm that the increase in REN1 activity due to phosphorylation in Ser_{267} led to reduced ROP1 activity, ROP1 activity assay was performed. ROP1 activity was visualized and quantified using active ROP1 marker, CFP-tagged RIC4ΔC (Hwang et al., 2005; Hwang et al., 2010). RIC4 is a downstream effector known to interact with active GTP-bound ROP1 (Hwang et al., 2005). Deletion of RIC4 C-terminal domain, which is involved in effector interaction, has been shown to prevent depolarized growth without affecting its interaction with active ROP1, making it a good marker for ROP1 activity (Hwang et al., 2005). Active ROP1 localization to and intensity at the apical PM is required for normal pollen tube growth (Hwang et al., 2010). An increase in ROP1 activity can be observed as both an increase in apical tip intensity and an expanded localization from the apical to the subapical PM region which eventually results in tip swelling phenotype (Hwang et al., 2010). Thus ROP1 activity can be quantified by factoring in pollen tube tip width, apical PM intensity of RIC4ΔC, and apical PM circumference length of RIC4ΔC signal (Hwang et al., 2010). Co-expression of WT REN1 and CFP-RIC4ΔC resulted in a reduced tip width, reduced tip-active ROP1 intensity, reduced active ROP1 domain, and three-fold reduction in ROP1 activity compared to CFP-RIC4ΔC OX control (Figure 2.4A-D; $p < 0.0001$). Similarly, co-expression of phosphomimic REN1 mutant, $S_{267}E$, and CFP-RIC4ΔC had a decreased tip width, reduced tip-active ROP1 intensity, reduced active ROP1 domain at the apical PM, and two-fold reduction in ROP1 activity compared to CFP-RIC4ΔC OX (Figure 2.4A-D;

$p < 0.0001$). In contrast, co-expression of nonphosphorylated REN1 mutant, $S_{267}A$, and CFP-RIC4ΔC, had an increased tip width, increased tip-active ROP1 intensity, expanded active ROP1 domain at the apical PM, and high ROP1 activity similar to CFP-RIC4ΔC OX (Figure 2.4A-D). These results further confirm that phosphorylation of REN1 at Ser_{267} is required for REN1 activity to suppress ROP1 activity, as evident from the high ROP1 activity when REN1 nonphosphorylated mutant was co-expressed with active ROP1 marker.

REN1 phosphorylation within the PH domain at $Ser_{70,71}$ reduces its activity

PH domain is known to be involved in lipid binding and thus contributes to protein localization to the PM (Lemmon et al., 1995; Ma et al., 1997). Based on the MS/MS analysis, REN1 can be phosphorylated on two PH-domain residues, Ser_{70} and Thr_{151}. Mutations on $Thr_{146,151}$ did not affect its localization but either mutation to A/E reduced REN1 activity toward suppressing ROP1 OX phenotype (Figure 2.5A,B). It seems that these residues are essential for REN1 function such that mutation impacts its activity and thus, it is likely that neither residue is regulated by phosphorylation.

A different set of mutations on $Ser_{70,71}$ had an effect on its sub-cellular localization and consequently on its activity. Overexpression of nonphosphorylated mutant, $S_{70,71}A$, displayed cytosolic localization similar to WT REN1 (Figure 2.6A). However, phosphomimic REN1 mutant, $S_{70,71}E$, localized to cytosolic patches whose identity is currently unknown (Figure 2.6A). Despite the localization change, the pollen tube tip width of REN1 $S_{70,71}E$ OX was comparable to WT and nonphosphorylated REN1

mutant. These results suggest that REN1 phosphorylation at $Ser_{70,71}$ affects protein localization but does not seem to affect pollen tube tip width at this condition.

Further co-expression analyses showed that co-expression of REN1 $S_{70,71}A$ mutant with ROP1 led to the suppression of ROP1 OX-induced tip swelling and produced pollen tubes with comparable tip width to WT REN1 co-expression (Figure 2.7A, B; $p < 0.0001$). In contrast, co-expression of REN1 $S_{70,71}E$, did not suppress the ROP1OX-induced tip swelling phenotype. These results further suggest that REN1 phosphorylation at $Ser_{70,71}$ leads to a reduction in REN1 activity in suppressing the ROP1 OX phenotype which is likely caused by its localization change. Since active ROP1 is localized to the apical PM where it interacts with REN1, the inability of REN1 to localize to the apical PM when it is phosphorylated would negatively impact its ability to regulate ROP1 activity.

DISCUSSION

Here we presented some evidence of the functional significance of REN1 phosphorylation on its activity. Our previous data showed that CPK16 can phosphorylate REN1 at several sites including the three sites, Ser_{70}, Thr_{151}, and Ser_{267} in a calcium-dependent manner. Ser_{267} lies in the GAP domain of REN1 and our data indicate that this residue is important for its activity since nonphosporylated mutation resulted in no (or significantly reduced activity) toward ROP1. Previous studies have reported enhanced GAP activity following phosphorylation. For example: p190 RhoGAP phosphorylation by Fyn tyrosine kinase at Tyr_{1105} near the RhoGAP domain resulted in enhanced

RhoGAP activity to regulate oligodendrocyte differentiation (Wolf et al., 2001) while p190 phosphorylation by c-Src tyrosine kinase also at Tyr_{1105} is important to stimulate its activity in regulating actin stress fibers disassembly (Haskell et al., 2001). In contrast, other studies have also reported inhibition of RhoGAP activity when phosphorylated. For example: yeast Bem2p and Bem3p phosphorylation by Cdc28p-Cln2p kinase led to inhibition of GAP activity and promotion of Cdc42p GTPase in regulating bud emergence (Knaus et al., 2007) and p190 phosphorylation by Rho-kinase at Ser_{1150} reduced its RhoGAP activity and enhanced RhoA activation in regulating contraction of vascular smooth muscle cells (Mori et al., 2009). Despite the contradictory effects of phosphorylation on RhoGAP, it is clear that phosphorylation is important for RhoGAP activity. While the phosphorylation data of RhoGAPs especially for mammalian RhoGAPs are plenty, currently there is no information regarding the phosphorylation of plant RhoGAPs. In addition, since most mammalian RhoGAPs are tyrosine-phosphorylated, the effects on their activities may not reflect serine/threonine phosphorylation found in plants. Interestingly, Ser_{267} residue is quite conserved in REN1-like proteins (At5g12150 and At5g19390) but not in other plant or mammalian RhoGAPs. This suggests that phosphorylation in this REN1 residue to regulate its activity may be unique to REN1 and/or REN1-like proteins.

To further validate the functional significance of REN1 phosphorylation at Ser_{267}, it is important to perform another key experiment to test for ROP1 GTPase activity in *vitro*. In this assay, ROP1 GTPase intrinsic activity is observable as low GTP-to-GDP exchange which can be enhanced when it is incubated with functional REN1. Based on

our transient co-expression data showing that nonphosphorylation mutant REN1 $S_{267}A$ had no activity against ROP1, we would expect to observe similar effects in *in vitro* GTPase assay such that only intrinsic ROP1 GTPase activity is present when it is incubated with REN1 nonphosphorylated mutant. Additional assay such as *in vitro* phosphorylation of WT REN1 and REN1 $S_{267}A$ prior to performing GTPase assay can also be useful to further investigate whether phosphorylation of REN1 at S_{267} is required for REN1 activity. We expect an enhanced ROP1 GTPase activity in the presence of WT REN1 pre-incubated with CPK16 but no ROP1 GTPase activity in the presence of REN1 $S_{267}A$ pre-incubated with CPK16. Upon implementation of these assays and observation of the expected phenotypes, it would then be fairly convincing to conclude that REN1 phosphorylation at S_{267} is required and sufficient for its activity toward ROP1.

Within the PH domain, mutation of Thr_{151} to either A/E resulted in a reduction in REN1 activity suggesting that this residue is important for activity and most likely not regulated by phosphorylation. In contrast, phosphomimic mutation at $Ser_{70,71}$ affected REN1 localization and subsequently its activity. PH domain is known to interact with phospholipids, such as PIP_2 or PIP_3, at the PM allowing PH domain-containing proteins to be targeted to the membrane (Lemmon et al., 1995; Ma et al., 1997; Harlan et al., 1994; Salim et al., 1996; Yu et al., 2004; Varnai et al., 2005). However, not all PH domain-containing proteins are membrane-targeted as well as interact strongly with phospholipids (Yu et al., 2004). Such is the case with REN1 since its association with PM can only be observed with strong ROP1 overexpression suggesting that its PM-localization requires binding with tip-active ROP1 (unpublished data). Structural studies

of PH-containing proteins have reported that PH domain displays positively-charged surface which promotes binding with the negatively-charged phospholipids (Ferguson et al., 1995; Ferguson et al., 1994). Mutation of the basic residues within the PH domain led to diminished interaction with phosphoinositides (Yu et al., 2004). Due to the delocalized electrostatic interactions between PH domain and phosphoinositides, we predict that introduction of negative charges in the phosphomimic mutant case may affect the overall positive charge of PH domain and as a result reduce or abolish its interaction with phospholipids (Figure 2.8). This is in fact the case as has been reported in various studies. For example: phosphorylation of pleckstrin by protein kinase C near the PH domain which is important for its activity led to inhibition of phosphoinositide hydrolysis (Abrams et al., 1995; Craig and Harley, 1996) and phosphorylation of PH domain of protein kinase B abolished its interaction to PIP3 and prevented its activation (Powell et al., 2003).

To further validate the functional significance of REN1 phosphorylation at $Ser_{70,71}$, it is also important to perform another key experiment to test for ROP1 GTPase activity *in vitro*. Our transient co-expression data showed that phosphomimic mutant REN1 $S_{70,71}E$ resulted in localization change which likely caused the loss (or highly reduced) activity toward ROP1. Thus if this is indeed the case, we would expect to observe similar activities of either mutation at REN1 $S_{70,71}$ in comparison to WT REN1 in *in vitro* GTPase assay. In addition, phospholipid-binding assays to determine changes in binding preferences between the two REN1 $S_{70,71}$ mutants would be important to further confirm our hypothesis. It has been reported that RhoGTPase proteins such as Rac2 and

At-Rac2 can specifically interact with $PI_{4,5}P$ at the plasma membrane (Tolias et al., 1995; Kost et al., 1999). Phospholipid-binding assay analyses of WT REN1 suggest its preferential binding to phosphatidylinositol phosphate PI_3P, PI_4P, and PI_5P as well as very weak binding to phosphatidylinositol bisphosphate $PI_{3,4}P$, $PI_{3,5}P$, and $PI_{4,5}P$ (data not shown). Based on our transient expression analysis, REN1 $S_{70,71}E$ mutant displayed protein accumulation in the cytosolic patches which may likely be due to the changes in its preferential binding to phosphoinositides. We expect that REN1 $S_{70,71}E$ mutation would result in the loss of the weak REN1 binding to $PI_{4,5}P$ (and possibly enhanced binding toward PIPs or other PIP_2s) which can be tested in phospholipid-binding assay using PIP strips. Upon implementation of these assays and observation of the expected phenotypes, it would then be fairly convincing to conclude that REN1 phosphorylation at $S_{70,71}$ affects its localization to the PM and subsequently its activity to regulate ROP1 activity at the PM.

Based on our current observations and past reports, we present a mechanistic model for the functional significance of REN1 phosphorylation by CPK16 (Figure 2.8). In this model, we show that in *in vitro* condition, REN1 can be phosphorylated at many sites including the Ser_{267} and Ser_{70} with contrasting effects. Ser_{267} phosphorylation is required for REN1 activity to regulate ROP1 while Ser_{70} phosphorylation reduced/abolished its interaction to the apical PM leading to activity loss. It is still unclear whether CPK16 display any preferences to phosphorylate distinct sites *in vivo* or whether CPK16 phosphorylation of distinct sites requires certain calcium concentration. Nevertheless, we speculate that *in vivo,* PH domain interaction with phospholipids may

prevent phosphorylation at Ser_{70} but not at Ser_{267}. As such, tip-localized REN1 bound to apical ROP1 can be phosphorylated at Ser_{267} (within the GAP domain) which then negatively regulates ROP1 activity. Following the release of REN1 from the apical PM, its phosphorylation in other residue such as Ser_{70} may occur and may or may not prevent REN1 tip-directed targeting as well. It remains to be tested whether this is indeed the case. In addition, it is yet to be investigated whether synergistic relationships exist between different phosphorylation sites such that phosphorylation in one residue may enhance the phosphorylation of another residue.

REFERENCES

Abramoff, M. D., Magalhaes, P. J., and Ram, S. J. (2004) Image processing with ImageJ. Biophotonics Int. **11(7)**: 36 – 42

Abrams, C. S., Zhao, W., Belmonte, E., and Brass, L. F. (1995) Protein kinase C regulates pleckstrin by phosphorylation of sites adjacent to the N-terminal pleckstrin homology domain. J. Biol. Chem. **270(40)**: 23317 – 23321

Bethke, P. C. and Jones, R. L. (1997) Reversible protein phosphorylation regulates the activity of the slow-vacuolar ion channel. Plant J. **11(6)**: 1227 – 1235

Boudsocq, M., Willmann, M. R., McCormack, M., Lee, H., Shan, L., He, P., Bush, J., Cheng, S-H., and Sheen, J. (2010) Differential innate immune signaling via Ca^{2+} sensor protein kinases. Nature **464**: 418 – 423

Choi, H-I, Park, H-J., Park, J. H., Kim, S., Im, M-Y., Seo, H-H., Kim, Y-W., Hwang, I., and Kim, S. Y. (2005) Arabidopsis calcium-dependent protein kinase AtCPK32 interacts with ABF4, a transcriptional regulator of abscisic acid-responsive gene expression, and modulates its activity. Plant Physiol. **139**: 1750 – 1761

Craig, K. L. and Harley, C. B. (1996) Phosphorylation of human pleckstrin on Ser-113 and Ser-117 by protein kinase C. Biochem. J. **314**: 937 – 942

Ferguson, K. M., Lemmon, M. A., Schlessinger, J., and Sigler, P. B. (1994) Crystal structure at 2.2 Å resolution of the pleckstrin homology domain from human dynamin. Cell **79**: 199 – 209

Ferguson, K. M., Lemmon, M. A., Schlessinger, J., and Sigler, P. B. (1995) Structure of the high affinity complex of inositol triphosphate with a phospholipase C pleckstrin homology domain. Cell **83**: 1037 – 1046

Fu, Y., Wu, G., and Yang, Z. (2001) Rop GTPase-dependent dynamics of tip-localized F-actin controls tip growth in pollen tubes. J. Cell Biol. **152(5)**: 1019 – 1032

Harlan, J. E., Hadjuk, P. J., Yoon, H. S., and Fesik, S. W. (1994) Pleckstrin homology domains bind to phasphatidylinositol-4,5-biphosphate. Nature **371**: 168 – 170

Harper, J.F., Breton, G., and Harmon, A. (2004) Decoding Ca^{2+} signals through plant protein kinases. Annu. Rev. Plant Biol. **55**: 263-288

Harper, J. F. and Harmon, A. (2005) Plants, symbiosis and parasites: a calcium signaling connection. Nat. Rev. Mol. Cell Biol. **6**: 555 – 566

Haskell, M. D., Nickles, A. L., Agati, J. M., Su, L., Dukes, B. D., and Parsons, S. J. (2001) Phosphorylation of p190 on Tyr1105 by c-Src is necessary but not sufficient for EGF-induced actin disassembly in C3H10T1/2 fibroblasts. J. Cell Sci. **114**: 1699 – 1708

Hwang, J-U., Gu, Y., Lee, Y-J., and Yang, Z. (2005) Oscillatory ROP GTPase activation leads the oscillatory polarized growth of pollen tubes. Mol. Biol. Cell **16:** 5385 – 5399

Hwang, I., Sze, H., and Harper, J. F. (2000) A calcium-dependent protein kinase can inhibit a calmodulin-stimulated Ca^{2+} pump (ACA2) located in the endoplasmic reticulum of Arabidopsis. Proc. Nat. Acad. Sci. **97(11)**: 6224 – 6229

Hwang, J-U., Wu, G., Yan, A., Lee, Y-J., Grierson, C. S., and Yang, Z. (2010) Pollen-tube tip growth requires a balance of lateral propagation and global inhibition of Rho-family GTPase activity. J. Cell Sci. **123**: 340 – 350.

Ishida, S., Yuasa, T., Nakata, M., and Takahashi, Y. (2008) A tobacco calcium-dependent protein kinase, CDPK1, regulates the transcription factor Repression of Shoot Growth in response to gibberellins. Plant Cell **20**: 3273 – 3288

Klahre, U., and Kost, B. (2006). Tobacco RhoGTPase ACTIVATING PROTEIN1 spatially restricts signaling of RAC/Rop to the apex of pollen tubes. Plant Cell ***18*:** 3033-3046

Knaus, M., Pelli-Gulli, M-P., van Drogen, F., Springer, S., Jaquenoud, M., and Peter, M. (2007) Phosphorylation of Bem2p and Bem3p may contribute to local activation of Cdc42p at bud emergence. EMBO J. **26**: 4501 – 4513

Kost, B., Lemichez, E., Spielhofer, P., Hong, Y., Tolias, K., Carpenter, C., and Chua, N-H. (1999) Rac homologues and compartmentalized phosphatidylinositol 4,5-bisphosphate act in a commong pathway to regulate polar pollen tube growth. J. Cell Biol. **145(2)**: 317 – 330

Lancaster, C. A., Taylor-Harris, P.M., Self, A. J., Brill, S., van Erp, H. E., and Hall, A. (1994) Characterization of rhoGAP. J. Biol. Chem. **269(2)**: 1137 – 1142

Lee, J-Y., Yoo, B-C., and Harmon, A. C. (1998) Kinetic and calcium-binding properties of three calcium-dependent protein kinase isoenzymes from soybean. Biochemistry **37**: 6801 – 6809

Lemmon, M. A., Ferguson, K. M., O'Brien, R., Sigler, P. B., and Schlessinger, J. (1995) Specific and high-affinity binding of inositol phosphates to an isolated pleckstrin homology domain. Proc. Natl. Acad. Sci. **92**: 10472 – 10476

Li, H., Lin, Y., Heath, R.M., Zhu, M.X., and Yang, Z. (1999) Control of pollen tube tip growth by a Rop GTPase-dependent pathway that leads to tip-localized calcium influx. Plant Cell **11**: 1731-1742

Lino, B., Baizabal-Aguirre, V. M., Gonzalez de la Vara, L. E. (1998) The plasma-membrane H_+-ATPase from beet root is inhibited by a calcium-dependent phosphorylation. Planta **204**: 352 – 359

Lourido, S., Shuman, J., Zhang, C., Shokat, K. M., Hui, R., and Sibley, L. D. (2010) Calcium-dependent protein kinase 1 is an essential regulator of exocytosis in *Toxoplasma*. Nature **465**: 359 – 363

Ma, A. D., Brass, L. F., and Abrams, C. S. (1997) Pleckstrin associates with plasma membranes and induces the formation of membrane projections: requirements for phosphorylation and the NH_2-terminal PH domain. J. Cell Biol. **136(5)**: 1071– 1079

Mori, K., Amano, M., Takefuji, M., Kato, K., Morita, Y., Nishioka, T., Matsuura, Y., Murohara, T., and Kaibuchi, K. (2009) Rho-kinase contributes to sustained RhoA activation through phosphorylation of p190A RhoGAP. J. Biol. Chem. **284(8)**: 5067 – 5076

Myers, C., Romanowsky, S. M., Barron, Y. D., Garg, S., Azuse, C. L., Curran, A., Davis, R. M., Hatton, J., Harmon, A. C., and Harper, J. F. (2009) Calcium-dependent protein kinases regulate polarized tip growth in pollen tubes. Plant J. **59(4)**: 528 – 539

Ohta, Y., Hartwig, J. H., and Stossel, T. P. (2006) FilGAP, a Rho- and ROCK-regulated GAP for Rac binds filamin A to control actin remodeling. Nat. Cell Biol. **8(8)**: 803 – 814

Pei, Z-M., Ward, J. M., Harper, J. F., and Schroeder, J. I. (1996) A novel chloride channel in *Vicia faba* guard cell vacuoles activated by the serine/threonine kinase, CDPK. EMBO J. **15(23)**: 6564 – 6574

Powell, D. J., Hajduch, E., Kular, G., and Hundal, H. S. (2003) Ceramide disables 3-phosphoinositide binding to the pleckstrin homology domain of protein kinase B (PKB)/Akt by a PKC ζ-dependent mechanism. Mol. Cell Biol. **23(21)**: 7794 – 7808

Rasband, W. S. ImageJ, US National Institute of Health, Bethesda, Maryland, USA. http://imagej.nih.gov/ij/ 1997 – 2011

Romeis, T., Ludwig, A. A., Martin, R., and Jones, J. D. G. (2001) Calcium-dependent protein kinases play an essential role in a plant defense response. EMBO J. **20(20)**: 5556 – 5567

Romeis, T., Piedras, P., and Jones, J. D. G. (2000) Resistance gene-dependent activation of a calcium-dependent protein kinase in the plant defense response. Plant Cell **12**: 803 – 815

Saijo, Y., Hata, S., Kyozuka, J., Shimamoto, K., and Izui, K. (2000) Over-expression of a single Ca^{2+}-dependent protein kinase confers both cold and salt/drought tolerance on rice plants. Plant J. **23(3)**: 319 – 327

Saijo, Y., Kinoshita, N., Ishiyama, K., Hata, S., Kyozuka, J., Hayakawa, T., Nakamura, T., Shimamoto, K., Yamaya, T. and Izui, K. (2001) A Ca^{2+}-dependent protein kinase that endows rice plants with cold- and salt-stress tolerance functions in vascular bundles. Plant Cell Phys. **42(11)**: 1228 – 1233

Salim, K., Bottomley, M. J., Querfurth, E., Zvelebil, M. J., Gout, I., Scaife, R., Margolis, R. L., Gigg, R., Smith, C. I. E., Driscoll, P. C., Waterfield, M. D., and Panayotou, G. (1996) Distinct specificity in the recognition of phosphoinositides by the pleckstrin homology domains of dynamin and Bruton's tyrosine kinase. EMBO J. **15(22)**: 6241 – 6250

Sheen, J. (1996) Ca^{2+}-dependent protein kinases and stress signal transduction in plants. Science **274**: 1900 – 1902

Tolias, K. F., Cantley, L. W., and Carpenters, C. L. (1995) Rho family GTPases bind to phosphoinositide kinases. J. Biol. Chem. **270(30)**: 17656 – 17659

Varnai, P., Bondeva, T., Tamas, P., Toth, B., Buday, L., Hunyady, L., and Balla, T. (2005) Selective cellular effects of overexpressed pleckstrin-homology domains that recognize PtdIns(3,4,5)P_3 suggest their interaction with protein binding partners. J. Cell Sci. **118**: 4879 – 4888

Witte, C-P., Keinath, N., Dubiella, U., Demouliere, R., Seal, A., and Romeis, T. (2010) Tobacco calcium-dependent protein kinases are differentially phosphorylated *in vivo* as part of a kinase cascade that regulates stress response. J. Biol. Chem **285(13)**: 9740 – 9748

Wolf, R. M., Wilkes, J. J., Chao, M. V., and Resh, M. D. (2001) Tyrosine phosphorylation of p190 RhoGAP by Fyn regulates oligodendrocyte differentiation. J. Neurobiol. **49(1)**: 62 – 78

Wu, G., Li, H., and Yang, Z. (2000) Arabidopsis RopGAPs are a novel family of rho GTPase-activating proteins that require the Cdc42/Rac-interactive binding motif for rop-specific GTPase stimulation. Plant Physiol. **124**: 1625-1636

Yoon, G. M., Dowd, P. E., Gilroy, S., and McCubbin, A. G. (2006) Calcium-dependent protein kinase isoforms in *Petunia* have distinct functions in pollen tube growth, including regulating polarity. Plant Cell **18**: 867 – 878

Yu, J. W., Mendrola, J. M., Audhya, A., Singh, S., Keleti, D., DeWald, D. B., Murray, D., Emr, S. D., and Lemmon, M. A. (2004) Genome-wide analysis of membrane targeting by *S. cerevisiae* pleckstrin homology domains. Mol. Cell. **13:** 677 – 688

Zhou, L., Fu, Y., and Yang, Z. (2009) A genome-wide functional characterization of *Arabidopsis* regulatory calcium sensors in pollen tubes. J Integr. Plant Biol. **51(8)**: 751 – 761

Zhu, S-Y., Yu, X-C., Wang, X-J., Zhao, R., Li, Y., Fan, R-C., Shang, Y., Du, S-Y., Wang, X-F., Wu, F-Q., Xu, Y-H., Zhang, X-Y., and Zhang, D-P. (2007) Two calcium-dependent protein kinases, CPK4 and CPK11, regulate abscisic acid signal transduction in *Arabidopsis*. Plant Cell **19**: 3019 – 3036

Figure 2.1. REN1 phosphorylation mutations from Ser to Ala (nonphosphorylation mutation) or Glu (phosphomimic mutation). Three sets of mutations were generated. Two sets were within the PH domain which included $Ser_{70,71}$ and $Thr_{146,151}$. The last set was a mutation within the GAP domain at Ser_{267}.

Figure 2.1.

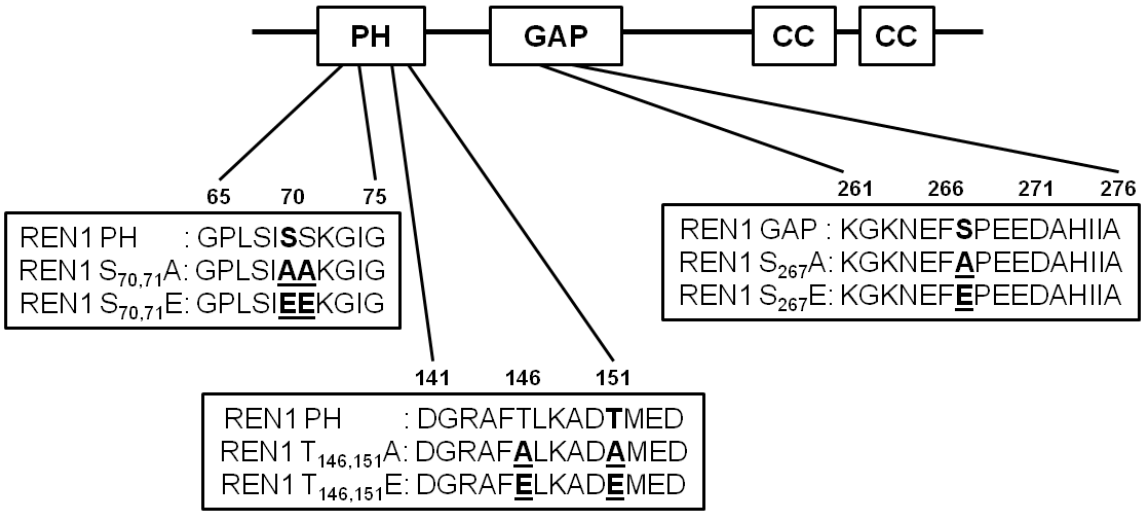
PH
GAP
CC
CC
65
70
75
REN1 PH : GPLSISSKGIG
REN1 S70,71A: GPLSIAAKGIG
REN1 S70,71E: GPLSIEEKGIG
261
266
271
276
REN1 GAP : KGKNEFSPEEDAHIIA
REN1 S267A: KGKNEFAPEEDAHIIA
REN1 S267E: KGKNEFEPEEDAHIIA
141
146
151
REN1 PH : DGRAFTLKADTMED
REN1 T146,151A: DGRAFALKADAMED
REN1 T146,151E: DGRAFELKADEMED

Figure 2.2. Transient expression analysis of GFP-REN1 Ser_{267} mutants in tobacco pollen tubes. A) Nonphophorylated REN1 mutant (REN1 $S_{267}A$) showed similar cytosolic localization pattern as WT REN1. Phophomimic REN1 mutant (REN1 $S_{267}E$) also showed similar cytosolic localization pattern as WT REN1 as well as internalization of proteins into the vegetative nucleus. B) Tip width quantification from each transient expression. Tip width is much reduced in OX of phophomimic REN1 mutant (REN1 $S_{267}E$) suggesting a potentially active REN1 form.

Figure 2.2.

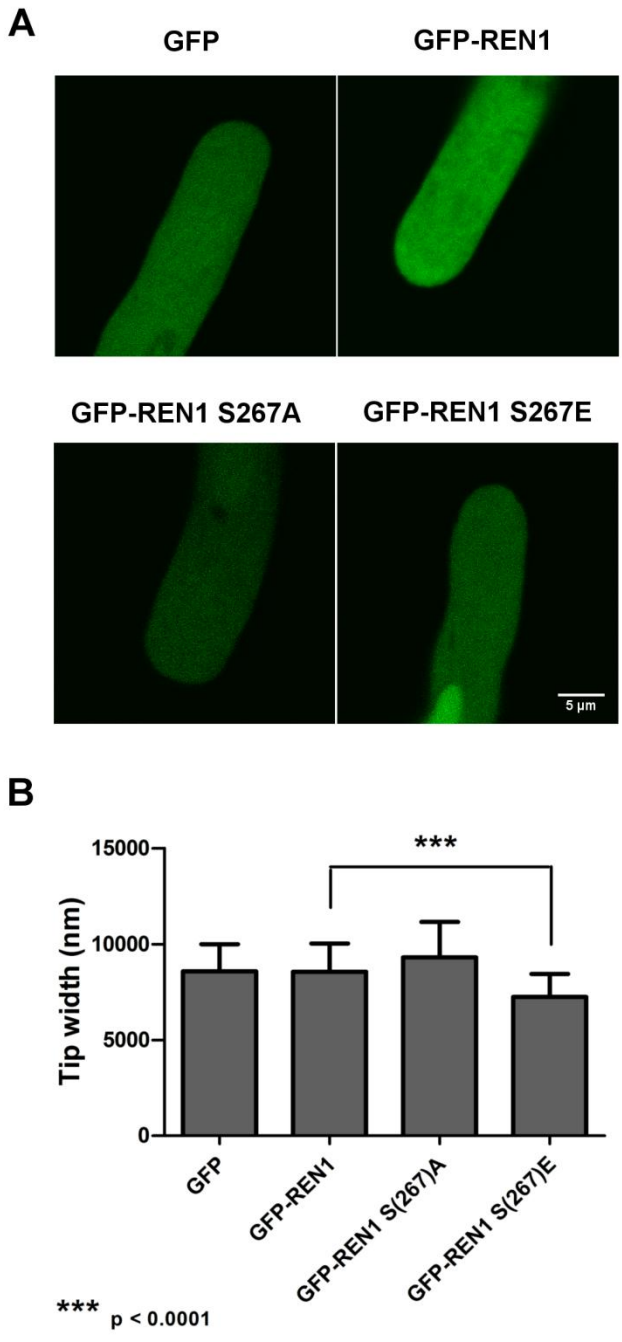
A
GFP
GFP-REN1
GFP-REN1 S267A
GFP-REN1 S267E
5 µm
B
Tip width (nm)
15000
10000
5000
0
***
GFP
GFP-REN1
GFP-REN1 S(267)A
GFP-REN1 S(267)E
*** p < 0.0001

Figure 2.3. Transient co-expression analysis of RFP-ROP1 and GFP-REN1 Ser$_{267}$ mutants in tobacco pollen tubes. A) Nonphophorylated REN1 mutant (REN1 $S_{267}A$) cannot suppress GFP-ROP1 OX-induced tip swelling phenotype. In contrast, phophomimic REN1 mutant (REN1 $S_{267}E$) can suppress GFP-ROP1 OX phenotype similar to WT REN1. B) Tip width quantification from each transient expression.

Figure 2.3.

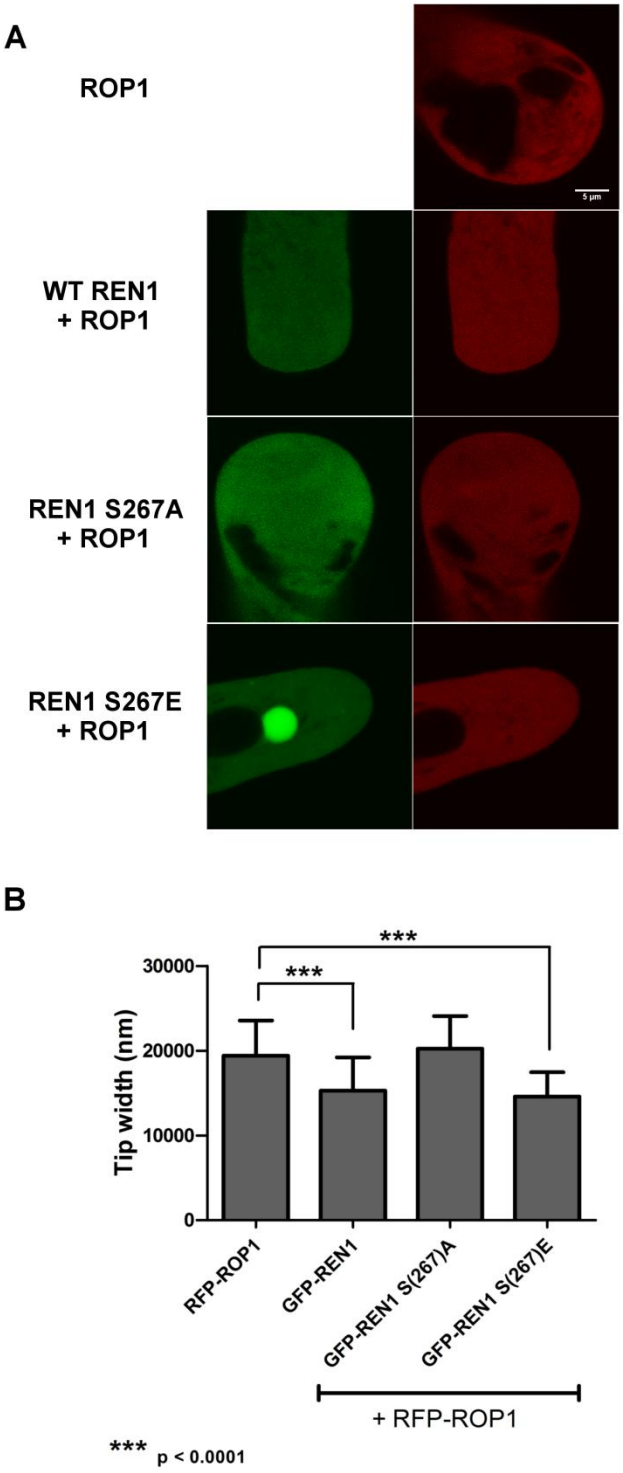
A
ROP1
5 µm
WT REN1
+ ROP1
REN1 S267A
+ ROP1
REN1 S267E
+ ROP1
B
***
***
30000
20000
10000
0
Tip width (nm)
RFP-ROP1
GFP-REN1
GFP-REN1 S(267)A
GFP-REN1 S(267)E
+ RFP-ROP1
*** p < 0.0001

Figure 2.4. ROP1 activity assay. A) Transient co-expression of active ROP1 marker, CFP-RIC4ΔC, with WT or mutant REN1 (S_{267}A/E) in tobacco pollen tubes. Co-expression with WT or phosphomimic REN1, S_{267}E, both reduced pollen tube width and reduced or slightly reduced CFP-RIC4ΔC expression at the apical PM consecutively. Co-expression with nonphosphorylated REN1 mutant, S_{267}A, did not reduce pollen tube width and did not reduce CFP-RIC4ΔC expression at the apical PM. B) Quantification analysis of pollen tube tip width as shown in part A. Co-expression with either WT REN1 or phosphomimic REN1 produced significantly reduced tip width ($p < 0.0001$). C) ROP1 activity is measured by incorporating three factors. The first factor is the length of apical cap where active ROP1 localizes to. The second factor is the intensity ratio between ROP1 signal at the apical cap to ROP1 signal at the cytosol. The third factor is tip width. D) ROP1 activity is quantified by multiplying all the numbers from the three factors mentioned in part C. ROP1 activity was the lowest when CFP-RIC4ΔC was co-expressed with WT REN1. ROP1 activity was low when CFP-RIC4ΔC was co-expressed with phosphomimic REN1 mutant.

Figure 2.4.

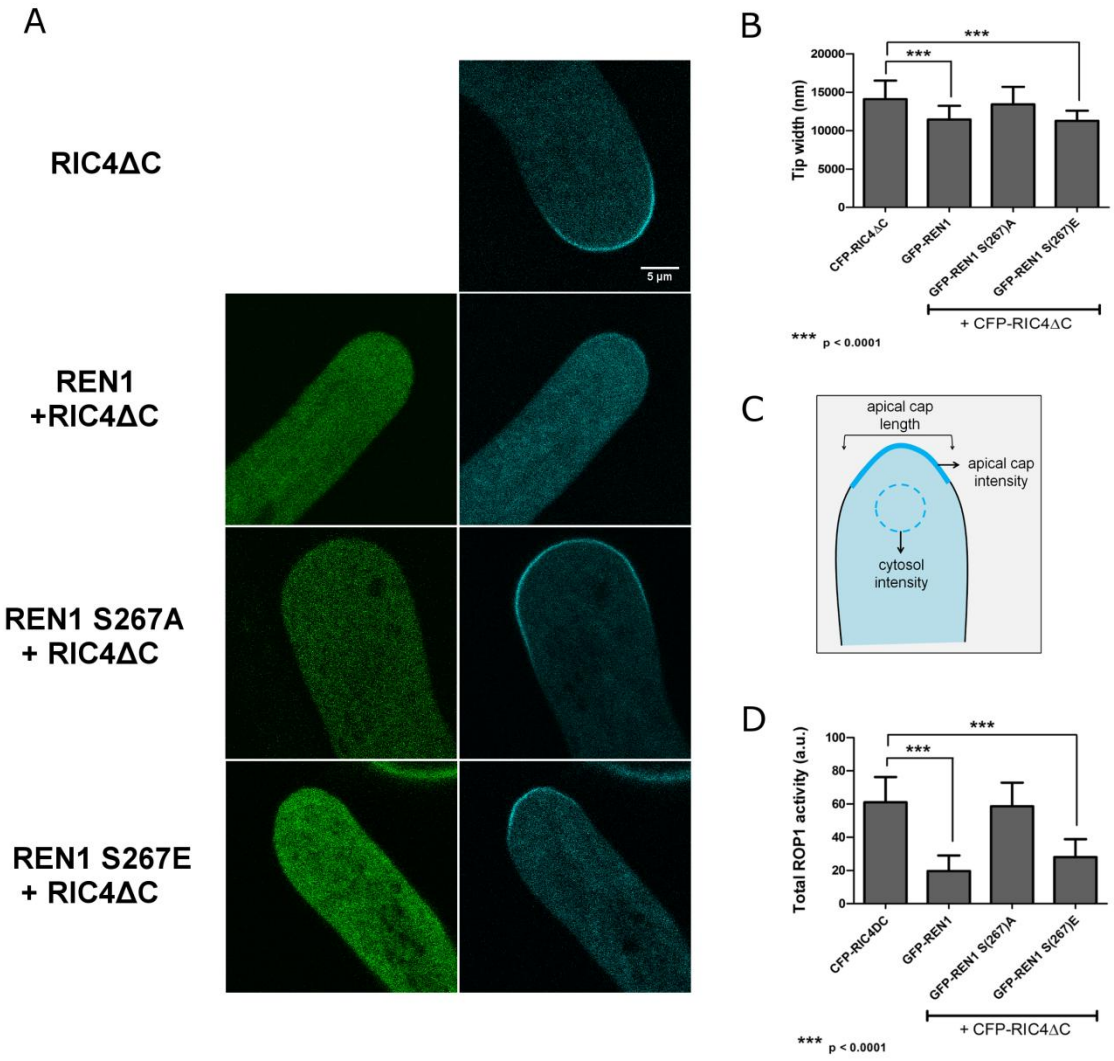
A
RIC4ΔC
REN1
+RIC4ΔC
REN1 S267A
+ RIC4ΔC
REN1 S267E
+ RIC4ΔC
5 µm
B
Tip width (nm)
20000
15000
10000
5000
0
***
***
CFP-RIC4ΔC
GFP-REN1
GFP-REN1 S(267)A
GFP-REN1 S(267)E
+ CFP-RIC4ΔC
*** p < 0.0001
C
apical cap length
apical cap intensity
cytosol intensity
D
Total ROP1 activity (a.u.)
100
80
60
40
20
0
***
***
CFP-RIC4DC
GFP-REN1
GFP-REN1 S(267)A
GFP-REN1 S(267)E
+ CFP-RIC4ΔC
*** p < 0.0001

Figure 2.5. Transient expression analysis of GFP-REN1 $Thr_{146,151}$ mutants in tobacco pollen tubes. A) Both the nonphophorylated REN1 mutant (REN1 $T_{146,150A}$) and phosphomimic REN1 mutant (REN1 $T_{146,150}$E) did not suppress GFP-ROP1 OX phenotype compared to WT REN1. B) Tip width quantification from each transient expression.

Figure 2.5.

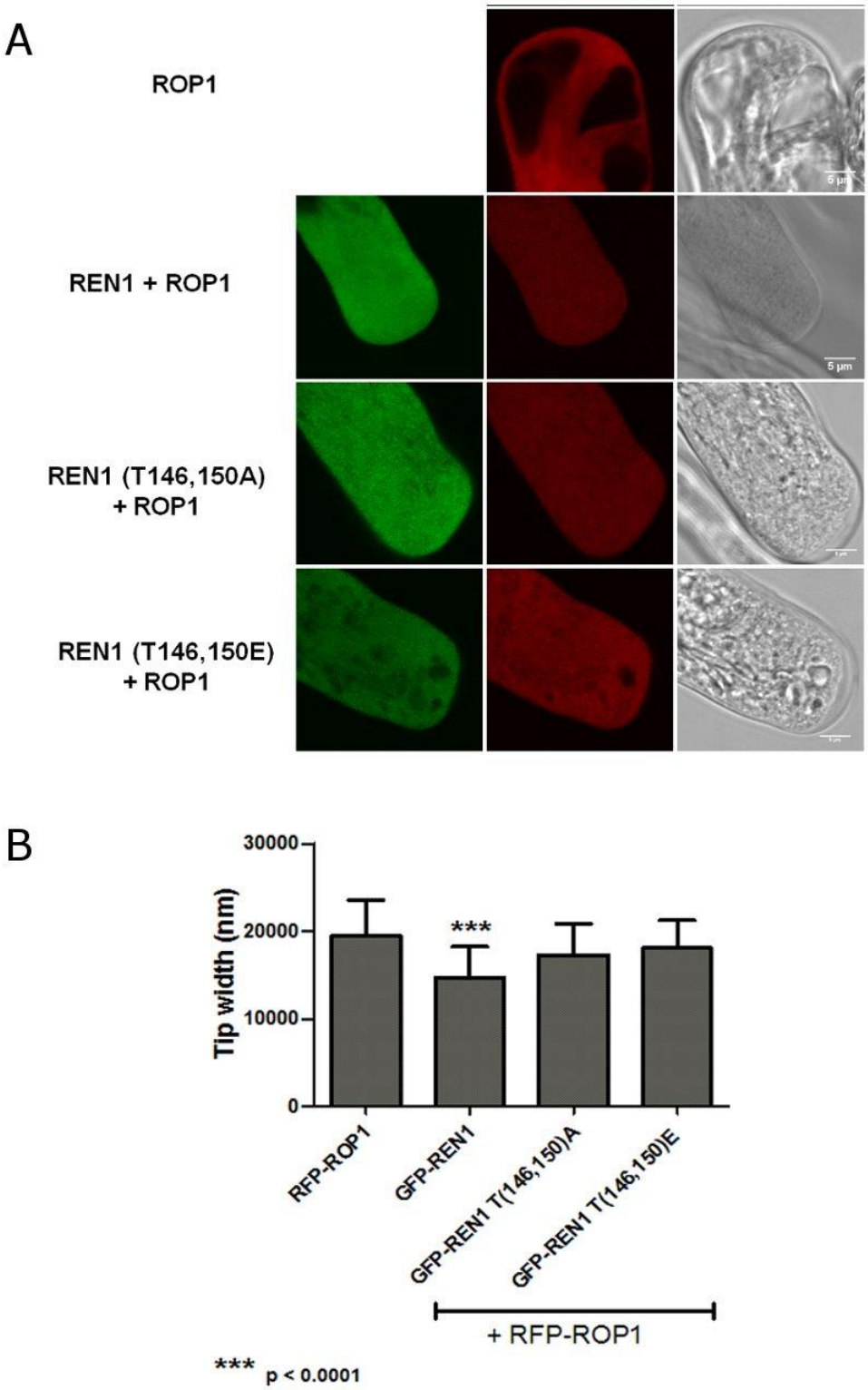
A
ROP1
REN1 + ROP1
REN1 (T146,150A)
+ ROP1
REN1 (T146,150E)
+ ROP1
5 µm
B
Tip width (nm)
30000
20000
10000
0
***
RFP-ROP1
GFP-REN1
GFP-REN1 T(146,150)A
GFP-REN1 T(146,150)E
+ RFP-ROP1
*** p < 0.0001

Figure 2.6. Transient expression analysis of GFP-REN1 Ser$_{70,71}$ mutants in tobacco pollen tubes. A) Nonphophorylated REN1 mutants (REN1 $S_{70,71}A$) showed similar cytosolic localization pattern as WT REN1. Phophomimic REN1 mutants (REN1 $S_{70,71}E$) showed internalization of proteins into unknown compartments. B) Tip width quantification from each transient expression. No significant difference was observed between the tip width of each expression.

Figure 2.6.

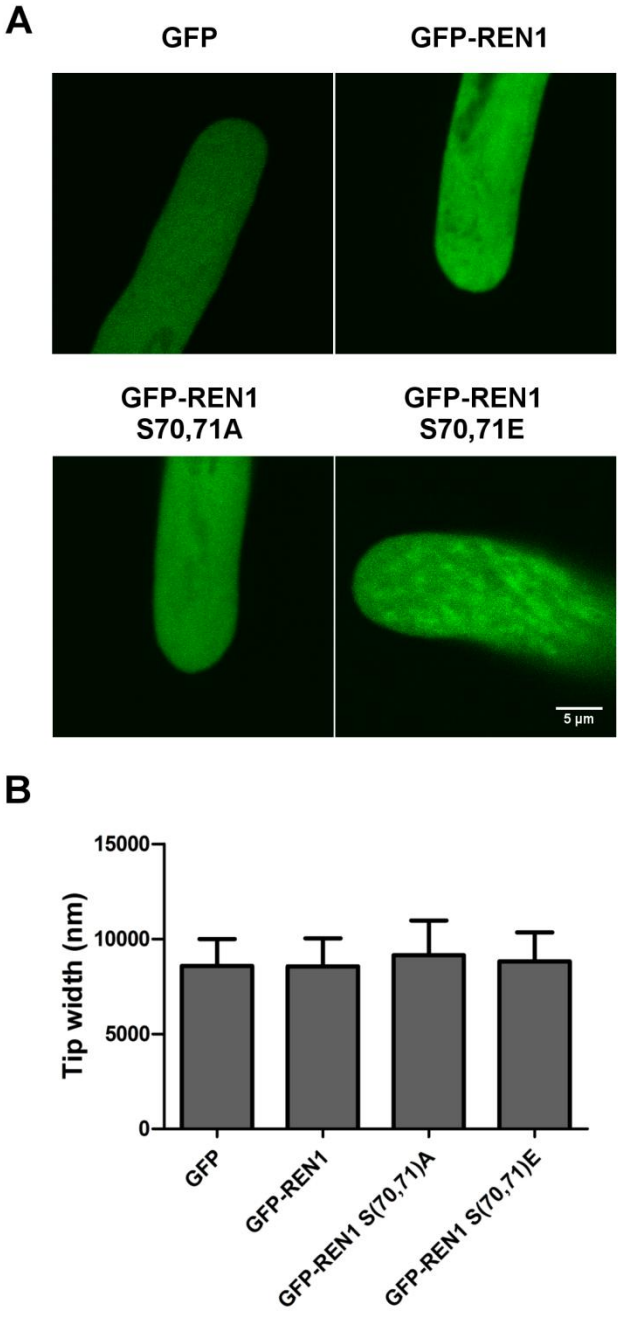
A
GFP
GFP-REN1
GFP-REN1
S70,71A
GFP-REN1
S70,71E
5 µm
B
Tip width (nm)
15000
10000
5000
0
GFP
GFP-REN1
GFP-REN1 S(70,71)A
GFP-REN1 S(70,71)E

Figure 2.7. Transient co-expression analysis of RFP-ROP1 and GFP-REN1 Ser$_{70,71}$ mutants in tobacco pollen tubes. A) Nonphophorylated REN1 mutant (REN1 $S_{70,71}A$) suppressed GFP-ROP1 OX phenotype similar as WT REN1. Meanwhile, phosphomimic REN1 mutant (REN1 $S_{70,71}A$) cannot suppress GFP-ROP1 OX phenotype. B) Tip width quantification from each transient expression. Phosphomimic REN1 mutant (REN1 $S_{70,71}E$) showed similar tip width as GFP-ROP1 OX pollen tubes.

Figure 2.7.

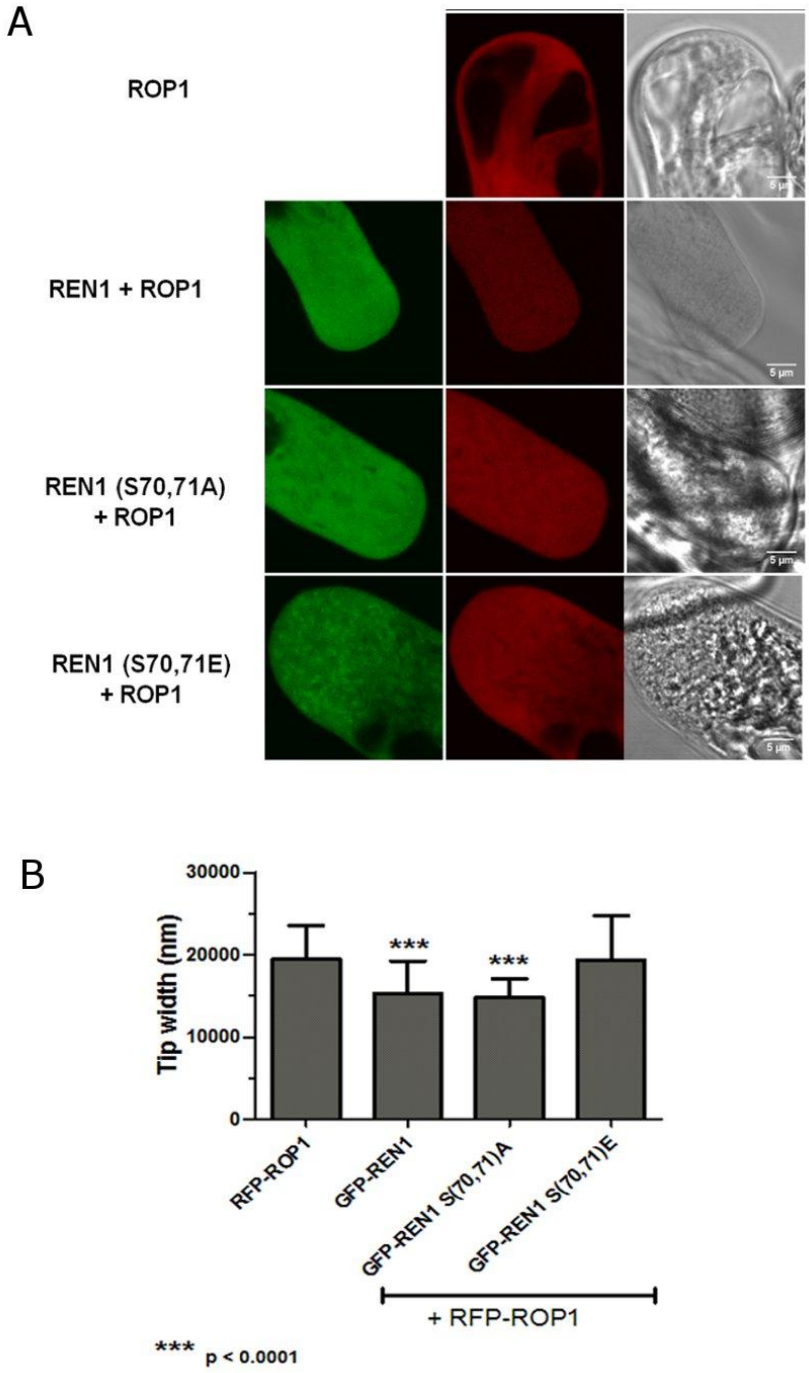
A
ROP1
REN1 + ROP1
REN1 (S70,71A)
+ ROP1
REN1 (S70,71E)
+ ROP1
5 µm
B
Tip width (nm)
30000
20000
10000
0
***
***
RFP-ROP1
GFP-REN1
GFP-REN1 S(70,71)A
GFP-REN1 S(70,71)E
+ RFP-ROP1
*** p < 0.0001

Figure 2.8. Model for the regulation of REN1 activity following phosphorylation within the PH and GAP domain. A) In vitro condition of REN1 phosphorylation by CPK16. At this condition, Ser_{70} and Ser_{267} (as well as other residues not pictured) can be phosphorylated. B) In vivo condition of REN1 phosphorylation by CPK16. At this condition, PH domain residues interact with the phospholipid PIP_2 at the PM and possibly prevent phosphorylation at Ser_{70} but not at Ser_{267}.

Figure 2.8.

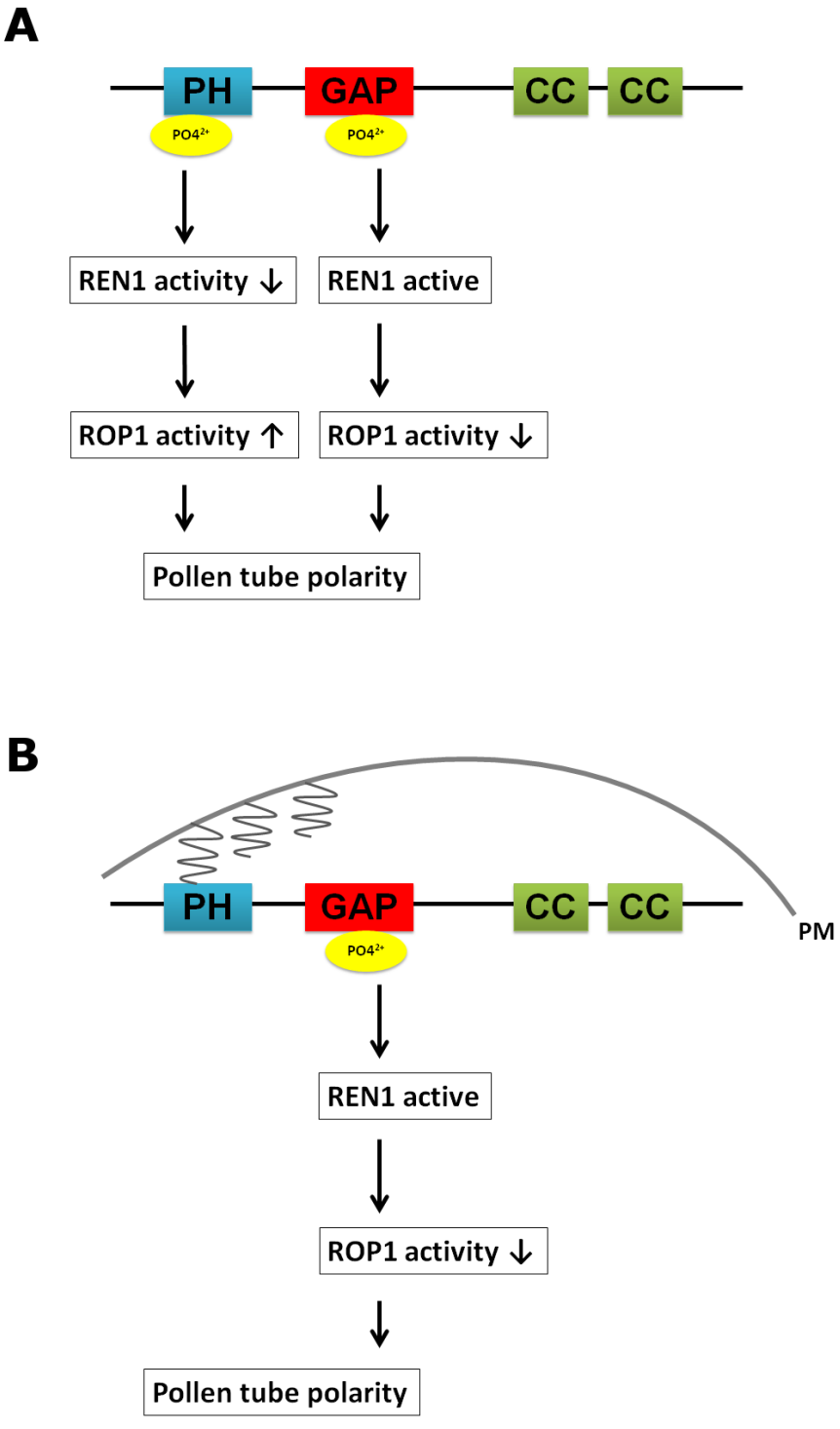
A
PH
GAP
CC
CC
PO4 2+
PO4 2+
REN1 activity ↓
REN1 active
ROP1 activity ↑
ROP1 activity ↓
Pollen tube polarity
B
PH
GAP
CC
CC
PM
PO4 2+
REN1 active
ROP1 activity ↓
Pollen tube polarity

Table 2.1. REN1 calcium-dependent phosphorylated sites by CPK16. Phosphorylation mutations were made at the residues indicated.

Table 2.1.

Residue	**Phosphopeptides**	**Domain**
Ser70	R.GGNTVFKSGPLSI**S**SK.G	PH
Thr151	K.AD**T**MELDLHEWK.A	PH
Ser267	K.GKNEF**S**PEEDAHIIADCLK.Y	GAP

Chapter 3

Functional characterization of CPK16 role in pollen tube growth

ABSTRACT

Polarized growth in pollen tube requires complex signaling events including ROP1 GTPase pathway and calcium signaling. Our previous data show that a calcium sensor, calcium-dependent protein kinases 16 (CPK16) can phosphorylate REN1 *in vitro* to modulate REN1 activity. CPK16 is expressed in mature pollen consistent with REN1 expression. Physiologically, loss-of-function *cpk16-3* mutant displayed enhanced pollen tube growth in low calcium media which is largely due to enhanced growth rate and germination frequency, but no polarity defect. Interestingly, depolarized growth and wider pollen tubes of *cpk16-3* mutant can be induced with chemical treatments of either brefeldin A (BFA) or latrunculin B (LatB). This enhanced phenotype somewhat mimic the same effects produced by chemical treatments of partially complemented *ren1-1 Lat52::GFP-REN1*. Thus CPK16 seems to partially regulate REN1 activity which explains the enhanced growth phenotype but not polarity defect in *cpk16-3* mutant and depolarized growth phenotype when REN1 tip-targeting is disrupted in chemical treatments. To test for genetic redundancy, T-DNA insertion mutant of CPK18 *cpk18-3* and double mutant *cpk16-3cpk18-3* were analyzed. *cpk18-3* mutant did not display any growth defect while double mutant *cpk16-3cpk18-3* displayed similar phenotype as *cpk16-3*. BFA and LatB treatments of *cpk16-3cpk18-3* resulted in slightly enhanced resistant to BFA as well as enhanced tip swelling with LatB treatments. This suggests that some redundancy may be present between CPK16 and CPK18. Thus the evidence presented here seem to indicate that CPK16 is involved in the regulation of pollen tube growth and polarity through ROP1/REN1 pathway.

INTRODUCTION

Pollen tube is essential for the success of plant reproduction since it serves as a key instrument in delivering sperm cells contained within it to the egg cells located in the ovary within the stigma (Waterings and Russell, 2004; Lord and Russell, 2002). Pollen tubes, similar to fungal hyphae or plant root hairs, grow by polarized tip growth which is a fast extension of the tip region resulted from complex interactions between many cell signaling processes including calcium signaling and the ROP1 pathway (Zonia, 2010; Krichevsky et al., 2007). Normal pollen tube tip growth requires certain tip calcium level/characteristics termed "calcium signatures" which are recognized by calcium binding proteins/sensors. One of the well studied calcium sensors are calcium-dependent protein kinases (CDPKs/CPKs). Several CPKs have been attributed to function in regulating pollen tube growth, polarity, or guidance. Pollen-expressed CPK17, and its homolog CPK34, have been shown to regulate pollen tube growth and guidance since *cpk17-2cpk34-2* or *cpk17-2cpk34-2*/+ showed reduced seed set and defect in ovule sensing (Myers et al., 2009). Overexpression of PiCDPK1, petunia ortholog of AtCPK17, and its dominant negative DN-PiCDPK1 resulted in tip swelling phenotype which mimics ROP1/CA-rop1 OX while CA-PiCDPK1 OX inhibited tube growth similar to DN-rop1 OX (Yoon et al., 2006). CPK32 OX resulted in swollen tubes similar to ROP1 OX (Zhou et al., 2009). Although the OX of some CPKs resulted in depolarized pollen tube phenotype which suggests its involvement in regulating tip polarity, there has been no report linking CPKs to the regulators of tip growth. One speculation based on PiCDPK1 studies was that CDPK phosphorylates inhibitor of tip growth activator to

promote activator activation and pollen tube growth (Yoon et al., 2006). It remains to be investigated whether this speculation holds true. Thus, in this study we present the first investigation of possible link between CPK16 and ROP1/REN1 pathway in regulating pollen tube growth and polarity.

MATERIALS AND METHODS

Plant materials and growth condition

Arabidopsis plants were grown at 22^{o}C growth room under 16 h light and 8 h dark. Tobacco plants were grown at 28^{o}C growth room under natural light. T-DNA insertion lines were annotated from T-DNA Express website (http://signal.salk.edu/cgi-bin/tdnaexpress) and obtained from either Salk or GABI-KAT T-DNA lines. The stock numbers for each insertions are as followed: *cpk16-1* (SALK 020716), *cpk16-2* (SALK 052257), and *cpk16-3* (GABI 226C09).

Cloning

REN1 phosphorylation mutants were generated using primers which carry mutations on the phosphorylated residues. The primer sets are as follows: REN1(S267A)-F GGAAAAAATGAGTTCGCTCCCGAGGAGG and REN1(S267A)-R CCTCCTCGGGAGCGAACTCATTTTTTCC; REN1(S267E)-F GGAAAAAATGAGTTCGAACCCGAGGAGG and REN1(S267E)-R CCTCCTCGGGTTCGAACTCATTTTTTCC. REN1 transient expression constructs were generated using PCR and subcloning into a pUC19-based vector harboring *Lat52* promoter fused to mGFP. REN1 stable expression constructs were generated by

subcloning PCR product into Gateway entry and destination vector (Invitrogen Corporation, Carlsbad, CA). CPK16 transient expression constructs were generated using PCR and subcloning into a pUC19-based vector harboring *Lat52* promoter fused to mGFP to produce C-terminal mGFP fusion. CPK16 stable expression constructs were generated by subcloning PCR product into Gateway entry and destination vector (Invitrogen Corporation, Carlsbad, CA).

T-DNA mutant analysis

T-DNA lines were confirmed using the recommended primers as obtained from the T-DNA Express website (http://signal.salk.edu/cgi-bin/tdnaexpress). The primers sets are as followed: for *cpk16-1*, LBb1.3 + R primer CAAGCCAGTATGCTGCAAAA (to check insertion) and F primer AATCAACCGAAGAAGATTCGC + R primer CAAGCCAGTATGCTGCAAAA (to check for homozygosity of insertion); for *cpk16-2*, LBb1.3 + F primer TATGCGAGGGTGGTGAATTAC (to check insertion) and F primer TATGCGAGGGTGGTGAATTAC + R primer ATCAATCGCATCAAACTGGTC (to check for homozygosity of insertion); and for *cpk16-3*, GABI-F + F primer TCTAGAATGGGTCTCTGTTTCTCC (to check insertion) and F primer TCTAGAATGGGTCTCTGTTTCTCC + R primer ATCAATCGCATCAAACTGGTC (to check for homozygosity of insertion); for *cpk18-2*, LBb1.3 + F primer GGTCTCTGTTTCTCGTCTCCTAAA (to check insertion) and F primer GGTCTCTGTTTCTCGTCTCCTAAA + R primer GAGCAGAATGTAAGTGATGACACC (to check for homozygosity of insertion); and for *cpk16-3*, GABI-F + F primer GAAAACCAAGTAAGCTCCCTCTCT (to check insertion) and F primer GAAAACCAAGTAAGCTCCCTCTCT + R primer GAGCAGAATGTAAGTGATGACACC (to

check for homozygosity of insertion).. DNA bands obtained from PCR products were extracted from the gel and sent to sequencing to confirm insertion sites.

RT-PCR

RT-PCR primers to check expression levels are as followed: for REN1 expression, F primer TGACCGTGGCAATAGGGTAA and R primer CACAGGGATCTGAGGACTACACGGAT (product size is 450 bp); for CPK16 expression, F primer ATTTACGCGGTTTGGTTCAC and R primer TACATTCTTCTCTGCGGGAGA (product size is 260 bp). ACT3 is used as a control: F primer GAAGATATTCAACCCCTTGTCTGT and R primer ATCTGAGTCATCTTCTCACGGTTA (product size is 350 bp).

In vitro pollen germination

Pollen grains were collected from open and mature flowers. Arabidopsis pollen was germinated on agar medium containing 18% sucrose, 0.01% H_3BO_3, 1 mM MgSO4, 2.5 mM $CaCl_2$, 2.5 mM $Ca(NO_3)_2$, and 0.45% agar, pH 7. Tobacco pollen was germinated on liquid medium containing 18% sucrose, 0.01% boric acid, 1 mM MgSO4, 5 µM $CaCl_2$, 5 µM $Ca(NO_3)_2$, pH 7. Pollen tubes were grown in 28^{o}C water bath for 3 – 6 hour. Variation of calcium concentration in Arabidopsis germination media was achieved by adjusting the amount of $CaCl_2$ and $Ca(NO_3)_2$ added. For example, 0.5 mM calcium-containing media contains of 0.25 mM $CaCl_2$ and 0.25 mM $Ca(NO_3)_2$.

Chemical treatments

Chemicals were added onto germination media prior to pollen tube germination. BFA stock concentration was 1 mg/mL prepared in DMSO and LatB stock concentration was 1 mM in DMSO.

Microscopy

For phenotypic analysis and chemical treatments, Nikon TE300 Eclipse inverted microscope (Nikon Instruments, Melville, NY) was utilized. For fluorescence observation and oscillation studies, confocal microscope Leica SP2 (Leica, Wetzlar, Germany) was used. Most images were obtained using either a 20x or a 63x water-immersion lens, zoomed 4x to 8x with 524 x 524 frame and 400-Hz scanning speed. Time-lapse images were obtained at 1 – 3 sec intervals.

Image Analysis

Image analysis such as pollen tube length and tip width measurements were performed using Metamorph software (Molecular Devices, Sunnyvale, CA). Pollen tube growth oscillation analyses were performed using ImageJ 1.43u software as available from http://rsbweb.nih.gov/ij/ (Abramoff et al., 2004; Rasband, 1997).

RESULTS

CPK16 is involved calcium-dependent regulation of pollen tube growth

Reverse transcriptase-PCR (RT-PCR) analysis showed that *CPK16* was expressed in mature flowers which contain mature pollen grains. Its expression was not detected in other tissues tested which included cotyledon, mature leaf, stem, cauline leaf, and silique

(Figure 3.1A). To investigate the role of CPK16 in regulating pollen tube growth, *CPK16* T-DNA insertion lines were characterized. Three T-DNA insertion lines were obtained from T-DNA Express: *cpk16-1* (SALK 020716), *cpk16-2* (SALK 052257), and *cpk16-3* (GABI 226C09). T-DNA insertion in *cpk16-1* line as annotated in T-DNA Express cannot be determined and no further analysis was done on these lines. *cpk16-2* insertion was confirmed to be within the 5^{th} intron by sequencing of PCR product. However, *cpk16-2* insertion lines did not display any pollen tube defects when grown in different Ca^{2+} conditions (data not shown). *cpk16-3* insertion was confirmed to be within the 6^{th} exon as annotated (Figure 3.1B). The 6^{th} exon of *CPK16* encodes CPK16 kinase domain which suggests that *cpk16-3* mutant likely produce truncated protein with partial kinase region. Furthermore, reverse transcriptase-PCR analysis of *cpk16-3* revealed that this mutation is a loss-of-function mutation (Figure 3.1C) suggesting that no protein products are made.

For phenotypic analysis of *cpk16-3* mutant, pollen tubes were germinated in different Ca^{2+} condition to determine any defects in Ca^{2+} sensing. Tubes grown in optimal germination media (5 mM Ca^{2+}) had a similar phenotype and tube growth as the *Col-0* wild type (WT) control (Figure 3.2A, B). Similarly, tubes grown in high Ca^{2+} media (20 mM) had a similar phenotype but shorter tubes compared to the WT control (Figure 3.2A, B; $p \leq 0.0001$). The shorter tubes in *cpk16-3* seemed to be due to earlier pollen tubes bursting compared to WT. In contrast, tubes grown in low Ca^{2+} media (0.2 mM) had a higher germination frequency and growth rate than the WT control (Figure 3.2A, B; $p \leq 0.0001$). These results seem to suggest that CPK16 is involved in suppressing pollen tube

growth in low Ca^{2+} media and as such, *cpk16-3* mutant is unable to detect the low extracellular Ca^{2+} level which then results in enhanced pollen tube growth.

Further analysis of the distribution frequencies for pollen tubes length were performed on *cpk16-3* tubes grown in different Ca^{2+} media, 3h and 5h after germination. In optimal Ca^{2+} media, the tube length distribution frequency between the *cpk16-3* and WT were comparable either 3h or 5h after germination, as expected from the results obtained previously (Figure 3.3B, E). Similar observation was also found in high Ca^{2+} media where the tube length distribution frequency between *cpk16-3* and WT was similar (Figure 3.3C, F); although, the amount of shorter pollen tubes was higher in *cpk16-3* compared to WT; for e.g. at 3HAG, 47.9% of *cpk16-3* pollen tubes reached 100 – 200 µm in length while only 18.6% of WT pollen tubes reached the same length (Figure 3.3C). In contrast, in low Ca^{2+} media, the pollen tube length distribution frequency was dramatically higher in the *cpk16-3* than the WT (Figure 3.3A, D) such that 3h after germination, 39.3% of *cpk16-3* pollen tubes had reached 200 – 300 µm in length while 46.4 % of WT pollen tubes had only reached 0 – 100 µm in length (Figure 3.3A). The higher distribution frequencies of pollen tube length in low Ca^{2+} media further show that CPK16 is involved in inhibiting pollen tube growth in response to extracellular low Ca^{2+} concentration.

***cpk16-3* pollen tubes enhanced growth can be contributed to higher growth rate and germination rate**

To further understand the enhanced pollen tube growth of *cpk16-3* mutant in low Ca^{2+} media, the growth patterns such as germination frequency, growth rate, and growth

oscillation were analyzed. In optimal Ca^{2+} media, *cpk16-3* pollen tubes display higher germination frequency compared to WT (Figure 3.4A, B). Even at 25 minutes after germination (MAG), *cpk16-3* pollen germination rate of 2.8% was 10 fold higher than the WT, and the same was observed at 1 HAG with rate of 11.5%. After 3H, the germination frequency of both genotypes reached above 60%. Similarly, in low Ca^{2+} media, *cpk16-3* pollen tubes also displayed higher germination frequency compared to WT especially at 3HAG when it reached 54% compared to 11% of WT pollen germination (Figure 3.4C, D). These results suggest that CPK16 negatively regulates Ca^{2+}–dependent pollen tube germination rate. With respect to growth rate which was measured from time recordings of pollen tube growth over the course of 3 – 5 minutes, it can be observed that in optimal Ca^{2+} condition, WT pollen tubes had higher growth rate of 37.9 nm/sec (± 7.0 nm/sec) compared to *cpk16-3* pollen tubes of 22 nm/sec (± 12.9 nm/sec). Interestingly, *cpk16-3* pollen tubes grown in low Ca^{2+} condition had a comparable growth rate of 37.9 nm/sec (± 11.4 nm/sec) to WT pollen tubes grown in optimal Ca^{2+} media. Meanwhile, WT pollen tubes grown in low Ca^{2+} media hardly grew within the time span of the experimental observations and so definite growth rate cannot be determined. However, it can be extrapolated based on the pollen tube length data that the growth rate is likely to be ~10 nm/sec, with the assumption that the growth rate is linear. Thus in addition to CPK16 role in inhibiting pollen tube germination, it also likely to have a role in controlling pollen tube growth rate in certain calcium condition.

Pollen tubes oscillatory growth has been reported in both lily and tobacco (Cardenas et al., 2008; Hwang et al., 2005; Holdaway-Clarke et al., 1997; Messerli and

Robinson, 1997; Pierson et al., 1996). Depending on growth oscillation period and frequency, pollen tube growth rates can vary between species. Thus it is possible that the enhanced growth phenotype in *cpk16-3* mutant may be due to the changes in growth oscillation frequency. However, pollen tube growth oscillation, though implied based on other species to oscillate in every 20 – 30 sec, has not been definitively reported in Arabidopsis and as such, its involvement in Arabidopsis pollen tubes needs to be carefully observed. For this analysis, growth oscillation was resolved by obtaining time lapse images of growing pollen tubes using Leica SP2 microscope 40x lens that scans every 1s 635ms or every 3s 325ms. Time lapse images were compiled to generate movies where growth was measured using overlapping successive time images. Using these measurements, growth curves were generated as a function of growth rate over time.

Unlike the growth oscillation pattern observed in lily and tobacco pollen tubes marked by a period of rapid growth and a period of slow growth, we were not able to observe the same for Arabidopsis pollen tubes. Instead, the oscillation patterns, if at all, were more irregular in either WT or *cpk16-3* mutant (Figure 3.5 and 3.6). A somewhat regular oscillation can only be observed in slow-growing pollen tubes (growth rate $\leq$ 20 nm/sec) (Figure 3.5G). As pollen tubes grow faster (growth rate > 20 nm/sec), it seems that the 'regular' growth oscillation can hardly be observed. Though the growth patterns vary between WT and *cpk16-3* pollen tubes, the period between growth spikes are quite obvious when tubes were grown in low Ca^{2+} media. The noticeable difference between the two genotypes was the lack of growth spikes in WT pollen tubes grown in low Ca^{2+} media. At this condition, pollen tube growth was not abolished since growth spikes can

still be observed at very low frequency (Figure 3.6A, B). Thus this observation seems to be consistent with the fact that WT pollen tubes grown in low Ca^{2+} media had very low growth rate and thus short tubes compared to those grown in optimal Ca^{2+} media. Unlike WT, *cpk16-3* pollen tubes in low Ca^{2+} media displayed growth spikes and oscillation patterns that were similar to both genotypes grown in optimal Ca^{2+} media. Thus it is consistent with the fact that this mutant had a high growth rate of 37.9 nm/sec at this condition. These observations imply that when CPK16 is nonfunctional, the cellular mechanisms driving pollen tube growth and germination frequency were not regulated properly which then allows for enhanced growth at condition that may not be favorable such as low Ca^{2+} environment.

cpk16-3 **displays wider tube and tip swelling phenotype with BFA and LatB treatment**

REN1 localization to the exocytic vesicles has been shown to be important for its activity (Hwang et al., 2008). This is evident from the observation that disruption of such localization by brefeldin-A (BFA) and latrunculinB (LatB) treatment led to shorter and swollen tubes (Hwang et al., 2008). BFA is a fungal metabolite that disrupts vesicle trafficking, targeting of secretory vesicles, and vacuolar protein transport (Rojas et al., 1999; Nebenfuhr et al., 2002; Wang et al., 2005; Zhang et al., 2010) while LatB is one of two marine compounds found to disrupt actin polymerization (Spector et al., 1989; Gibbon et al., 1999). The two processes regulated by these compounds are interconnected since actin dynamics is involved in the regulation of vesicle trafficking including F-actin-dependent tip targeting of exocytic vesicles (Lee et al., 2008; Zhang et al., 2010). To

address the involvement of CPK16 in regulating REN1, BFA and LatB treatments were performed in *cpk16-3* mutant. We reasoned that in this mutant, REN1 activity is likely reduced and further inhibition of REN1 tip-directed targeting may result in enhanced *cpk16-3* mutant phenotype. Treatment of WT pollen tubes with 0.1 µg/mL BFA for 20 – 30 min resulted in some growth retardation (Hwang et al., 2008). However, in this assay, since pollen grains were germinated and grown in the presence of chemical, no WT tube germination was observed at 0.1 µg/mL. (Figure 3.7A). Interestingly at this condition, *cpk16-3* mutant tubes display some resistant to the BFA treatment since germination and growth can still be observed (Figure 3.7A) but were completed abolished at higher concentration of 0.15 µg/mL BFA (data not shown). Treatment of as low as 0.05 µg/mL of BFA in WT pollen tubes produced slightly enhanced tip width but the same treatment in *cpk16-3* pollen dramatically produced a significant increase in tip width ($p < 0.0001$; Figure 3.7A, B). In both cases, reduced pollen tube length was also observed (Figure 3.7A, C). This enhanced swelling phenotype observed in *cpk16-3* pollen somewhat mimic, though not as severe, that of BFA treatment of partially complemented *ren1-1 Lat52::GFP-REN1* (Hwang et al., 2008). This suggests that in *cpk16-3* mutant, REN1 partial activity may likely be present and is only completely abolished when REN1 tip targeting is prevented via BFA treatment.

Similar to BFA results, LatB treatment also affected pollen tube growth and tip width (Figure 3.8A, B, C). Treatment of WT pollen tubes with 1.5 nM LatB completely inhibited germination while that of *cpk16-3* mutant still germinated up to 2.0 nM LatB (Figure 3.8A). Consistent with the BFA resistant previously observed, *cpk16-3* mutant

tubes are also more resistant to LatB treatment than WT control. LatB treatment of WT pollen tubes slightly enhanced tip width but the same treatment of *cpk16-3* mutant dramatically enhanced tip width with as little as 1 nM LatB and almost two-fold enhancement in 2 nM LatB treatment (Figure 3.8A, B). In contrast, pollen tube length was not inhibited up to 1 nM LatB treatment in WT but was dramatically inhibited in *cpk16-3* mutant tubes (Figure 3.8C). Overall, these enhanced swelling phenotypes observed in *cpk16-3* pollen with LatB treatment is consistent with BFA treatment as well as what was previously reported for the same treatments in partially complemented *ren1-1 Lat52::GFP-REN1* (Hwang et al., 2008). These further suggest that in *cpk16-3* mutant, REN1 partial activity may likely be present and is only completely abolished when REN1 tip targeting is prevented via inhibition of either exocytosis or actin-mediated tip targeting.

Mutation in CPK16 homolog, CPK18, did not result in abnormal pollen phenotypes and *cpk16-3cpk18-3* pollen displayed similar phenotypes as *cpk16-3*

To determine whether genetic redundancy takes place to compensate for the loss of CPK16 activity in *cpk16-3* mutant, CPK16 homolog, CPK18, was analyzed. Phylogenetic analysis of Arabidopsis CPKs revealed that CPK16 belongs to the least complex subgroup IV which also includes CPK18 and CPK28 (Cheng et al., 2002). The similarity between full length protein of CPK16 and CPK18 is ~76% and between the kinase domain ~84%. In addition, microarray studies have identified CPK18 to be expressed in mature pollen in a very low level (Becker et al., 2003). To investigate the role of CPK18 in regulating pollen tube growth, *CPK18* T-DNA insertion lines were

characterized. Three T-DNA insertion lines were purchased from T-DNA Express: *cpk18-1* (SALK 061352), *cpk18-2* (SALK 069578), and *cpk18-3* (GABI 071G03). *cpk18-1* was unavailable. Nevertheless, both *cpk18-2* and *cpk18-3* were analyzed and theirs insertions confirmed as annotated to be within the 2th intron and the 6th exon. Phenotypic analysis showed that both insertion lines did not display any pollen tube defects when grown in different Ca^{2+} conditions (Figure 3.9; data shown only for *cpk18-3* mutant). However, reverse transcriptase-PCR analysis of *cpk18-3* was not able to confirm whether these mutations are loss-of-function mutations and this is likely due to the very low expression level of the transcript since our attempt to amplify *CPK18* cDNA has been unsuccessful thus far. Nevertheless, since *cpk18-3* line has T-DNA inserted in the exon 6 which encodes the kinase domain, it is likely that the CPK18 transcripts in this line are nonfunctional. To determine whether CPK18 is genetically redundant to CPK16, double mutant *cpk16-3cpk18-3* was generated. Phenotypic observation of *cpk16-3cpk18-3* tubes grown in different calcium media seems to suggest that the phenotypes mimic those of *cpk16-3* mutant (Figure 3.9). As such, in low calcium condition, *cpk16-3cpk18-3* tubes displayed enhanced germination frequency and enhanced growth rate (Figure 3.9). It is possible that CPK18 does not play a major role in regulating pollen tube growth unlike CPK16, and therefore no significant change in pollen tube phenotypes was observed in *cpk16-3cpk18-3.*

cpk16-3cpk18-3 displays wider tube and tip swelling phenotype with BFA and LatB treatment

To address whether *cpk16-3cpk18-3* displays enhanced phenotypes compared to *cpk16-3* with respect to chemical treatments, we also germinated and grown *cpk16-3cpk18-3* pollen tubes with either BFA or LatB. *cpk18-3* pollen tubes responses to either treatments were similar to WT pollen tubes which included inhibition of germination and growth with increasing concentration but did not severely affect pollen tube tip width (Figure 3.10 and 3.11). In contrast, *cpk16-3cpk18-3* mutant tubes seemed to display similar phenotypes as *cpk16-3* tubes such as resistant to the chemical treatments and significantly enhanced tip width (Figure 3.10 and 3.11). With BFA treatment, the tip width and tube length were comparable between *cpk16-3cpk18-3* and *cpk16-3* tubes; however few *cpk16-3cpk18-3* tubes still germinated in 0.15 µg/mL BFA while no germination was observed in *cpk16-3* tubes at the same condition (Figure 3.10; data not shown for *cpk16-3*). With respect to LatB treatment, the tip width was more enhanced in *cpk16-3cpk18-3* than *cpk16-3* tubes (Figure 3.11A, B). In addition, *cpk16-3cpk18-3* pollen tube length was longer at 0.8 nM LatB compared to the same treatment in *cpk16* tubes (Figure 3.11A, C). Overall, both BFA and LatB treatments suggest slightly enhanced phenotypes either in the form of enhanced resistant or enhanced tip width in *cpk16-3cpk18-3* compared to single mutants *cpk16-3* or *cpk18-3*. This suggests that some redundancy may occur between CPK16 and CPK18. It remains to be investigated whether other CPKs not currently studied may be genetically redundant to CPK16 as well.

DISCUSSION

Here we presented evidence of the role of CPK16 in regulating pollen tube growth and germination in a calcium-dependent manner. Our data indicate that CPK16 is involved in calcium sensing and calcium response to negatively regulate the proper pollen tube germination and growth in low extracellular calcium condition. However, *cpk16-3* single mutant did not display tip polarity phenotype as expected if it is to be involved in regulating pollen tube polarity. Based on our analysis on REN1 phosphorylation by CPK16 and *cpk16-3* mutant phenotype, it is likely that REN1 activity is reduced due to reduced phosphorylation in *cpk16-3* mutant but not completely abolished since polarity loss associated with the absence of REN1 activity was not observed (Figure 3.12). Interestingly, only when *cpk16-3* mutants were treated with BFA, which inhibits exocytosis, or LatB, which inhibits actin polymerization and tip-directed targeting of secretory vesicles, then tip swelling phenotypes can be observed. These phenotypes mimic those observed with the same chemical treatments of partial complemented *ren1-1 Lat52::GFP-REN1* (Hwang et al., 2008) which suggests that CPK16 may indeed be involved in ROP1 pathway via its partial regulation of REN1 activity.

To elucidate the CPK16's functions in regulating REN1 activity, a model incorporating the phenotypes observed in *cpk16-3* mutant and chemical treatments is presented (Figure 3.12). In this model, we speculated that the highly dynamic REN1 exists in heterogeneous populations of phosphorylated and nonphosphorylated states at the apical region and at the exocytic vesicles. It is assumed that REN1 population at the

apical region is mainly phosphorylated at S_{267} and few nonphosphorylated at S_{70} and S_{267}. REN1 S_{267} is active in negatively regulating ROP1 activity at the apical PM leading to normal pollen tube tip growth in the WT background. Such may not be the case in *cpk16-3* background where REN1 S_{267} still has some activity but not complete in controlling ROP1 activity which then resulted in enhanced pollen tube growth with no polarity defect possibly due to increased ROP1 activation. Finally, only with additional treatment of BFA or LatB which likely inhibits the tip-directed targeting of the limited REN1 S_{267} then depolarized growth phenotype can be observed as a result of much enhanced ROP1 activity..

Since *cpk16-3* mutant phenotype did not result in polarity defect and such depolarized growth can only be enhanced with BFA or LatB treatment, other CPKs may potentially play a role in compensating for the loss of CPK16. Although CPK18 is the closest homolog to CPK16, it does not seem to play a major role in regulating pollen tube growth even in the absence of CPK16. The double mutant *cpk16-3cpk18-3* only displayed slightly enhanced phenotypes with BFA or LatB treatment. Another close homolog of CPK16, CPK28, expresses highly in vegetative tissues but not in mature pollen as reported in microarray studies. *CPK28* single mutants did not display any pollen tube defects (data not shown). It remains to be investigated whether CPK28 may be genetically redundant to CPK16. In addition, it is also possible that other CPKs may be involved in the feedback regulation of ROP1 pathway. Here, we presented the initial study of characterizing a potential regulator linking calcium signaling and ROP1 pathway. Our findings will provide future insights into the identifications of more CPKs

which are likely involved in regulating pollen tube polarity via negative feedback regulation of ROP1 pathway.

REFERENCES

Abramoff, M. D., Magalhaes, P. J., and Ram, S. J. (2004) Image processing with ImageJ. Biophotonics Int. **11(7)**: 36 – 42

Becker, J. D., Boavida, L. C., Carneiro, J., Haury, M., and Feijo, J. A. (2003) Transcriptional profiling of Arabidopsis tissues reveals the unique characteristics of the pollen transcriptome. Plant Physiol. **133**: 713 – 725

Cardenas, L., Lovy-Wheeler, A., Kunkel, J. G., and Hepler, P. K. (2008) Pollen tube growth oscillations and intracellular calcium levels are reversibly modulated by actin polymerization. Plant Physiol. **146**: 1611 – 1621

Cheng, S-H., Willmann, M. R., Chen, H-C., and Sheen, J. (2002) Calcium signaling through protein kinases. The *Arabidopsis* calcium-dependent protein kinase gene family. Plant Physiol. **129**: 469 – 485

Gibbon, B. C., Kovar, D. R., and Staiger, C. J. (1999) Latrunculin B has different effects on pollen germination and tube growth. Plant Cell **11**: 2349 – 2363

Harper, J.F., Breton, G., and Harmon, A. (2004) Decoding Ca^{2+} signals through plant protein kinases. Annu. Rev. Plant Biol. **55**: 263-288

Harper, J. F. and Harmon, A. (2005) Plants, symbiosis and parasites: a calcium signaling connection. Nat. Rev. Mol. Cell Biol. **6**: 555 – 566

Holdaway-Clarke, T.L., Feijo, J.A., Hackett, G.R., Kunkel, J.G., and Hepler, P.K. (1997) Pollen tube growth and the intracellular cytosolic calcium gradient oscillate in phase while extracellular calcium influx is delayed. Plant Cell **9**: 1999-2010

Hwang, J-U., Gu, Y., Lee, Y-J., and Yang, Z. (2005) Oscillatory ROP GTPase activation leads the oscillatory polarized growth of pollen tubes. Mol. Biol. Cell **16:** 5385 – 5399

Hwang, J.U., Vernoud, V., Szumlanski, A., Nielsen, E., and Yang, Z. (2008) A tip-localized RhoGAP controls cell polarity by globally inhibiting Rho GTPase at the cell apex. Curr. Biol. **18**: 1907-1916

Krichevsky, A., Kozlovsky, S. V., Tian, G-W., Chen, M-H., Zaltsman, A., and Citovsky, V. (2007) How pollen tubes grow. Dev. Biol. **303**: 405 – 420

Lee, Y. J., Szumlanski, A., Nielsen, E., and Yang, Z. (2008) Rho-GTPase-dependent filamentous actin dynamics coordinate vesicle targeting and exocytosis during tip growth. J. Cell Biol. **181(7)**: 1155 – 1168

Lord, E. M. and Russell, S. D. (2002) The mechanisms of pollination and fertilization in plants. Annu. Rev. Cell Dev. Biol. **18**: 81 – 105

Messerli, M. and Robinson, K. R. (1997) Tip localized Ca^{2+} pulses are coincident with peak pulsatile growth rates in pollen tubes of *Lilium longiflorum*. J. Cell Sci. 110: 1269 – 1278

Myers, C., Romanowsky, S. M., Barron, Y. D., Garg, S., Azuse, C. L., Curran, A., Davis, R. M., Hatton, J., Harmon, A. C., and Harper, J. F. (2009) Calcium-dependent protein kinases regulate polarized tip growth in pollen tubes. Plant J. **59(4)**: 528 – 539

Nebenfuhr, A., Ritzenthaler, C., and Robinson, D. G. (2002) Brefeldin A: deciphering an enigmatic inhibitor of secretion. Plant Physiol. **130(3)**: 1102 – 1108

Pierson, E.S., Miller, D.D., Callaham, D.A., van Aken, J., Hackett, G., and Hepler, P.K. (1996) Tip-localized calcium entry fluctuates during pollen tube growth. Dev. Biol. **174**: 160-173

Rasband, W. S. ImageJ, US National Institute of Health, Bethesda, Maryland, USA. http://imagej.nih.gov/ij/ 1997 – 2011

Rojas, M., Owen Jr., T. P., and Lindahl, K. N. (1999) Brefeldin A inhibits secondary cell wall synthesis in developing tracheary elements of *Zinnia elegans*. Int. J. Plant Sci. **160(4)**: 683 – 690

Spector, I., Shochet, N. R., Blasberger, D., and Kashman, Y. (1989) Latrunculins – novel marine macrolides that disrupt microfilament organization and affect cell growth: I. comparison with cytochalasin D. Cell Motil. Cyto. **13**: 127 – 144

Wang, Q., Kong, L., Hao, H., Wang, X., Lin, J., Samaj, J., and Baluska, F. (2005) Effects of brefeldin A on pollen germination and tube growth. Antagonistic effects on endocytosis and secretion. Plant Physiol. **139**: 1692 – 1703

Waterings, K. and Russell, S. D. (2004) Experimental analysis of the fertilization process. Plant Cell **16**: S107 – S118

Yoon, G. M., Dowd, P. E., Gilroy, S., and McCubbin, A. G. (2006) Calcium-dependent protein kinase isoforms in *Petunia* have distinct functions in pollen tube growth, including regulating polarity. Plant Cell **18**: 867 – 878

Zhang, Y., He, J., Lee, D., and McCormick, S. (2010) Interdependence of endomembrane trafficking and actin dynamics during polarized growth of Arabidopsis pollen tubes. Plant Physiol. **152**: 2200 – 2210

Zhou, L., Fu, Y., and Yang, Z. (2009) A genome-wide functional characterization of *Arabidopsis* regulatory calcium sensors in pollen tubes. J Integr. Plant Biol. **51(8)**: 751 – 761

Zonia, L. (2010) Spatial and temporal integration of signaling networks regulating pollen tube growth. J. Exp. Bot. **61(7)**: 1939 – 1957

Figure 3.1. CPK16 expression and mutant analysis. A) RT-PCR analysis showed that *CPK16* is expressed in mature flower. Expression is not detected in other tissues. *ACTIN 3* (*ACT3*) is used as internal control. B) *CPK16* gene structure. Black boxes indicate exons and lines between the exons indicate introns. *cpk16-3* has T-DNA insertion within the 6th exon. C) RT-PCR analysis of *cpk16-3* showed no CPK16 expression indicating loss-of-function of *cpk16-3* mutant.

Figure 3.1.

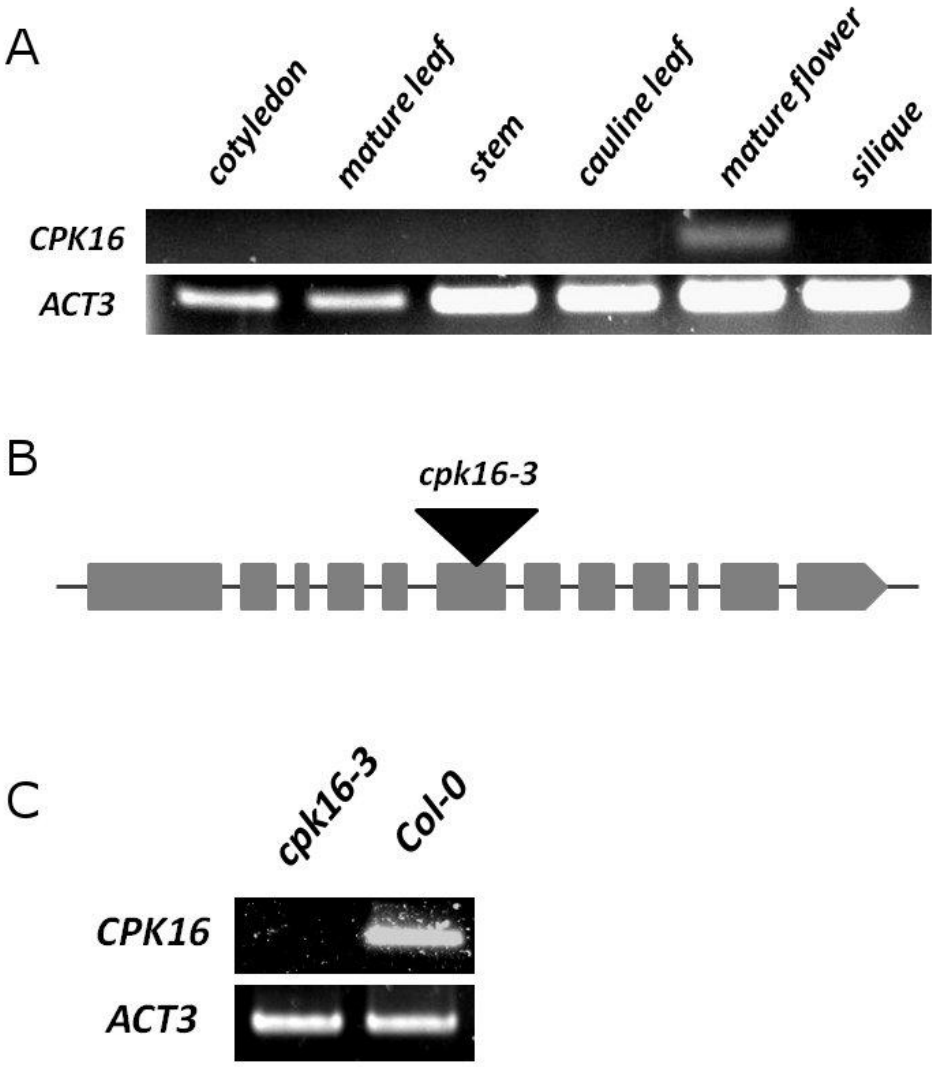
A
cotyledon
mature leaf
stem
cauline leaf
mature flower
silique
CPK16
ACT3
B
cpk16-3
C
cpk16-3
Col-0
CPK16
ACT3

Figure 3.2. In vitro pollen tube germination assay of Col-0 (WT) and *cpk16-3*. A) Pollen tubes were grown in three different Ca^{2+}-containing pollen germination media: 0.2, 5, and 20 mM Ca^{2+}. B) Quantification of pollen tube length from in vitro germination assay described in A. Each experiment was done in triplicate using pollen grains that come from three generations. Significant difference ($p < 0.0001$) was indicated by *** symbol.

Figure 3.2.

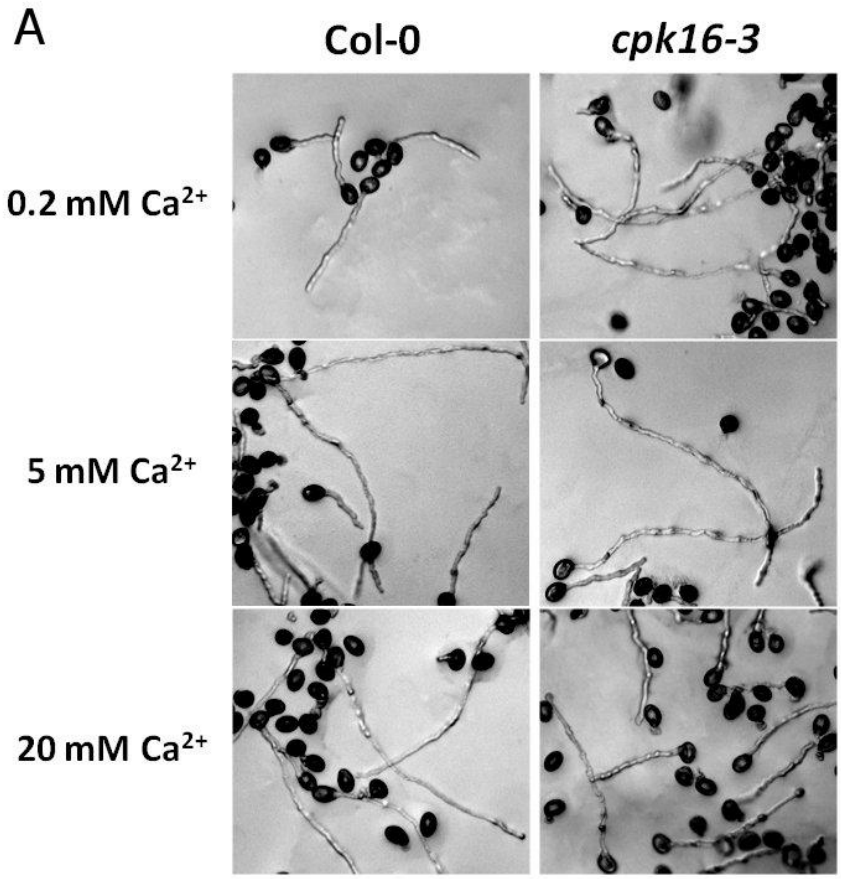
A
Col-0
cpk16-3
0.2 mM Ca2+
5 mM Ca2+
20 mM Ca2+

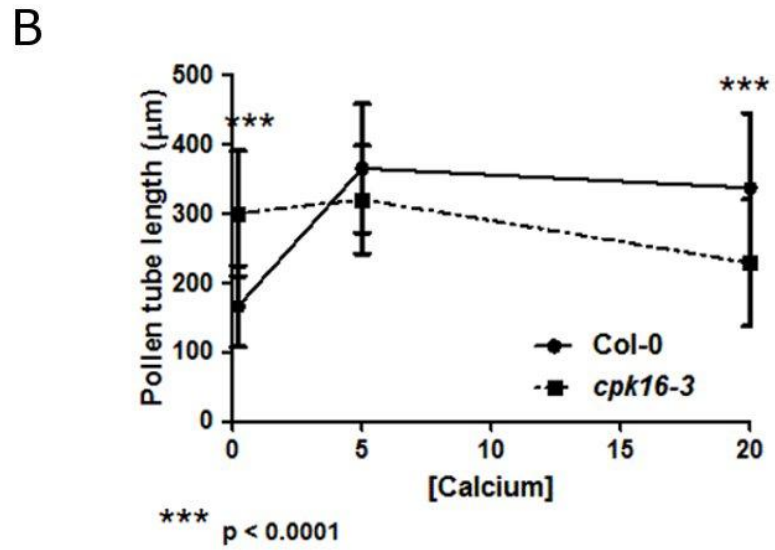
B
Pollen tube length (µm)
500
400
300
200
100
0
***
***
Col-0
cpk16-3
0
5
10
15
20
[Calcium]
*** p < 0.0001

Figure 3.3. The distribution frequencies of pollen tube length in Col-0 WT versus *cpk16-3*. Pollen tubes were grown *in vitro* in different Ca^{2+} media. A – C) measurement of pollen tube length 3 hours after germination. D – F) measurement of pollen tube length 5 hours after germination. A) and D) pollen tubes grown in 0.2 mM Ca^{2+}. B) and E). pollen tubes grown in 5 mM Ca^{2+}. C) and F). pollen tubes grown in 20 mM Ca^{2+}.

Figure 3.3.

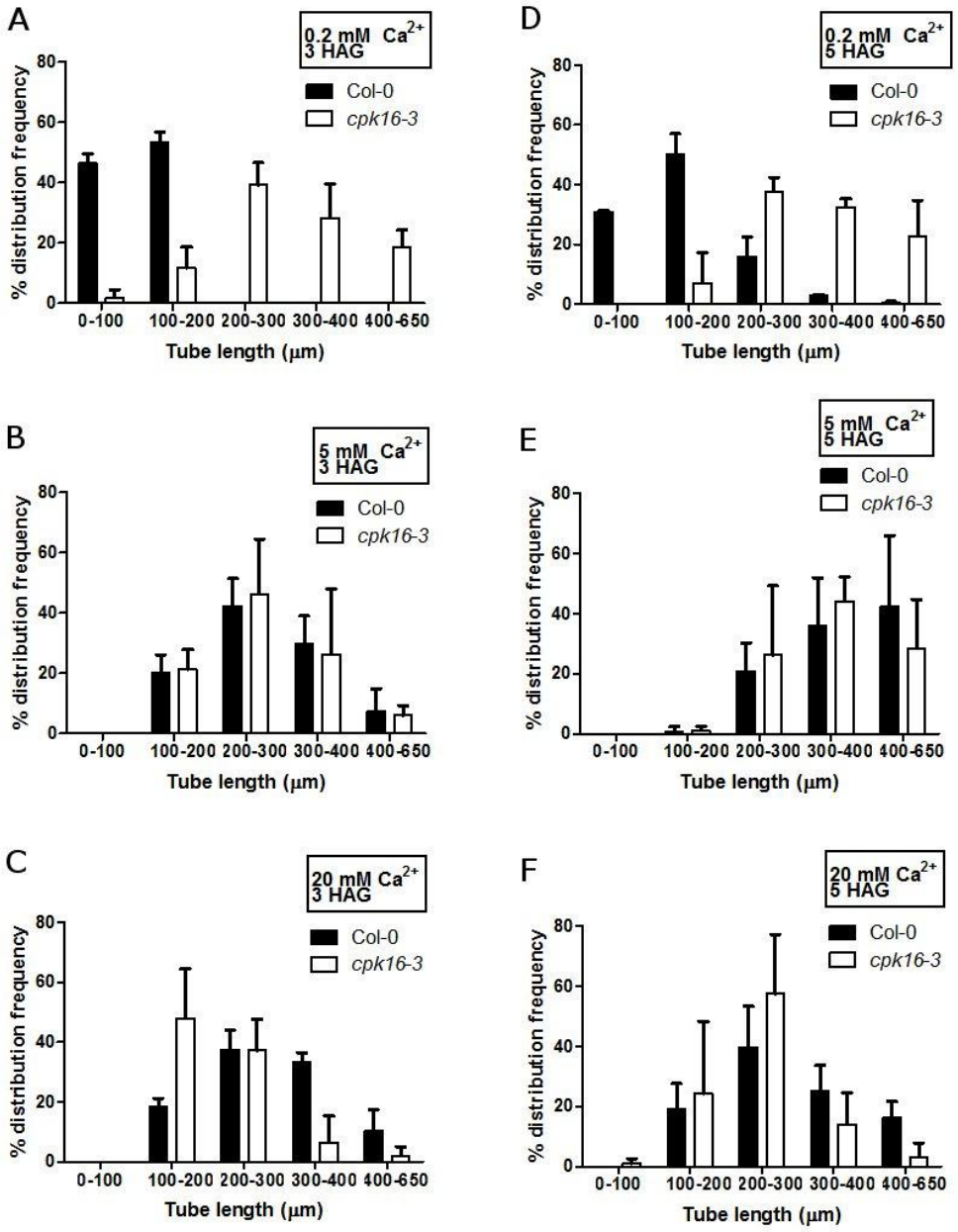
A
0.2 mM Ca2+
3 HAG
Col-0
cpk16-3
% distribution frequency
0
20
40
60
80
0-100
100-200
200-300
300-400
400-650
Tube length (μm)
D
0.2 mM Ca2+
5 HAG
Col-0
cpk16-3
% distribution frequency
Tube length (μm)
B
5 mM Ca2+
3 HAG
Col-0
cpk16-3
% distribution frequency
Tube length (μm)
E
5 mM Ca2+
5 HAG
Col-0
cpk16-3
% distribution frequency
Tube length (μm)
C
20 mM Ca2+
3 HAG
Col-0
cpk16-3
% distribution frequency
Tube length (μm)
F
20 mM Ca2+
5 HAG
Col-0
cpk16-3
% distribution frequency
Tube length (μm)

Figure 3.4. Pollen tube germination patterns between Col-0 WT versus *cpk16-3*. Germination was performed at various time points in two different calcium condition 2 mM and 0.2 mM Ca^{2+}. A, C) pollen tube germination and growth, B, D) quantification of pollen tube germination as represented in figure A and C. A – B) pollen tube germination in optimal Ca^{2+} media containing 2 mM Ca^{2+}. C – D) pollen tube germination in low Ca^{2+} media containing 0.2 mM Ca^{2+}.

Figure 3.4.

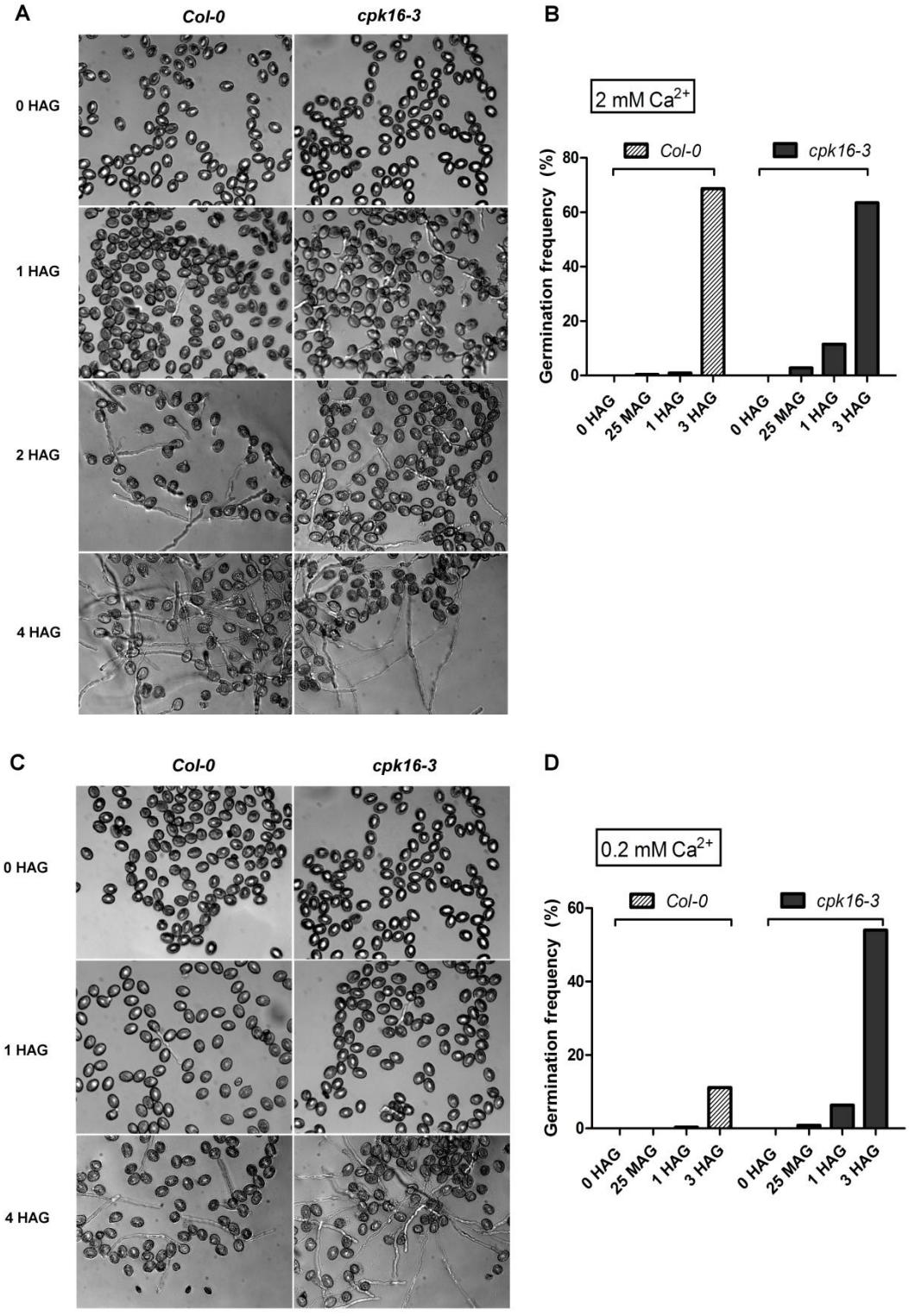
A
Col-0
cpk16-3
0 HAG
1 HAG
2 HAG
4 HAG
B
2 mM Ca2+
Col-0
cpk16-3
Germination frequency (%)
0
20
40
60
80
0 HAG
25 MAG
1 HAG
3 HAG
0 HAG
25 MAG
1 HAG
3 HAG
C
Col-0
cpk16-3
0 HAG
1 HAG
4 HAG
D
0.2 mM Ca2+
Col-0
cpk16-3
Germination frequency (%)
0
20
40
60
0 HAG
25 MAG
1 HAG
3 HAG
0 HAG
25 MAG
1 HAG
3 HAG

Figure 3.5. Growth oscillation of Col-0 WT versus *cpk16-3* pollen tubes grown *in vitro* in 2 mM Ca^{2+} media. A – D) oscillatory growth of WT pollen tubes. E – H) oscillatory growth of *cpk16-3* pollen tubes. Time lapse images were performed 4HAG and images were obtained every 3.3 sec. Growth oscillation curve was plotted as a function of growth rate versus time. Growth oscillations were compared between three growth populations: slow-growing (growth rate up to 20 nm/sec), medium-growing (growth rate 20 – 40 nm/sec), and fast-growing (growth rate greater than 40 nm/sec) pollen tubes. A) and B) Representation of WT medium-growing pollen tube. A) Growth oscillation curve for a medium-growing WT pollen tube. B) Time lapse curve of pollen tube depicted in panel A. C and D) Representation of WT fast-growing pollen tube. C) Growth oscillation curve for a fast-growing WT pollen tube. D) Time lapse curve of pollen tube depicted in panel B. E) and F) Representation of *cpk16-3* medium-growing pollen tube. E) Growth oscillation curve for a medium-growing *cpk16-3* pollen tube. F) Time lapse curve of pollen tube depicted in panel E. G) and H) Representation of *cpk16-3* slow-growing pollen tube. G) Growth oscillation curve for a slow-growing *cpk16-3* pollen tube. H) Time lapse curve of pollen tube depicted in panel G.

Figure 3.5.

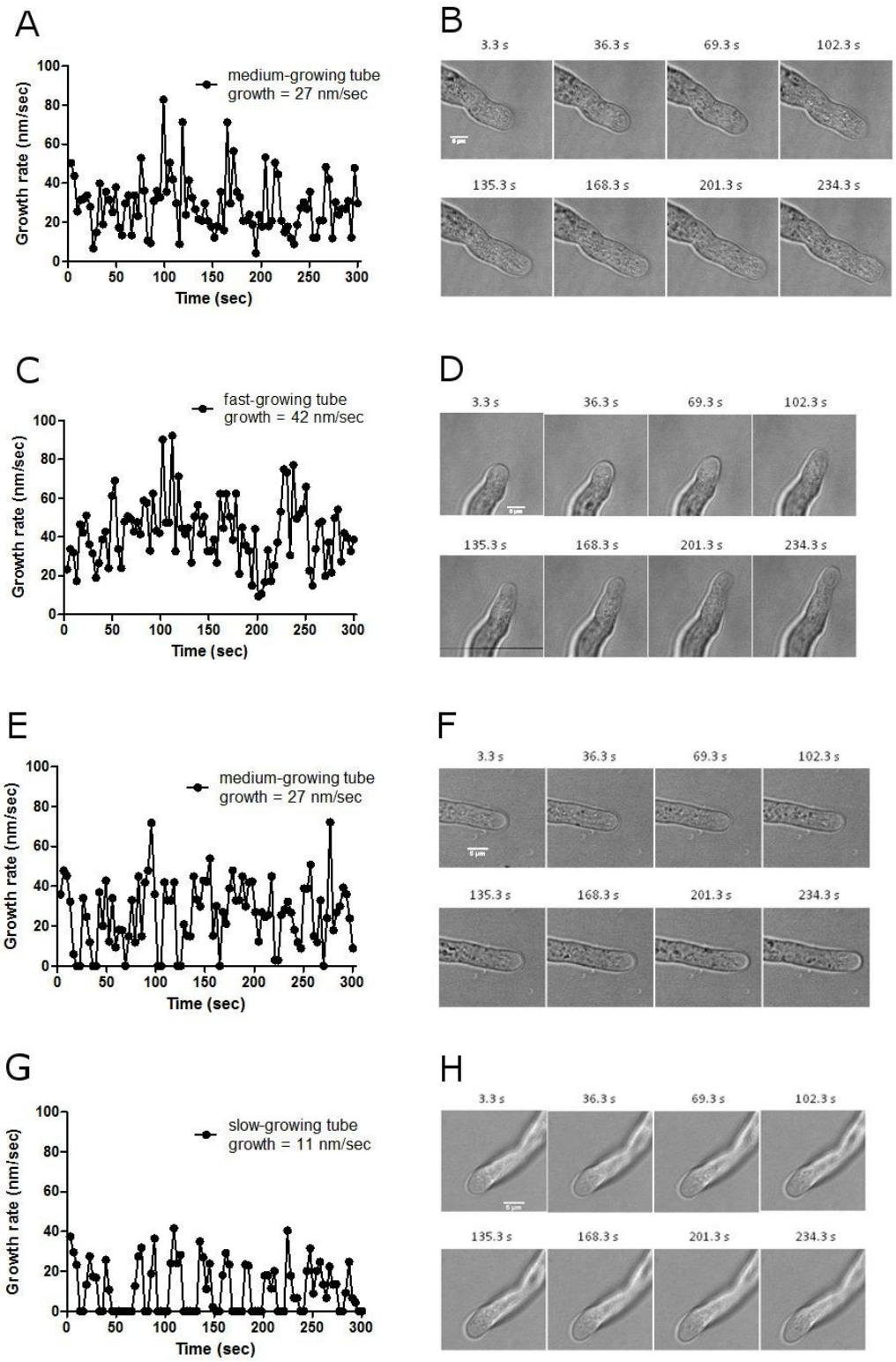
A
Growth rate (nm/sec)
Time (sec)
medium-growing tube
growth = 27 nm/sec
B
3.3 s
36.3 s
69.3 s
102.3 s
135.3 s
168.3 s
201.3 s
234.3 s
C
fast-growing tube
growth = 42 nm/sec
D
E
medium-growing tube
growth = 27 nm/sec
F
G
slow-growing tube
growth = 11 nm/sec
H

Figure 3.6. Growth oscillation of Col-0 WT versus *cpk16-3* pollen tubes grown *in vitro* in 0.2 mM Ca^{2+} (low Ca^{2+}) media. A – B) oscillatory growth of WT pollen tubes. C – F) oscillatory growth of *cpk16-3* pollen tubes. A) and B) WT slow-growing pollen tube. A) Growth oscillation curve for a slow-growing WT pollen tube. B) Time lapse curve of pollen tube depicted in panel A. C and D) Representation of WT medium-growing pollen tube. C) Growth oscillation curve for a medium-growing WT pollen tube. D) Time lapse curve of pollen tube depicted in panel B. E) and F) Representation of *cpk16-3* fast-growing pollen tube. E) Growth oscillation curve for a fast-growing *cpk16-3* pollen tube. F) Time lapse curve of pollen tube depicted in panel E.

Figure 3.6.

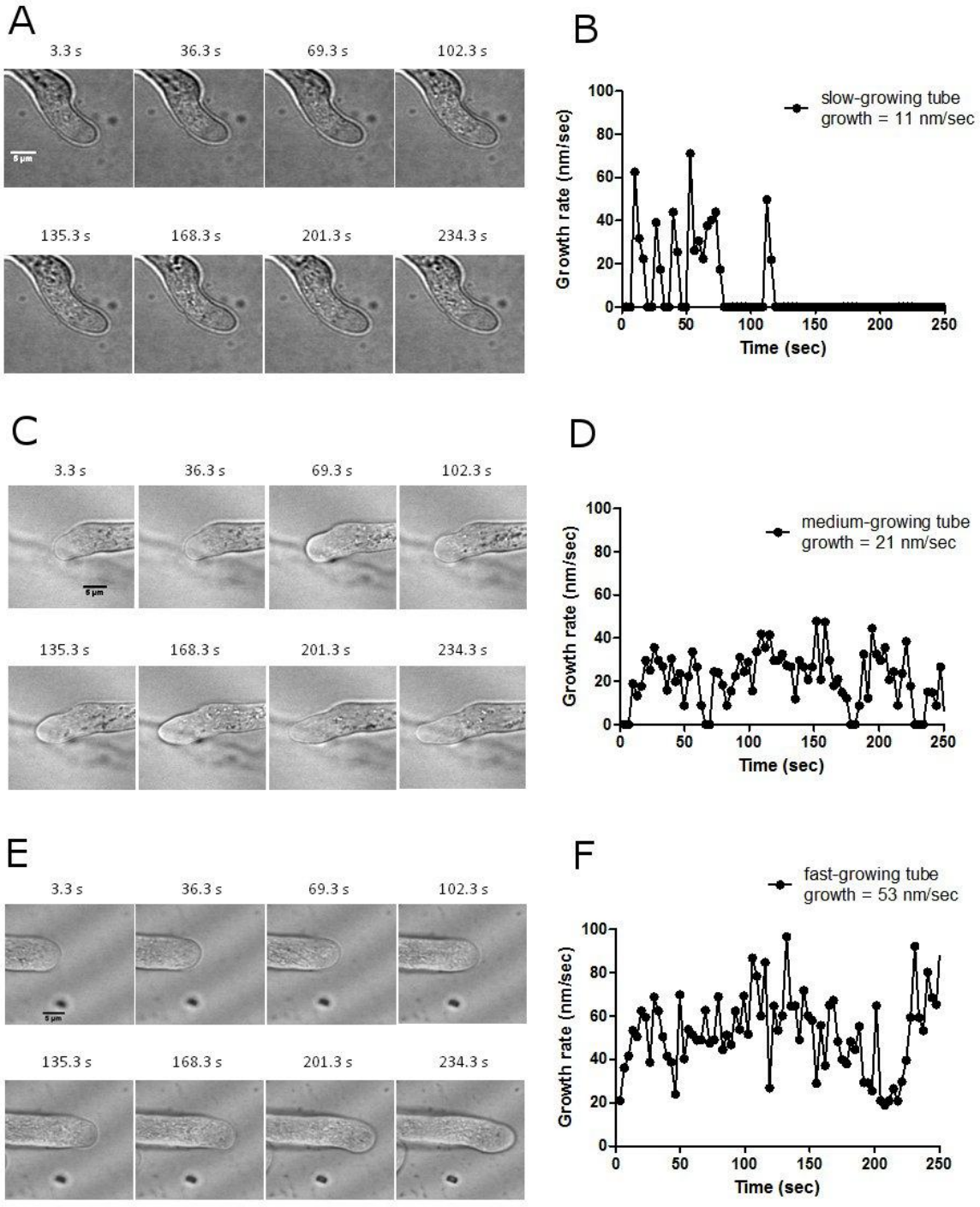
A
3.3 s
36.3 s
69.3 s
102.3 s
5 µm
135.3 s
168.3 s
201.3 s
234.3 s
B
slow-growing tube
growth = 11 nm/sec
Growth rate (nm/sec)
Time (sec)
C
3.3 s
36.3 s
69.3 s
102.3 s
5 µm
135.3 s
168.3 s
201.3 s
234.3 s
D
medium-growing tube
growth = 21 nm/sec
Growth rate (nm/sec)
Time (sec)
E
3.3 s
36.3 s
69.3 s
102.3 s
5 µm
135.3 s
168.3 s
201.3 s
234.3 s
F
fast-growing tube
growth = 53 nm/sec
Growth rate (nm/sec)
Time (sec)

Figure 3.7. BFA treatment of WT and *cpk16-3* pollen tubes grown in 2 mM Ca^{2+}. Pollen tubes were germinated and grown in the presence of chemicals for 3.5 hours after which pollen tube images were taken. A) Images of pollen tube grown in 0.15% DMSO control, 0.05 µg/mL BFA, 0.065 µg/mL BFA, 0.08 µg/mL BFA, and 0.1 µg/mL BFA. B) Quantification of pollen tube tip width. C) Quantification of pollen tube length.

Figure 3.7.

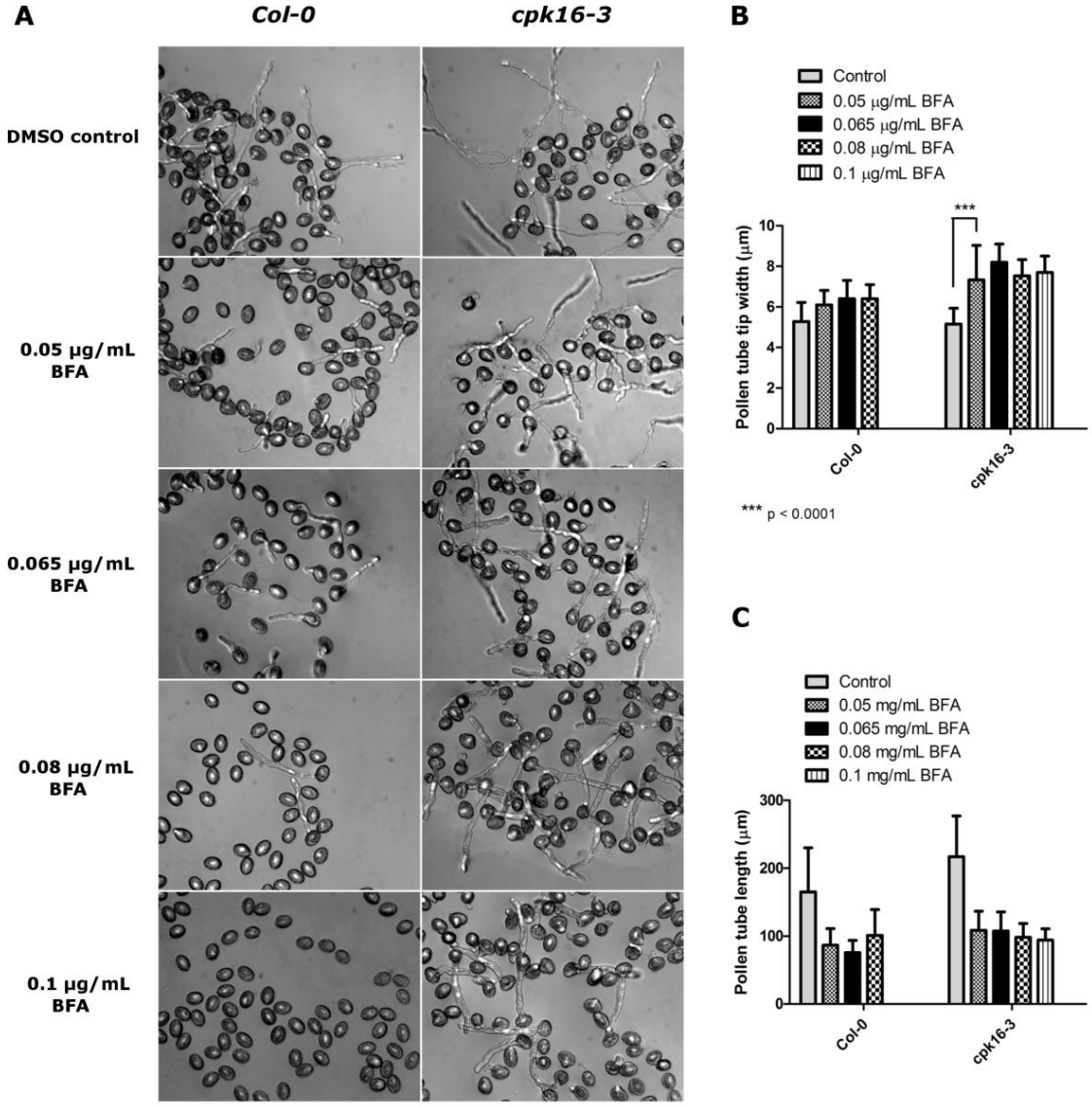
A
Col-0
cpk16-3
DMSO control
0.05 µg/mL BFA
0.065 µg/mL BFA
0.08 µg/mL BFA
0.1 µg/mL BFA
B
Control
0.05 µg/mL BFA
0.065 µg/mL BFA
0.08 µg/mL BFA
0.1 µg/mL BFA
Pollen tube tip width (µm)
***
Col-0
cpk16-3
*** p < 0.0001
C
Control
0.05 mg/mL BFA
0.065 mg/mL BFA
0.08 mg/mL BFA
0.1 mg/mL BFA
Pollen tube length (µm)
Col-0
cpk16-3

Figure 3.8. LatB treatment of WT and *cpk16-3* pollen tubes grown in 2 mM Ca^{2+}. Pollen tubes were germinated and grown in the presence of chemicals for 3.5 hours after which pollen tube images were taken. A) Images of pollen tube grown in 0.15% DMSO control, 0.8 nM LatB, 1.0 nM LatB, 1.5 nM LatB, and 2.0 nM LatB. B) Quantification of pollen tube tip width. C) Quantification of pollen tube length.

Figure 3.8.

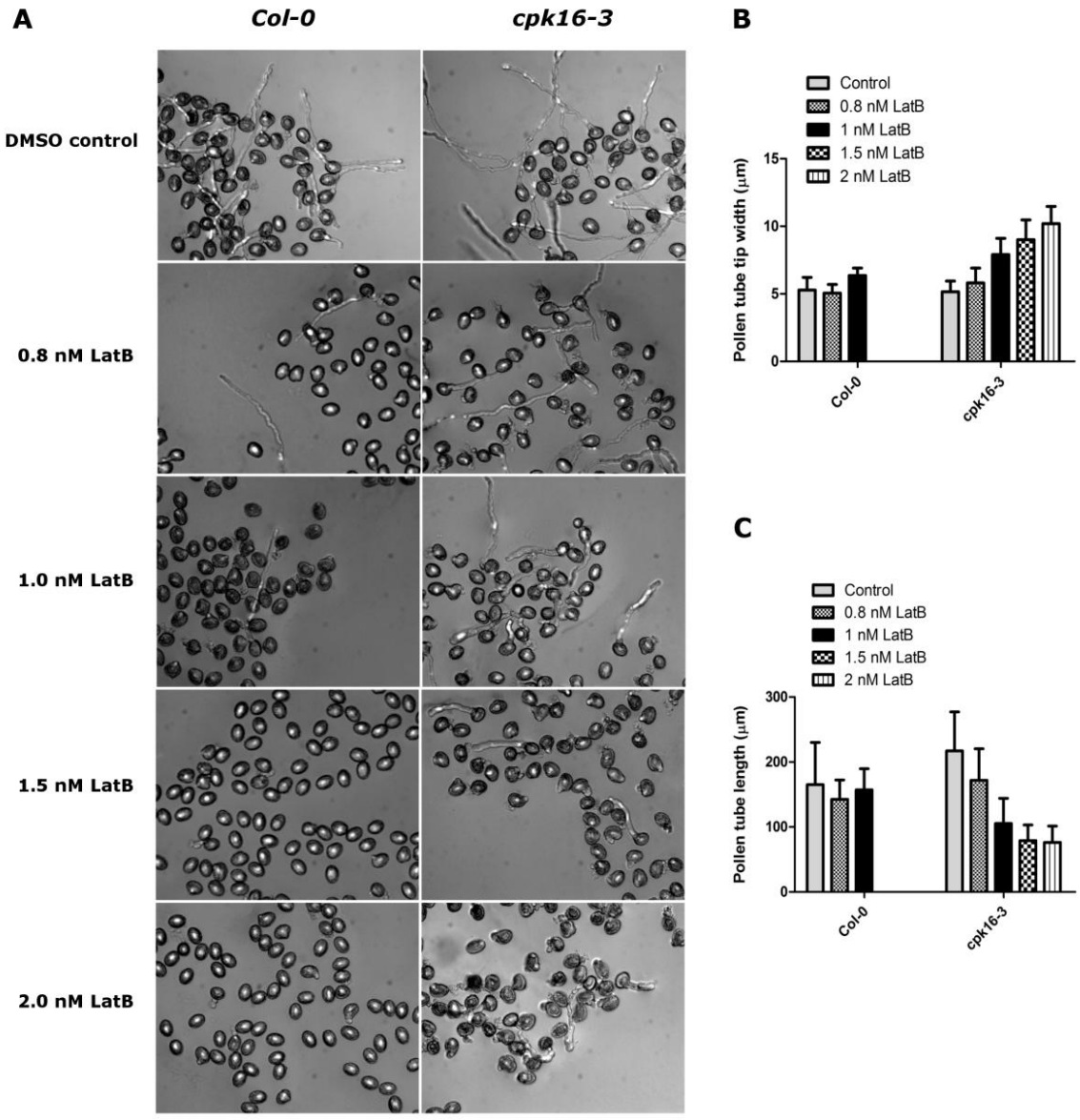
A
Col-0
cpk16-3
DMSO control
0.8 nM LatB
1.0 nM LatB
1.5 nM LatB
2.0 nM LatB
B
Control
0.8 nM LatB
1 nM LatB
1.5 nM LatB
2 nM LatB
Pollen tube tip width (μm)
15
10
5
0
Col-0
cpk16-3
C
Control
0.8 nM LatB
1 nM LatB
1.5 nM LatB
2 nM LatB
Pollen tube length (μm)
300
200
100
0
Col-0
cpk16-3

Figure 3.9. In vitro pollen germination assays for *cpk18-3* and double mutant *cpk16-3cpk18-3*. Pollen tubes were germinated in different calcium media: 0.2 mM, 2 mM, and 10 mM Ca^{2+}. *cpk18-3* mutant pollen tubes displayed similar growth as WT Col-0 control. In contrast, *cpk16-3cpk18-3* mutant pollen tubes growth and germination were enhanced in low 0.2 mM Ca^{2+} condition.

Figure 3.9.

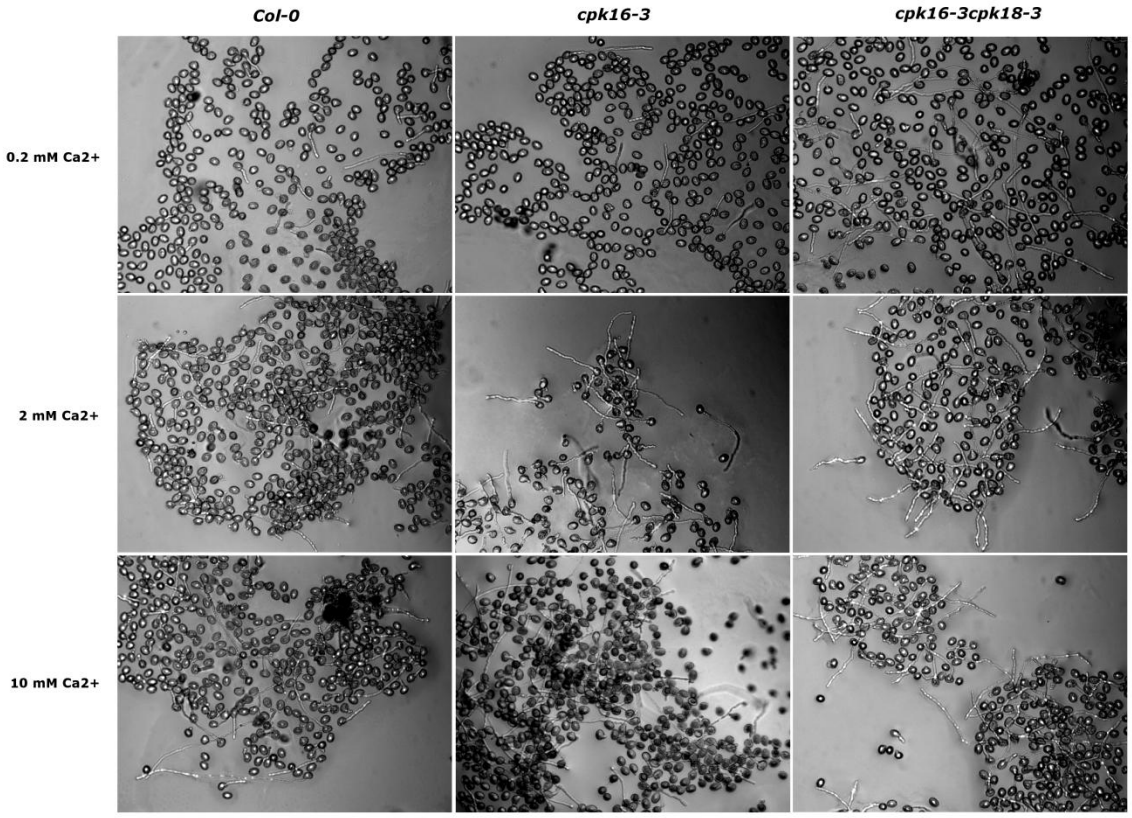

Figure 3.10. BFA treatment of *cpk18-3* and double mutant *cpk16-3cpk18-3* grown in 2 mM Ca^{2+}. Pollen tubes were germinated in the presence of chemicals for 3.5 hours after which pollen tube images were taken. A) Images of pollen tube grown in 0.15% DMSO control, 0.05 µg/mL BFA, 0.065 µg/mL BFA, 0.08 µg/mL BFA, 0.1 µg/mL, and 0.15 µg/mL BFA. B) Quantification of pollen tube tip width. C) Quantification of pollen tube length.

Figure 3.10.

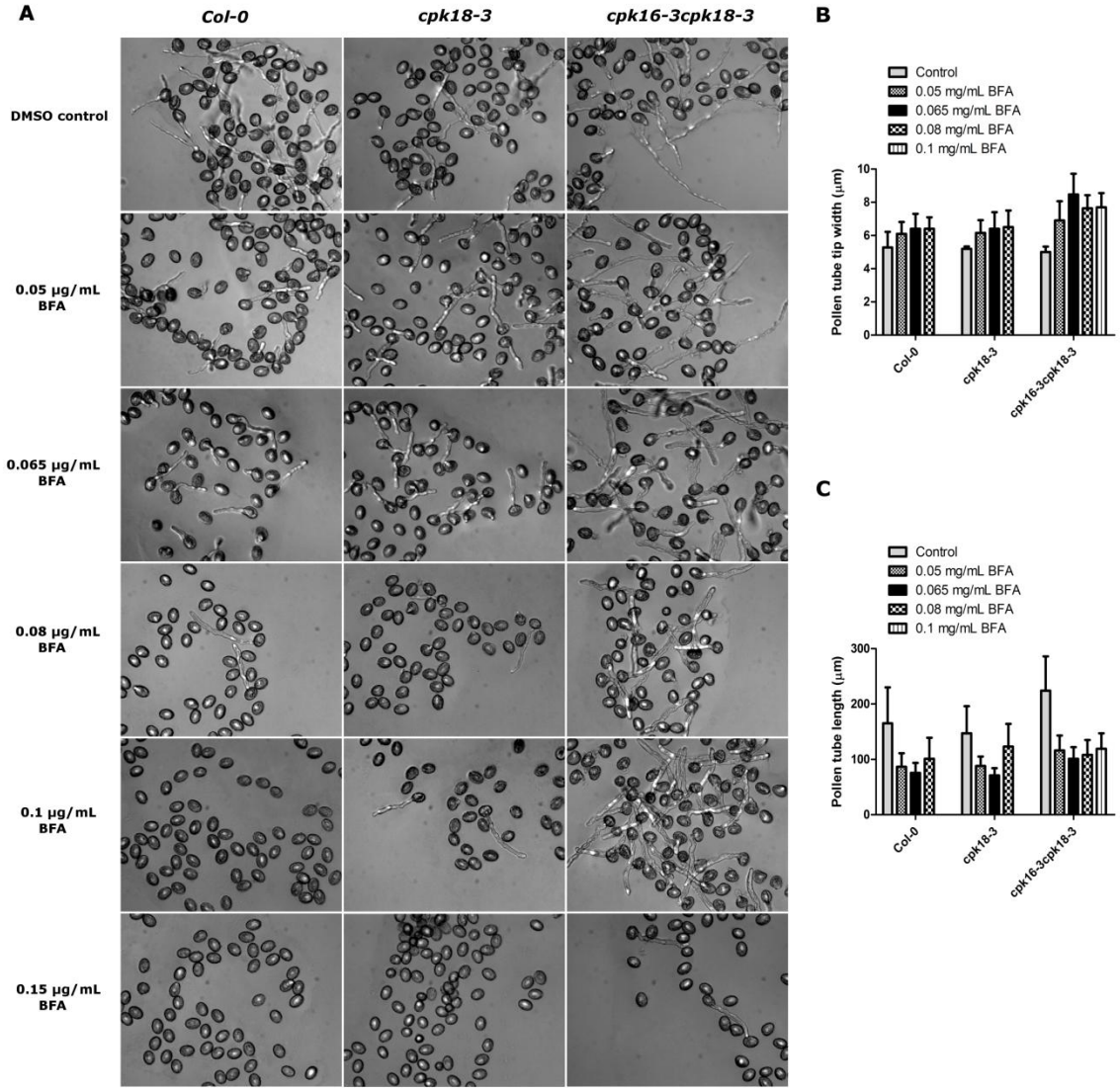
A
Col-0
cpk18-3
cpk16-3cpk18-3
DMSO control
0.05 µg/mL BFA
0.065 µg/mL BFA
0.08 µg/mL BFA
0.1 µg/mL BFA
0.15 µg/mL BFA
B
Control
0.05 mg/mL BFA
0.065 mg/mL BFA
0.08 mg/mL BFA
0.1 mg/mL BFA
Pollen tube tip width (µm)
0
2
4
6
8
10
Col-0
cpk18-3
cpk16-3cpk18-3
C
Control
0.05 mg/mL BFA
0.065 mg/mL BFA
0.08 mg/mL BFA
0.1 mg/mL BFA
Pollen tube length (µm)
0
100
200
300
Col-0
cpk18-3
cpk16-3cpk18-3

Figure 3.11. LatB treatment of *cpk18-3* and double mutant *cpk16-3cpk18-3* grown in 2 mM Ca^{2+}. Pollen tubes were germinated and grown in the presence of chemicals for 3.5 hours after which pollen tube images were taken. A) Images of pollen tube grown in 0.15% DMSO control, 0.8 nM LatB, 1.0 nM LatB, 1.5 nM LatB, and 2.0 nM LatB. B) Quantification of pollen tube tip width. C) Quantification of pollen tube length.

Figure 3.11.

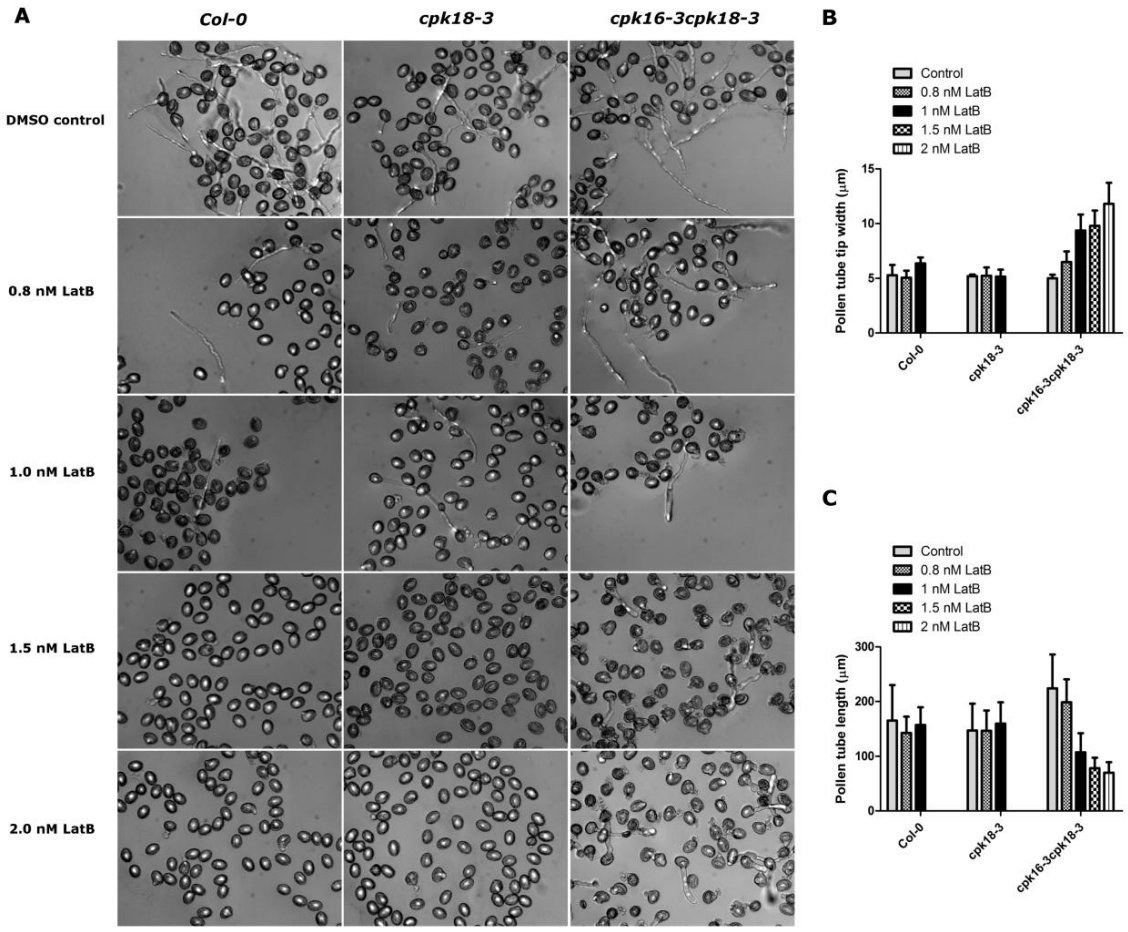
A
Col-0
cpk18-3
cpk16-3cpk18-3
DMSO control
0.8 nM LatB
1.0 nM LatB
1.5 nM LatB
2.0 nM LatB
B
Control
0.8 nM LatB
1 nM LatB
1.5 nM LatB
2 nM LatB
Pollen tube tip width (μm)
15
10
5
0
Col-0
cpk18-3
cpk16-3cpk18-3
C
Control
0.8 nM LatB
1 nM LatB
1.5 nM LatB
2 nM LatB
Pollen tube length (μm)
300
200
100
0
Col-0
cpk18-3
cpk16-3cpk18-3

Figure 3.12. Model of CPK16 function in potentially regulating pollen tube tip polarity. Activation of ROP1 (represented by blue circles) at the tip region leads to the promotion of tip-localized calcium gradient. In the wild-type background, high tip calcium activates CPK16 and promotes phosphorylation of REN1 at Ser_{267} (red circles) which then enhances ROP1 GTPase activity leading to ROP1 inactivation. Nonphosphorylated REN1 may also be present at the tip region as REN1 is targeted there by exocytic vesicles. However, phosphorylation of REN1 at Ser_{70} may inhibit its tip-directed targeting based on our observation. The localization of phosphorylated REN1 remains a speculation in this model and requires further investigation. In the *cpk16-3* background, high tip calcium still accumulates following ROP1 activation, but in the absence of CPK16, other CPKs may be involved in phosphorylating REN1 at Ser_{267}. However, REN1 regulation at this condition may not be optimal and as such, ROP1 activity is slightly higher than normal leading to higher growth and germination but no polarity loss. Only when *cpk16-3* mutant tubes were treated with BFA or LatB which can inhibit REN1 tip-directed targeting, then polarity loss can be observed. At this condition, we speculate that although REN1 may be partially phosphorylated, its inability to be targeted to the right compartment inhibits its potential to negatively regulate ROP1 resulting in enhanced ROP1 activity and tip swelling phenotype.

Figure 3.12.

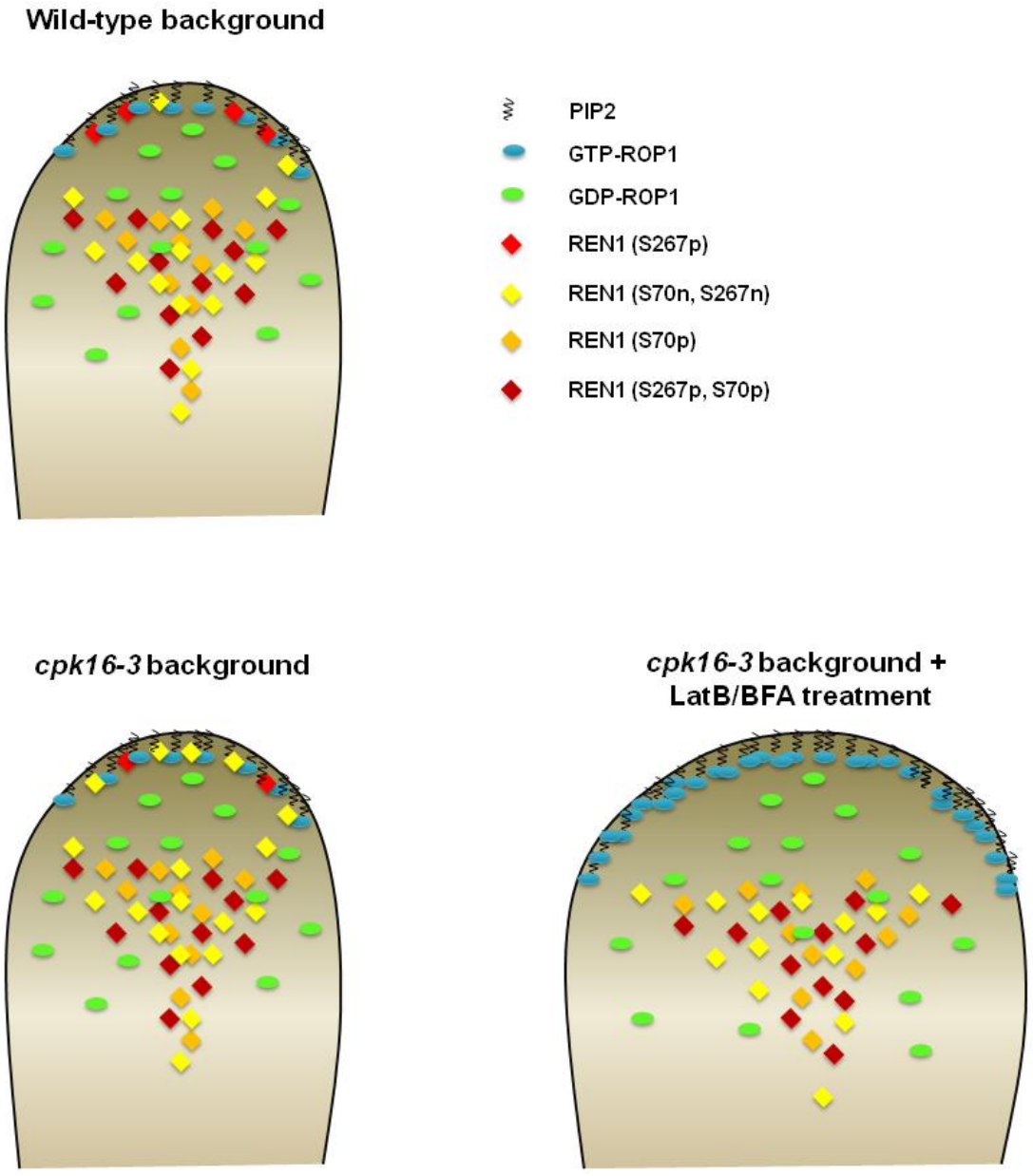
Wild-type background
PIP2
GTP-ROP1
GDP-ROP1
REN1 (S267p)
REN1 (S70n, S267n)
REN1 (S70p)
REN1 (S267p, S70p)
cpk16-3 background
cpk16-3 background +
LatB/BFA treatment

CHAPTER 4

Chemical Genetics Approach to Identify Inhibitors of ROP1 and REN1 Interaction

ABSTRACT

The regulation of pollen tube tip growth involves ROP1 pathway which controls actin dynamics, tip calcium influx, and vesicle trafficking. In this highly dynamic pollen tube system, oscillations of growth, active ROP1, F-actin dynamics, and tip-focused calcium were observed to be associated with one another. Thus, the dissection of phase relationships between these processes will be difficult when using a conventional genetics approach which would lead to terminal phenotypes such as tip swelling or growth inhibition. To address these challenges, we propose a chemical genetics approach to identify small molecules that would specifically lead to activation of ROP1. One way to reach this goal is by targeting protein-protein interaction between active ROP1 and its negative regulatory protein REN1GAP. Thus cell-based yeast two hybrid screens were performed to identify potential inhibitors of protein-protein interactions. From this initial screen, ten hit compounds were identified. Further screens including pollen tube phenotypic screen identified one compound, #7, which slightly enhanced pollen tube tip width and whose inhibition of ROP1-REN1 interactions was further confirmed using *in vitro* pulldown assays and GTPase assays. Interestingly, treatment of ROP1 OX with compound 7 severely enhanced tip swelling and reduced growth while the same treatment of weak *ren1-3* allele only slightly increased tip width which suggests that compound 7 primarily targets ROP1. Further tests of compound 7-related analogs in inducing tip swelling revealed no activities which suggested that compound 7 may have the optimal structures to inhibit ROP-type interaction. Finally, docking experiments of compound 7 to the protein interaction interface between RhoA and p190RhoGAP further suggests its

possibility in binding to the GTP-binding pocket within the Rho-GAP interface in potentially disrupting protein-protein interaction.

INTRODUCTION

Pollen tube tip growth is regulated by ROP1 pathway which controls many processes including assembly of tip F-actin, promotion of tip-localized calcium, and trafficking of secretory vesicles (Fu et al., 2001; Gu et al., 2003; Gu et al., 2005; Li et al., 1999; Yan et al., 2009: Lee et al., 2008). In addition to this highly dynamic system, the regulations of tip polarity in pollen tubes are further complicated by the oscillatory nature of the aforementioned processes. For example: pollen tube growth oscillates between a period of growth burst and a period of still phase (Holdaway-Clarke et al., 1997; Pierson et al., 1996; Hwang et al., 2005) while apical ROP1 activity, tip F-actin, and tip calcium oscillates between a period of high tip intensity and a period of low tip intensity (Hwang et al., 2005; Fu et al., 2001). These oscillations are not independent from one another; instead phase relationships seem to exist between them. Following ROP1 activation, ROP1 effector RIC4 mediates tip F-actin assembly which then leads to pollen tube growth burst (Hwang et al., 2005). Another ROP1 effector, RIC3 mediates tip-focused calcium accumulation by promoting extracellular calcium influx which over time, the high tip-focused calcium led to the slowing of pollen tube growth (Hwang et al., 2005). Dissection of the spatial and temporal relationships between these different processes will give a better understanding of the causal relationships of ROP1 activation in this complex pollen tube oscillatory system. However, manipulation of ROP1 activities via mutations such as constitutive-active or dominant-negative mutation only led to terminal phenotypes such as tip swelling or growth inhibition (Li et al., 1999; Kost et al. 1999). To address these challenges, we propose to use a chemical genetics approach which will be

useful to specifically affect ROP1 activity. In this manner, spatial and temporal studies of ROP1 in live cell would be feasible once the effect of chemicals have been optimized.

Reverse chemical genetics is a useful tool for functional study of a particular gene or protein of interest by identification of small molecules which are specific to the target gene or protein (Blackwell and Zhao, 2003; Zheng and Chan, 2002; Walsh and Chang, 2006). The use of small molecule to perturb dynamic biological system is advantageous especially since its effects are rapid, reversible, and tunable which would allow for real time observations (Blackwell and Zhao, 2003; Zheng and Chan, 2002; Walsh and Chang, 2006). Our goal was to identify small molecules which can lead to activation of ROP1. An attractive approach to activate ROP1 is by disrupting the interaction between active ROP1 and its negative regulator, REN1, by utilizing yeast two-hybrid system. In this assay, two hypothetically interacting proteins are each fused to split domains of transcription factors, one containing a DNA-binding domain while another containing an activation domain. Only when the two proteins interact, then functional transcription factor can be formed and transcription machinery can be reconstituted to drive the expression of reporter genes (Fields and Song, 1989; Chien et al., 1991). Using this assay, disruption of protein-protein interaction can technically be easily identified by the absence of reporter genes expression which can be selected for in the appropriate yeast media. Identification of inhibitors of protein-protein interactions has proven to be difficult and new methods continue to be developed in order to circumvent the many challenges associated with this goal (Arkin and Wells, 2004; Chene, 2006; Fry, 2006). Nevertheless, previous studies have in fact reported the successful use of yeast two-

hybrid to identify inhibitors of protein-protein interaction (Khazak et al., 2006; Igarashi et al., 1998; Young et al., 1998; Huang and Schreiber, 1997). Thus we are confident with the possibility of identifying inhibitor(s) of ROP1-REN1 protein interactions by using this assay.

MATERIALS AND METHODS

Plasmids construction and yeast transformation

CArop1 (contains mutation G15V) and *CArop2* (G15V) were PCR-amplified using Gateway attL sequence-containing primers and *CArop1/CArop2* templates (Li et al., 1999; Li et al., 2001). BP recombination reactions were performed between attL-containing PCR product and pDONR Zeo (Invitrogen, Carlsbad, CA) to produce entry clones. The same protocol was done with full length *RopGAP1* and *RopGAP3* (Wu et al., 2000), *RENGAP1* (Hwang et al., 2008), and *PHGAP2* and *PHGAP3*. LR recombination reactions were performed using entry clones and destination vectors, pDEST32 to generate the bait which contains GAL4 DNA binding domain (*GAL4DB*) or pDEST 22 to generate the prey which contains GAL4 DNA activation domain (*GAL4AD*). *GAL4DB* and *GAL4AD* constructs were co-transformed into yeast strains *MaV203* with genotype MATα, *leu*2-3,112, *trp*1-901, *his*3Δ200, *ade*2-101, *gal*4Δ, *gal*80Δ, *SPAL*10*::URA*3, *GAL*1::*lac*Z, *HIS*3UAS GAL1*::HIS*3*@LYS*2, *can*1R, *cyh*2R (Invitrogen Corporation, Carlsbad, CA). This yeast strain has three independent selectable markers: *HIS3*, *lacZ*, and *URA*.

Yeast two-hybrid chemical screen

Transformed yeast strains were grown in complete dropout media, Leu^-/Trp^-, or appropriate selective dropout media, $Leu^-/His^-/Trp^-$ containing 3-amino-1,2,4-triazole which is a competitive inhibitor of *HIS3*-encoded enzyme (Vidal and Legrain, 1999). Yeast starter culture was used to inoculate fresh complete or selective media that contains chemical. Optical density (OD) of chemical-containing yeast culture was measured at 630 nm. Yeast culture was grown overnight at 30^{o}C after which point the OD was again measured. DMSO-treated yeast culture was used as positive control.

Chemical libraries

Two chemical libraries from the UCR-IIGB collections, ChemBridge Diverset (ChemBridge Corporation, San Diego, CA) and Sigma/TimTec Myriascreen (TimTec LLC, Newark, DE), were screened.

Plant materials and growth condition

Arabidopsis plants were grown at 22^{o}C growth room under 16 h light and 8 h dark. Tobacco plants were grown at 28^{o}C growth room under natural light.

Protein overexpression and purification

All recombinant protein was expressed in E. coli BL21 cells. ROP1 fused to glutathione S-transferase (GST) and REN1 fused to 6xHIS were expressed at 30^{o}C for 4-6 h after induction with 1 mM isopropyl-b-D-thiogalactopyranoside (Wu et al., 2001). Cells were pelleted by centrifugation at 5000 rpm for 10 min and resuspended in GST-binding buffer (50 mM HEPES, 1 mM EDTA, pH 7.4) or HIS-lysis buffer (50 mM HEPES, 10 mM imidazole, pH 7.4). Following sonication, cell lysate was collected after

centrifugation at 10,000 rpm for 15 min and incubated with glutathione-agarose beads (Sigma-Aldrich, St. Louis, MO) for GST-fusion protein or Ni-NTA agarose beads (New England Biolabs, Ipswich, MA) for HIS-fusion protein for batch affinity purification method. After 1-2 h of incubation, beads were washed with GST-binding buffer or HIS-wash buffer (50 mM HEPES, 250 mM NaCl, and 30 mM imidazole, pH 7.4). Proteins were eluted with GST-elution buffer (50 mM HEPES, 30 mM glutathione, pH 7.4) or His- elution buffer (50 mM HEPES, 300 mM imidazole, pH 7.4).

In vitro pulldown assay

To obtain immobilized proteins as the bait, GST-ROP1 fusion bound to glutathione agarose beads was washed but not eluted. Immobilized GST-ROP1 was preloaded with 3 mM GTP prior to pulldown assay (Wu et al., 2001). Approximately 10 µg of GST-ROP1 and 5 µg of HIS-REN1 was incubated in interaction buffer (20 mM HEPES, 5 mM $MgCl_2$, 1 mM EDTA, pH 7.4) for 1-2 h. After binding, beads were washed and bound proteins were released by boiling in the presence of SDS-PAGE loading buffer and resolved using SDS-PAGE. Western blot was performed to detect bound proteins using HIS polyclonal antibody.

Particle bombardment-mediated transient expression in tobacco pollen tubes

Mature tobacco (*Nicotiana tabacum*) pollen grains were collected in tobacco germination media (Fu et al., 2001). Approximately 0.3 – 0.7 mg of plasmids were used to coat 0.5 mg gold (1.0 mm in diameter). Freshly collected pollen grains were bombarded by the plasmid-coated gold using a PDS-1000/He particle delivery system

(Bio-Rad Laboratories, Hercules, CA) as described previously (Fu et al., 2001). Following bombardment, pollen tubes were allowed to germinate in room temperature.

In vitro pollen germination

Pollen grains were collected from open flowers. Arabidopsis pollen was germinated on agar medium containing 18% sucrose, 0.01% H_3BO_3, 1 mM MgSO4, 1-2.5 mM $CaCl_2$, 1-2.5 mM $Ca(NO_3)_2$, and 0.45% agar, pH 7. Tobacco pollen was germinated on liquid medium containing 18% sucrose, 0.01% boric acid, 1 mM MgSO4, 5 µM $CaCl_2$, 5 µM $Ca(NO_3)_2$, pH 7. Pollen tubes were grown in 28^{o}C water bath. Pollen tube growth was examined 3-6 h under a light/DIC Nikon microscope. For chemical treatment, chemicals were added onto germination media prior to pollen tube germination.

RESULTS

Cell-based chemical screen identified putative inhibitors of ROP-GAP protein-protein interaction

To identify inhibitors of active ROP1 and REN1 interaction, chemical screen was performed using yeast-two-hybrid system (Figure 4.1A). Since ROP1 and REN1 interaction is not strong, interaction between other ROP-GAP: constitutive-active mutant form of ROP2, CArop2, and PHGAP2 was utilized. About 20,000 chemicals from two chemical libraries, ChemBridge Diverset and Sigma/TimTec Myriascreen were screened on yeast expressing both CArop2 and PHGAP2 at chemical concentration ranging from 5 – 70 µM. High-throughput screens were performed by observing the expression of *HIS3*

reporter gene in the form of yeast growth in histidine-lacking media. Only when the expression of reporter gene was reduced or eliminated due to disruption of protein-protein interaction, then the chemicals were considered as "hits". Yeast growth was measured by obtaining its optical density (OD) at 600 nm after 24 hour of chemical treatment. For consistency, OD ratio (OD_{24hr}/OD_{0hr}) was calculated and ratio < 2 was arbitrarily chosen as the "hits" where at this limit significant yeast growth was not observed. Our initial screen identified 162 hits (0.81% hit ratio), some of which were potential growth inhibitors. To eliminate such chemicals, chemically-treated yeast was also grown in histidine-containing media where yeast growth should be observed. From this screen, 137 chemicals were found to be toxic to yeast growth and were eliminated. Primary hits from this chemical screen were further tested for the expression of another reporter gene, *lacZ*, which is driven by a different promoter than *HIS3* gene to remove false positives. Following this assay, ten chemicals were identified as putative inhibitors of CArop2-PHGAP interaction.

All ten chemical hits were purchased and further analyzed (Figure 4.1.B). To determine the minimum chemical concentration required for inhibition of protein-protein interaction, titration curve of each compound was generated and found to range between 5µM up to 25µM (data not shown). To identify compounds that are permeable in pollen tubes as well as produce the tip swelling phenotype expected when ROP-GAP interaction is disrupted, we further screened these compounds in WT tobacco pollen tubes. This screen resulted in one compound, #7, which slightly induced pollen tube tip swelling phenotype at 25 µM (Figure 4.1C). However, in addition to tip swelling phenotype,

compound 7 also inhibited pollen tube growth and treatment with 50μM chemical almost completely inhibited pollen tube germination.

***In vitro* protein interaction analyses confirmed the effect of compound 7 in disrupting GTP-ROP1 and REN1 protein-protein interaction.**

To confirm that compound 7 acts by disrupting protein-protein interaction between active ROP1 and REN1, GTPase assay and *in vitro* pulldown assay were performed. GTPase assay is utilized to measure the activity of RhoGTPase (Webb and Hunter, 1992; Nixon et al., 1995) which has the ability to catalyze its GTP-to-GDP exchange with low intrinsic activity, but can be enhanced by interacting with GTPase-activating protein (Nixon et al., 1995). Thus high GTPase activity can be associated with high inorganic phosphate released from GTP hydrolysis which correlated with higher absorbance measured at 360 nm in our assay. After performing this assay, we found that chemical treatment of at least 25 μM of compound 7 resulted in reduced ROP1 GTPase activity compared to DMSO control (Figure 4.2A). This suggests that the reduced GTPase activity was potentially due to disruption of ROP1 and REN1 interaction. To further confirm GTPase assay results, we also performed *in vitro* pulldown assays. Recombinant protein of constitutive-active (GTP-locked) ROP1 was used to pulldown REN1. Bead-bound ROP1 was incubated with REN1 in the presence of DMSO control or compound 7 for at least 1h, after which bound REN1 was released and blotted onto the membrane for western blot analysis. Using this assay, we found that the amount of bound REN1 was decreased as the chemical concentration increased (Figure 4.2.B). Significant reduction in the amount of bound REN1 can be observed with treatment of 25 μM

compound 7 in comparison to DMSO control (Figure 4.2.B). This result is consistent with the GTPase assay result and further confirms that compound 7 seems to disrupt protein-protein interaction between ROP1 and REN1 *in vitro*.

Chemically-induced tip swelling phenotype is dose-dependent on functional ROP1.

To further investigate whether chemically-induced tip swelling phenotype requires ROP1, we tested two ROP1 mutants: *rop1RNAi (rop1* knockdown) and *GFP-ROP1OX* (*rop1* overexpression) pollen tubes. In *Col-0* WT pollen tubes, treatment with 25 µM compound #7 reduced pollen tube germination by 50% (data not shown) which was accompanied by slightly enhanced tip width and reduced pollen tube tip width ($p < 0.0001$; Figure 4.3B, C). In *rop1RNAi* background, pollen tube germination and growth was severely affected (Figure 4.3A). However, treatment with 25 µM compound #7 did not seem to affect tip width or tube length (Figure 4.3B, C). In addition, this background seemed to be more sensitive to chemical treatment since at 50 µM, pollen tube germination was not observed (Figure 4.3A). In contrast, treatment of *GFP-ROP1OX* pollen tubes with 25 µM compound #7 severely enhanced pollen tube tip width (Figure 4.3A, B) but not tube length which is partially because *GFP-ROP1OX* background itself already displayed shorter tubes with wider tube width (Figure 4.3C). In addition, treatment with 50 µM of chemical produced a severe effect with enhanced tip width and shorter tube length (Figure 4.3A, B). At this condition, polarized growth was almost abolished and pollen tube tip seemed to have expanded in all direction creating what looked to be a ballooning phenotype (Figure 4.3A). This ballooning effect mimics the loss of function *ren1-1* phenotype (Hwang et al., 2008) which suggests that ROP1

activity may have increased following chemical treatment as was observed in *ren1-1* mutant. Furthermore, this indicates that functional ROP1 is required to produce the chemically-induced tip swelling and that ROP1 is the potential chemical target *in vivo*.

Next, we also treated weak *REN1* allele, *ren1-3* pollen tubes to further test whether the same chemical effects can be observed in this background. *ren1-3* pollen tubes display a mixture of pollen tube defects which include wavy and long tubes, irregular tube width that tapers at the tip, or slightly wider tubes (Hwang et al., 2008). Treatment of *ren1-3* pollen in 25 μM chemical slightly induced tip width compared to DMSO treatment, however it was still comparable to the same effects observed in wild type pollen tubes. This seems to further suggest that compound 7 primarily targets ROP1 and subsequently affects its interaction with REN1 proteins.

Compound 7 has some specificity to ROP-type interaction.

To test whether compound 7 effects in disrupting protein-protein interaction may be specific to ROP-GAP interaction, yeast expressing an unrelated TMK1-SPIKE1 interaction was utilized. Transmembrane kinase 1 (TMK1) is a membrane-bound receptor kinase protein whose function is currently unknown (Chang et al., 1992; Schaller and Bleecker, 1993). On the other hand, SPIKE1 is a guanine exchange factor (RopGEF) which is required for actin-dependent cellular morphogenesis (Qiu et al., 2002; Uhrig et al., 2007; Basu et al., 2008). We currently have evidence showing that TMK1 and SPIKE1 can interact from yeast two-hybrid analysis as well as other assays (unpublished data). For a weak protein-protein interaction control, control C which expresses Drosophila DP and EF2 was utilized (Proquest Two Hybrid System; Invitrogen,

Carlsbad, CA). In this assay, we found that control C growth was inhibited as chemical concentration was increased (Figure 4). It has been observed in the initial screen that this compound also affected yeast growth. However, in this retest, this compound also inhibited control C yeast growth in histidine-lacking media. Since control C interaction is weak, it seemed that compound 7 may be toxic to the yeast when it was grown in histidine-lacking condition. It is possible that compound 7 may disrupt protein-protein interaction nonspecifically but this may not likely by the case since TMK1-SPIKE1 interaction displayed normal yeast growth up to 20 μM of compound 7 treatment (Figure 4). With the ROP-GAP interaction, yeast growth was inhibited with a minimum of 10 μM of compound 7 (Figure 4). Thus compound 7 seems to disrupt ROP-GAP protein interactions, though it also partially inhibits yeast growth. More ROP-GAP-unrelated protein-protein interactions should be tested to further confirm the chemical mode-of-actions.

Structure activity relationships (SAR) analysis did not identify more potent and more selective inhibitor of ROP-type interaction

To identify more potent and more specific inhibitor(s), analogs of compound 7 were searched using Chemine under atom pair similarity search. The search identified five analogs which were available commercially from Sigma/TimTec: R874000 (00), R875406 (06), R850446 (46), R852066 (66), and R855081 (81) (the last two digits were used for easier analog identification). None of these compounds has high similarity to compound 7, the closest was 40% similar. All analogs contain the thienopyrimidine backbone (Ivachtchenko et al., 2004; Munchhof et al., 2003) with varying side residues.

Out of the five compounds, compound 00 and 46 did not dissolve in a number of solvents tested which included DMSO, isopropanol, methanol, and DMF; thus we were unable to use these for further testing. Analyses of the rest of the analogs in yeast two-hybrid assay did not yield any functional compound as none of them inhibited yeast growth in histidine-lacking media (Figure 4.6) even with treatment of up to 100 µM chemical (data not shown). The common denominator between these three analogs was the absence of an amine tail or a benzyl group which suggests that either side residue may contribute to compound 7's function in potentially inhibiting protein-protein interaction. Studies of more chemical analogs would provide additional insights into the significance of these side residues. In the meantime, it seems that compound 7 has the best structure for its function in disrupting ROP-GAP protein interactions.

Ligand-protein docking revealed potential compound binding site within Rho-GAP protein interaction interface.

In silico virtual screening approach can be a valuable tool to identify inhibitors of protein-protein interaction (Toogood, 2002; Berg, 2003; Sugaya et al., 2007) as many approaches are often required to address the challenges in finding inhibitors of protein-protein interaction. Some of these challenges can be contributed to several factors such as the shape of protein-protein interface which are often flat and quite large with no clear chemical-binding pocket ('hot spot') as well as the unknown binding site and binding stoichiometry (Arkin and Wells, 2004; Chene, 2006; Fry, 2006; Toogood, 2002). Nevertheless, several studies have reported the identification of protein-protein interaction inhibitors via *in silico* studies; for example, between toll-like receptor 4

(TLR4) and myeloid differentiation factor 2 (MD-2) (Joce et al., 2010), between cyclin-dependent kinase 5 (CDK5) and non-cyclin protein p25 (Zhang et al., 2011), and between tumor suppressor p53 and its negative regulator MDM2 (Lawrence et al., 2009). Based on the importance of structural requirements for chemical binding as presented in these studies, we were interested to determine whether compound 7 can be 'docked' within ROP-GAP protein interaction interface. However, this study may not be conclusive as there is a possibility that compound 7 may bind to allosteric sites within ROP1 or REN1 which can lead to protein conformational changes and affect protein-protein interaction (Berg, 2003). Prior to docking analysis, protein databank was searched for existing co-crystal structure between ROP and GAP protein which yielded no structures. The closest Rho-GAP type interaction whose co-crystal structures were available was that of human RhoA-p50RhoGAP (Rittinger et al., 1997). Full length AtROP1 is 47% similar to human RhoA while GAP domain of AtREN1 is 21% similar to human p190RhoGAP. These co-crystal structures were then used as the template for ligand docking. Docking analyses were done using Vdoc modeling software which uses docking algorithm of mining minima method to find the minimum energy required for the formation of ligand-receptor complex (Kairys and Gilson, 2002; Kairys et al., 2006). For each docking analysis, protein interaction interface between Rho-GAP which included the two GTP-binding sites was determined as the ligand-binding sites. As a result, two docking analyses (for each GTP-binding sites) were generated (Figure 4.7). The first interface was set to include amino acid residues 13 – 16 within RhoA and residues 29 – 32 within the GAP domain of p190RhoGAP and the second interface was set to include amino acid residues

62 – 67 within RhoA and residues 64 – 70 within the GAP domain of p190RhoGAP (Figure 4.7.A, B). For each docking, the potential energy required for ligand binding was calculated and the lowest negative number correlated with the most favorable binding. DMSO was used as a negative control and DMSO docking was found to be the least favorable (Figure 4.7). Two tester compounds (* and **) unrelated to compound 7 were also utilized as controls to test docking specificity. In comparison to these two compounds, compound 7 was found to dock favorably into either binding interfaces with the least energy required. This analysis provided compelling evidence of the two potential binding sites of compound 7 within the GTP-binding domain of Rho-GAP interface.

DSICUSSION

In this study, we have implemented a cell-based assay using yeast two-hybrid system to screen for chemicals that disrupt ROP-GAP protein interactions. Yeast two-hybrid chemical screens have been reported in the past with successful results and proven to be useful to identify inhibitors of protein-protein interaction (Khazak et al., 2006; Igarashi et al., 1998; Young et al., 1998; Huang and Schreiber, 1997). In our attempt to identify such inhibitors, ten initial hit compounds were identified based on the chemical screen yeast two-hybrid assay. From these ten hits, one compound #7 was the only one that induced slight tip swelling phenotype in tobacco pollen tubes. Pollen tube tip polarity loss in the form of tip swelling can be associated with increased ROP1 activity (Li et al., 1999). Thus, increased ROP1 activity following chemical treatment would be consistent

with the inhibition of ROP-GAP interaction which is important to downregulate ROP1 activity (Hwang et al., 2008; Wu et al., 2000). Consistently, treatment of *ROP1 OX* with 25 μM of compound 7 severely induced depolarized growth phenotype; though, the same treatment of *ren1-3* only slightly induced tip width but not more significant than the WT. Thus it seems that compound 7 primarily targets ROP1 in disrupting ROP1-REN1 interaction which was further confirmed using *in vitro* pulldown and GTPase assay. However, compound 7 may not only affect ROP-GAP interactions as it also affected ROP-GEF interaction. As such, the growth inhibition caused by chemical treatment in all genotypes tested may not only caused by the general inhibition of growth but also caused by the inhibition of other ROP-type interactions such as ROP-GEF. Nevertheless, the extent of the effects of compound 7 to disrupt ROP-type interactions still needs further investigations.

Compound 7 contains a thienopyrimidine backbone with amine tail. The activities of thienopyrimidines in disrupting biological functions have been reported; for example, as an inhibitor of VEGF receptor-2 kinase (Munchhof et al., 2003), inhibitor of phosphatidylinositol-3-kinase p110α (Folkes et al., 2008), and antibacterial and antifungal compound (Rahman et al., 2003). The antifungal activity of compound 7 can also be observed in our assay as it inhibits the weaker protein-protein interaction in our test control, control C. Due to this nonspecific effects, several chemical analogs were tested to identify more potent and specific compound(s) but none of the analogs seemed to have activity in our assays. It is possible that compound 7 has the optimal structures

required for its activity in affecting ROP-type interactions. However, more analyses of untested compound analogs would be needed to further confirm our results.

Finally, ligand-receptor docking analysis provided a model for the potential interactions between compound 7 and Rho-GAP interactions. In silico docking analysis can be a useful tool to screen for inhibitors of protein-protein interactions (Toogood, 2002; Berg, 2003; Sugaya et al., 2007) which we utilize in our study to predict for chemical-protein binding sites. By using Vdoc software, we were able to analyzed possible compound 7 binding site within the two known GTP-binding pockets at RhoA and p190GAP binding interface. Compared to DMSO control and other compounds tested, compound 7 docked the likeliest at either GTP-binding sites within the RhoA-p190RhoGAP interaction interfaces. These results provided compelling evidence of the two potential binding sites of compound 7 within the GTP-binding domain of Rho-GAP interface. It remains to be tested experimentally whether these potential compound binding sites are indeed significant. Future mutation studies of these binding interfaces would be required to validate these results.

REFERENCES

Arkin, M. R. and Wells, J. A. (2004) Small-molecule inhibitors of protein-protein interactions: progressing towards the dream. Nat. Rev. Drug Discovery **3**: 301 – 317

Basu, D., Le, J., Zakharova, T., Mallery, E. L., and Szymanski, D. B. (2008) A SPIKE1 signaling complex controls actin-dependent cell morphogenesis through the heteromeric WAVE and ARP2/3 complexes. Proc. Natl. Acad. Sci. **105(10)**: 4044 – 4049

Blackwell, H. E. and Zhao, Y. (2003) Chemical genetic approaches to plant biology. Plant Physiol. **133**: 448 – 455

Chang, C., Schaller, G. E., Patterson, S. E., Kwok, S. F., Meyerowitz, E. M., and Bleecker, A. B. (1992) The TMK1 gene from Arabidopsis codes for a protein with structural and biochemical characteristics of a receptor protein kinase. Plant Cell **4**: 1263 – 1271

Chene, P. (2006) Drugs targeting protein-protein interactions. Chem. Med. Chem. **1(4)**: 400 – 411

Chien, C. T., Bartel, P. L., Sternglanz, R., and Fields, S. (1991) The two-hybrid system: a method to identify and clone genes for proteins that interact with a protein of interest. Proc. Natl. Acad. Sci. **88(21)**: 9578 – 9582

Fields, S and Song, O. (1989) A novel genetic system to detect protein-protein interactions. Nature **340(6230)**: 245 – 246

Folkes, A. J., Ahmadi, K., Alderton, W. K., Alix, S., Baker, S. J., Box, G., Chuckowree, I. S., Clarke, P. A., Depledge, P., Eccles, S. A., Friedman, L. S., Hayes, A., Hancox, T. C., Kugendradas, A., Lensun, L., Moore, P., Olivero, A. G., Pang, J., Patel, S., Pergl-Wilson, G. H., Raynaud, F. I., Robson, A., Saghir, N., Salphati, L., Sohal, S., Ultsch, M. H., Valenti, M., Wallweber, H. J. A., Wan, N. C., Wiesmann, C., Workman, P., Zhyvoloup, A., Zvelebil, M. J., and Shuttleworth, S. J. (2008) The identification of 2-(1H-Indazol-4-yl)-6-(4-methanesulfonyl-piperazin-1-ylmethyl)-4-morpholin-4-yl-thieno[3,2-d]pyrimidine (GDC-0941) as a potent, selective, orally bioavailable inhibitor of class I PI3 kinase for the treatment of cancer. J. Med. Chem. **51:** 5522 – 5532

Fry, D. C. (2006) Protein-protein interactions as targets for small molecule drug discovery. Peptide Sci. **84(6)**: 535 – 552

Fu, Y., Wu, G., and Yang, Z. (2001) Rop GTPase-dependent dynamics of tip-localized F-actin controls tip growth in pollen tubes. J Cell Biol. **152**: 1019-1032

Gu, Y., Fu, Y., Dowd, P., Li, S., Vernoud, V., Gilroy, S., and Yang, Z. (2005) A Rho family GTPase controls actin dynamics and tip growth via two counteracting downstream pathways in pollen tubes. J. Cell Biol. **169**: 127-138

Gu, Y., Vernoud, V., Fu, Y., and Yang, Z. (2003) ROP GTPase regulation of pollen tube growth through the dynamics of tip-localized F-actin. J. Exp. Bot. **54**: 93-101

Holdaway-Clarke, T.L., Feijo, J.A., Hackett, G.R., Kunkel, J.G., and Hepler, P.K. (1997) Pollen tube growth and the intracellular cytosolic calcium gradient oscillate in phase while extracellular calcium influx is delayed. Plant Cell **9**: 1999-2010

Huang, J and Schreiber, S. L. (1997) A yeast genetic system for selecting small molecule inhibitors of protein-protein interactions in nanodroplets. Proc. Natl. Acad. Sci. **94**, 13396 – 13401

Hwang, J.U., Gu, Y., Lee, Y.J., and Yang, Z. (2005) Oscillatory ROP GTPase activation leads the oscillatory polarized growth of pollen tubes. Mol. Biol. Cell **16**: 5385-5399

Igarashi, K., Shigeta, K., Kohno, S., Isohara, T., Yamano, T., and Uno, I. (1998) A novel indication of the activities of small molecule inhibitors of protein-protein interactions: application of the yeast two-hybrid system. J. Antibiotics **51(9)**: 886 – 888

Ivachtchenko, A., Kovalenko, S., Tkachenko, O. V., and Parkhomenko, O. (2004) Synthesis of substituted thienopyrimidine-4-ones. J. Comb. Chem. **6**: 573 – 583

Joce, C., Stahl, J. A., Shridhar, M., Hutchinson, M. R., Watkins, L. R., Fedichev, P. O., and Yin, H. (2010) Application of a novel *in silico* high throughput screen to identify selective inhibitors for protein-protein interactions. Bioorg. Med. Chem. Lett. **20(18)**: 5411 – 5413

Kairys, V., M. X. Fernandes, and M. K. Gilson. (2006) Screening druglike compounds by docking to homology models: a systematic study. J. Chem. Inf. Model. **46**: 365–379

Kairys, V., and M. K. Gilson. (2002) Enhanced docking with the mining minima optimizer: acceleration and side-chain flexibility. J. Comput. Chem. **23**: 1656–1670

Khazak, V., Kato-Stankiewicz, Tamanoi, F., and Golemis, E. A. (2006) Yeast screens for inhibitors of Ras-Raf interaction and characterization of MCP inhibitors of Ras-Raf interaction. Methods Enzymology **407(48)**: 612 – 629

Kost, B., Lemichez, E., Spielhofer, P., Hong, Y., Tolias, K., Carpenter, C., and Chua, N.H. (1999) Rac homologues and compartmentalized phosphatidylinositol 4, 5-bisphosphate act in a common pathway to regulate polar pollen tube growth. J. Cell Biol. **145**: 317-330

Lawrence, H. R., Li, Z., Yip, M. L. R., Sung, S-S., Lawrence, N. J., McLaughlin, M. L., McManus, G. J., Zaworotko, M. J., Sebti, S. M., Chen, J., and Guida, W. C. (2009) Identification of a disruptor of the MDM2-p53 protein-protein interaction facilitated by high-throughput in silico docking. Bioorg. Med. Chem. Lett. **19(14)**: 3756 – 3759

Lee, Y.J., Szumlanski, A., Nielsen, E., and Yang, Z. (2008) Rho-GTPase-dependent filamentous actin dynamics coordinate vesicle targeting and exocytosis during tip growth. J. Cell Biol. **181**: 1155-1168

Li, H., Lin, Y., Heath, R.M., Zhu, M.X., and Yang, Z. (1999) Control of pollen tube tip growth by a Rop GTPase-dependent pathway that leads to tip-localized calcium influx. Plant Cell **11**: 1731-1742

Munchhof, M. J., Beebe, J. S., Casavant, J. M., Cooper, B. A., Doty, J. L., Higdon, R. C., Hillerman, S. M., Soderstrom, C. I., Knauth, E. A., Marx, M. A., Rossi, A. M. K., Sobolov, S. B., and Sun, J. (2003) Design and SAR of thienopyrimidine and thienopyridine inhibitors of VEGFR-2 kinase activity. Bioorg. Med. Chem. Lett. **14**: 21 – 24

Nixon, A. E., Brune, M., Lowe, P. N., and Webb, M. R. (1995) Kinetics of inorganic phosphate release during the interaction of p21ras with the GTPase-activating proteins, p120-GAP and neurofibromin. Biochemistry **34**: 15592 – 15598

Pierson, E.S., Miller, D.D., Callaham, D.A., van Aken, J., Hackett, G., and Hepler, P.K. (1996) Tip-localized calcium entry fluctuates during pollen tube growth. Dev. Biol. **174**: 160-173

Qiu, J-L., Jilk, R., Marks, M. D., and Szymanski, D. B. (2002) The Arabidopsis *SPIKE1* gene is required for normall cell shape control and tissue development. Plant Cell **14**: 101 – 118

Rahman, K. M., Chowdhury, A. Z. M. S., Bhuiyan, M. M. H., Hossain, M. K., and Uddin, M. K. (2003) Synthesis and anti-microbial activity of some heterocycles: part-II. Pak. J. Sci. Ind. Res. **46(2)**: 95 – 98

Rittinger, K., Walker, P. A., Eccleston, J. F., Smerdon, S. J., and Gamblin, S. J. (1997) Structure of 1.65 A of RhoA and its GTPase-activating protein in complex with a transition-state analogue. Nature **389**: 758 – 762

Schaler, G. E. and Bleecker, A. B. (1993) Receptor-like kinase activity in membranes of *Arabidopsis thaliana*. FEBS **333(3)**: 306 – 310

Sugaya, N., Ikeda, K., Tashiro, T., Takeda, S., Otomo, J., Ishida, Y., Shiratori, A., Toyoda, A., Noguchi, H., Takeda, T., Kuhara, S., Sakaki, Y., and Iwayanagi, T. (2007) An integrative in silico approach for discovering candidates for drug-targetable protein-protein interactions in interactome data. BMC Pharm. **7**: 10 – 25

Toogood, P. L. (2002) Inhibition of protein-protein association by small molecules: approaches and progress. J. Med. Chem. **45(8)**: 1543 – 1558

Uhrig, J. F., Mutondo, M., Zimmermann, I., Deeks, M. J., Machesky, L. M., Thomas, P., Uhrig, S., Rambke, C., Hussey, P. J., and Hulskamp, M. (2007) The role of Arabidopsis SCAR genes in ARP2-ARP3-dependent cell morphogenesis. Development **134**: 967 – 977

Walsh, D.P., and Chang, Y.T. (2006) Chemical genetics. Chem. Rev. **106**: 2476-2530

Webb, M. R. and Hunter, J. L. (1992) Interaction of GTPase-activating protein with p21ras, measured using a continuous assay for inorganic phosphate release. Biochem. J. **287**: 555 – 559

Wu, G., Li, H., and Yang, Z. (2000) Arabidopsis RopGAPs are a novel family of rho GTPase-activating proteins that require the Cdc42/Rac-interactive binding motif for rop-specific GTPase stimulation. Plant Physiol. **124**: 1625-1636

Yan, A., Xu, G., and Yang, Z.B. (2009) Calcium participates in feedback regulation of the oscillating ROP1 Rho GTPase in pollen tubes. Proc. Natl. Acad. Sci. **106**: 22002-22007

Young, K., Lin, S., Sun, L., Lee, E., Modi, M., Hellings, S., Husbands, M., Ozenberger, B., and Franco, R. (1998) Identification of a calcium channel modulator using a high throughput yeast two-hybrid screen. Nat. Biotech. **16**: 946 – 950

Zhang, B., Corbel, C., Gueritte, F., Couturier, C., Bach, S., and Tan, V. B. C. (2011) An *in silico* approach for the discovery of CDK5/p25 interaction inhibitors. Biotechnol. J. **6**, 871 – 881

Zheng, X. F. and Chan, T-F. (2002) Chemical genomics: a systematic approach in biological research and drug discovery. Curr. Issues Mol. Biol. **4**: 33 – 43

Figure 4.1. Schematic representation of yeast two-hybrid chemical screen and hits identified from the screen. A) General work flow of the screen from initial yeast two-hybrid screen, secondary screens, and follow-up tobacco pollen assay. At the end, one putative inhibitor of ROP-GAP interaction was identified. B) Chemical structures of ten hits purchased and tested in pollen tube germination assays. C) Slight pollen tube swelling was observed with treatment of 25 μM of compound #7.

Figure 4.1.

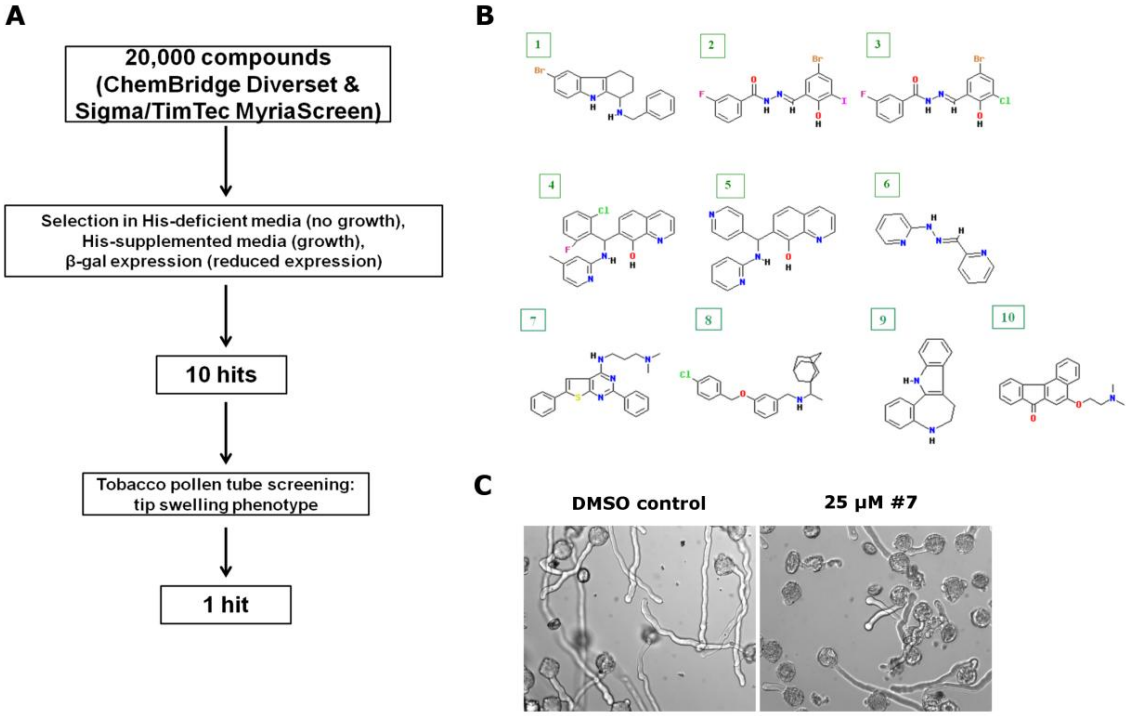
A
20,000 compounds
(ChemBridge Diverset &
Sigma/TimTec MyriaScreen)
Selection in His-deficient media (no growth),
His-supplemented media (growth),
β-gal expression (reduced expression)
10 hits
Tobacco pollen tube screening:
tip swelling phenotype
1 hit
B
1
2
3
4
5
6
7
8
9
10
C
DMSO control
25 μM #7

Figure 4.2. *In vitro* protein interaction analysis of ROP1 and REN1 interaction in the presence of compound 7. A) GTPase assay to measure the amount of inorganic phosphate released from GTPase reaction which positively correlates with the Δ absorbance measured at 360 nm. Increasing chemical concentration resulted in reduced Δ absorbance suggesting reduced inorganic phosphate present in the assay. B) In vitro pulldown assay where bead-bound GST-ROP1 used to pulldown HIS-REN1 in the presence of DMSO control or compound 7. Increasing chemical concentration led to reduced REN1 being pulldown by bead-bound ROP1.

Figure 4.2.

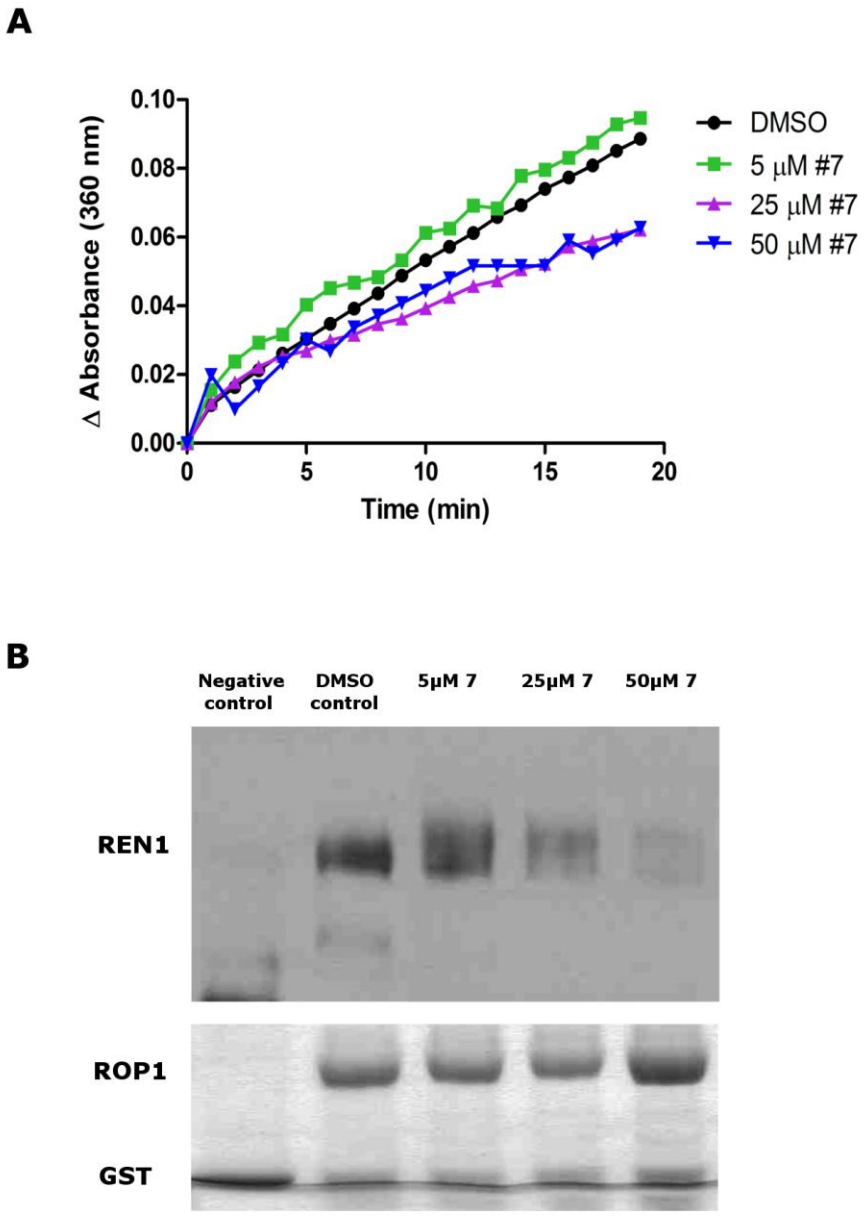
A
0.10
0.08
0.06
0.04
0.02
0.00
Δ Absorbance (360 nm)
0
5
10
15
20
Time (min)
DMSO
5 μM #7
25 μM #7
50 μM #7
B
Negative control
DMSO control
5μM 7
25μM 7
50μM 7
REN1
ROP1
GST

Figure 4.3. *In vitro* pollen tube germination assay of *Col-0* WT, *rop1RNAi*, and *GFP-ROP1 OX* treated with varying concentration of compound 7. Pollen tubes were germinated and grown in the presence of chemical for 4 h, after which images were captured. A) Pollen tube images of the different genotypes in different chemical concentration. B) Quantification of pollen tube tip width. C) Quantification of pollen tube length.

Figure 4.3.

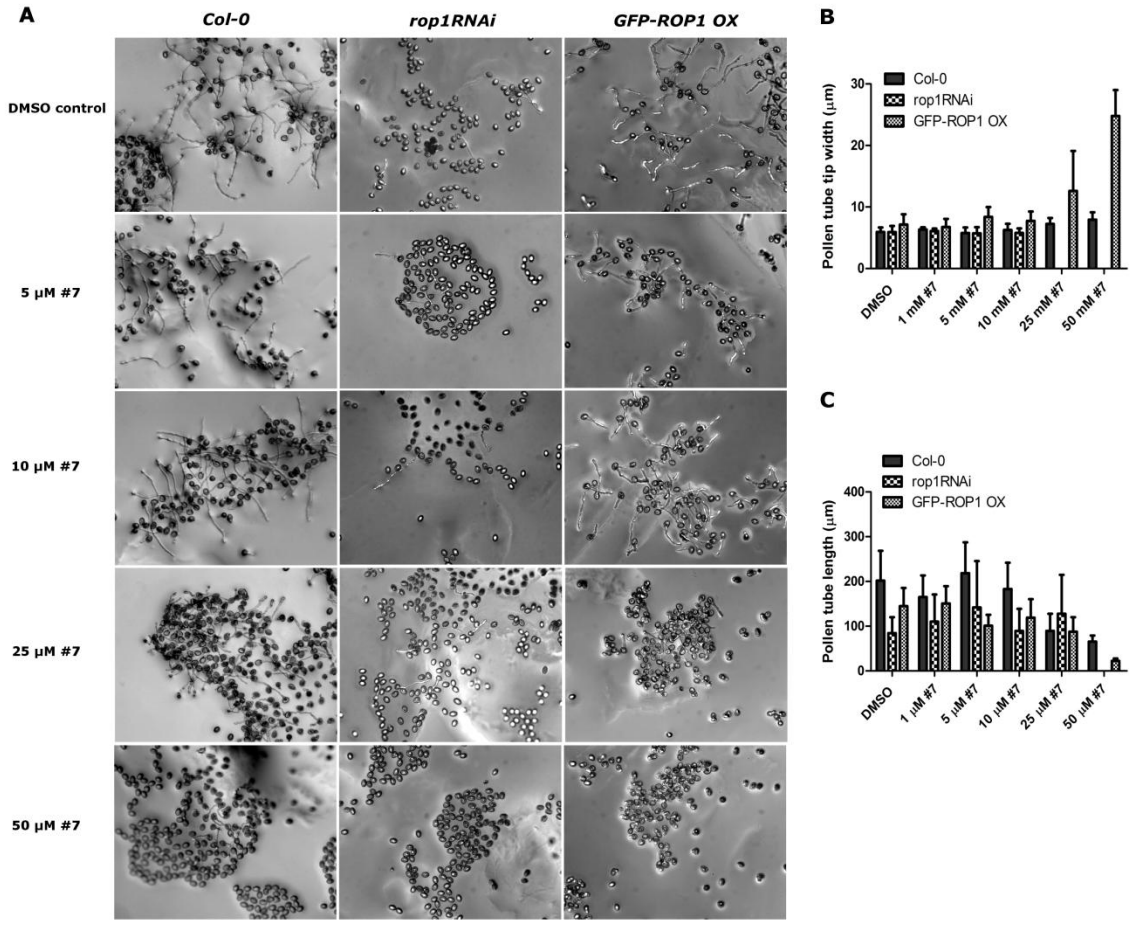
A
Col-0
rop1RNAi
GFP-ROP1 OX
DMSO control
5 µM #7
10 µM #7
25 µM #7
50 µM #7
B
Col-0
rop1RNAi
GFP-ROP1 OX
Pollen tube tip width (µm)
0
10
20
30
DMSO
1 mM #7
5 mM #7
10 mM #7
25 mM #7
50 mM #7
C
Col-0
rop1RNAi
GFP-ROP1 OX
Pollen tube length (µm)
0
100
200
300
400
DMSO
1 µM #7
5 µM #7
10 µM #7
25 µM #7
50 µM #7

Figure 4.4. *In vitro* pollen tube germination assay of *Col-0* WT and *ren1-3* treated with varying concentration of compound 7. Pollen tubes were germinated and grown in the presence of chemical for 4 h, after which images were captured. A) Pollen tube images of the different genotypes in different chemical concentration. B) Quantification of pollen tube tip width.

Figure 4.4.

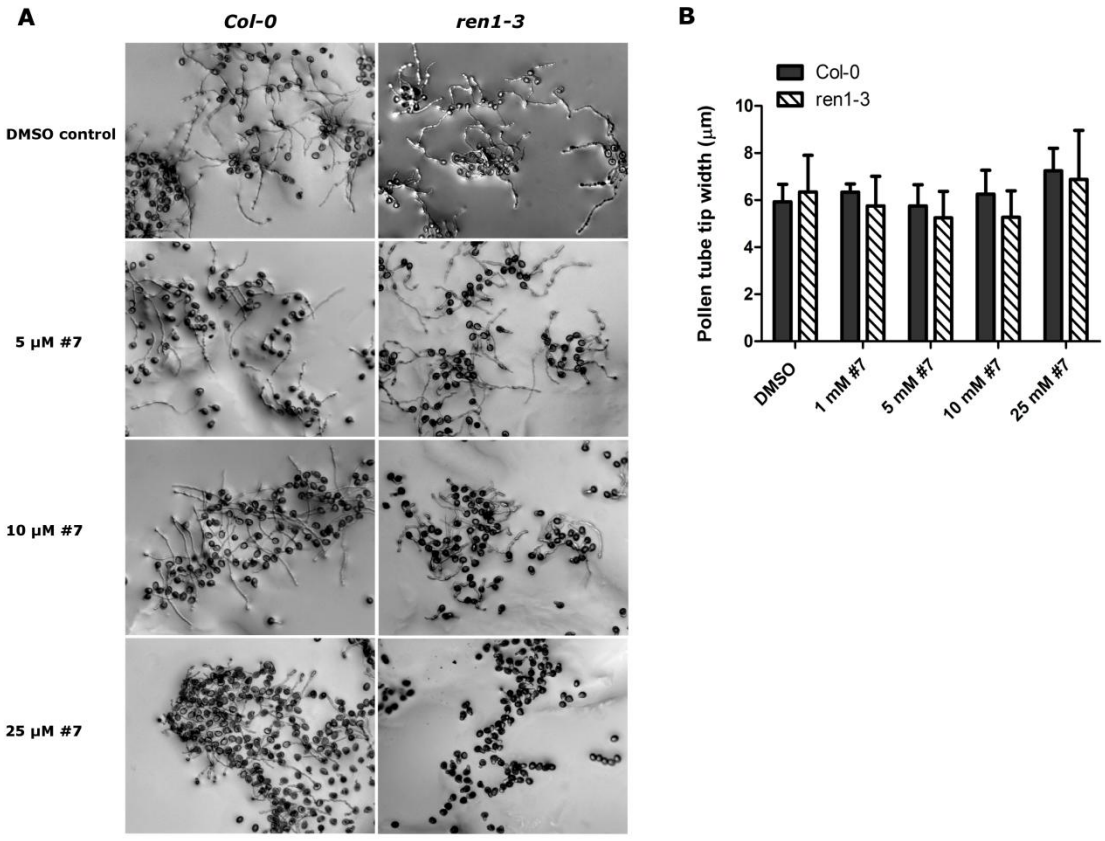
A
Col-0
ren1-3
DMSO control
5 µM #7
10 µM #7
25 µM #7
B
Col-0
ren1-3
Pollen tube tip width (µm)
0
2
4
6
8
10
DMSO
1 mM #7
5 mM #7
10 mM #7
25 mM #7

Figure 4.5. Yeast two-hybrid assay of various protein-protein interactions in the presence of compound 7. Yeast growth was assayed in histidine-complete media and histidine-lacking media and measured in the form of optical density ratio at 600 nm after 24 h incubation period. Control C is a weak protein interaction control. TMK1-SPIKE1(SPK1) is another protein interaction control unrelated to ROP-GAP interaction.

Figure 4.5.

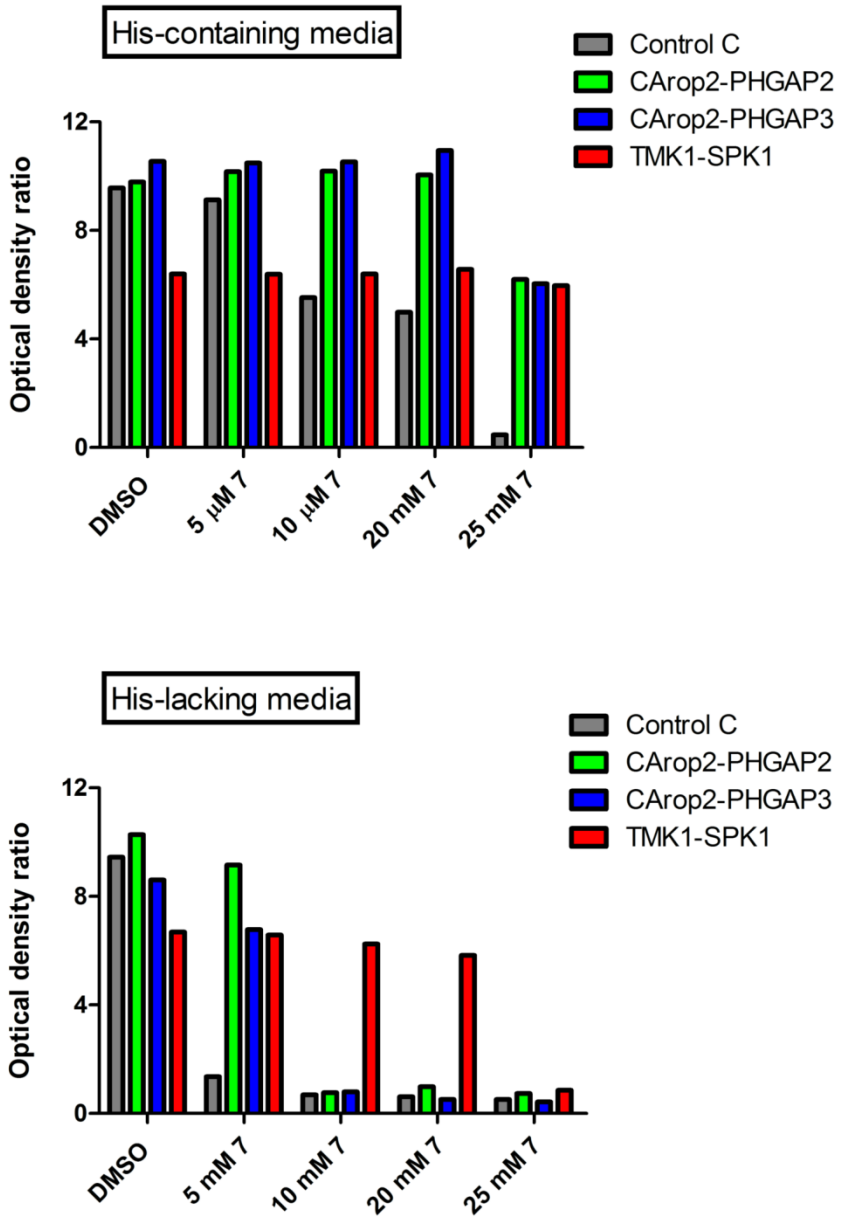
His-containing media
Control C
CArop2-PHGAP2
CArop2-PHGAP3
TMK1-SPK1
Optical density ratio
12
8
4
0
DMSO
5 μM 7
10 μM 7
20 mM 7
25 mM 7
His-lacking media
Control C
CArop2-PHGAP2
CArop2-PHGAP3
TMK1-SPK1
Optical density ratio
12
8
4
0
DMSO
5 mM 7
10 mM 7
20 mM 7
25 mM 7

Figure 4.6. Analogs analysis of compound #7. A) Five analogs purchased for analyses. Compound 7 is circled in black. Green circle indicates side residues which differ from that of compound 7. Compound similarity was indicated in parenthesis.

Figure 4.6.

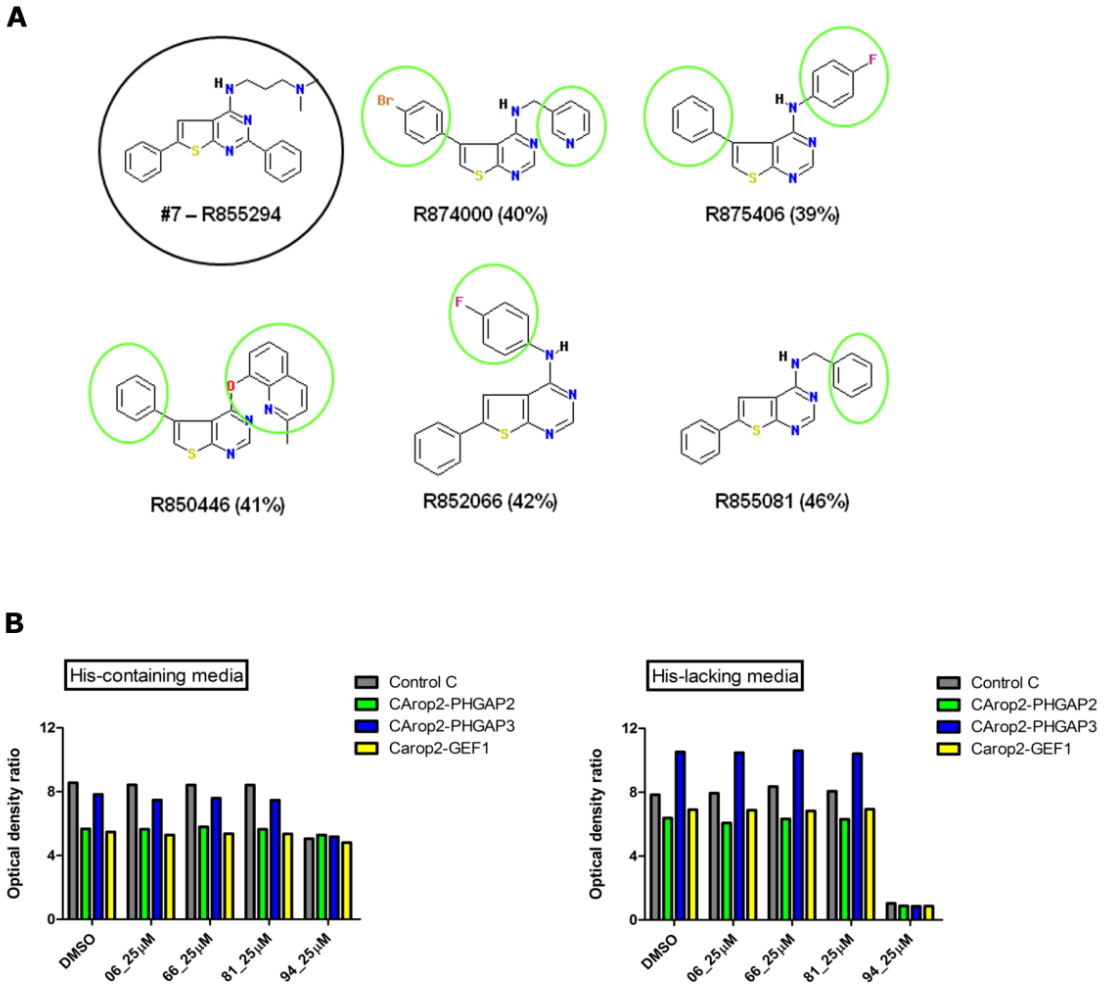
A
#7 – R855294
R874000 (40%)
R875406 (39%)
R850446 (41%)
R852066 (42%)
R855081 (46%)
B
His-containing media
His-lacking media
Control C
CArop2-PHGAP2
CArop2-PHGAP3
Carop2-GEF1
Optical density ratio
12
8
4
0
DMSO
06_25μM
66_25μM
81_25μM
94_25μM

Figure 4.7. Ligand-protein docking using RhoA-p190RhoGAP crystal structures. Compounds were docked within the GTP-binding pockets where the two proteins interact. The larger images display the compound docked to the binding interface. The smaller images display the GTP-binding pockets defined as the binding interface. Red/green ribbons represent full length RhoA while blue ribbons represent the GAP domain of p190RhoGAP. Red and yellow highlights on the ribbons represent the GTP-binding sites. A) Ligand-protein docking where the GTP-binding interface was set between amino acid residues 13 – 16 within RhoA and residues 29 – 32 within the GAP domain of p190RhoGAP. B) Ligand-protein docking where the GTP-binding interface was set between amino acid residues 62 – 67 within RhoA and residues 64 – 70 within the GAP domain of p190RhoGAP. DMSO was used as negative control, compound 7 was the test compound, compound 8 was identified from the screen but did not induce tip swelling phenotype was also tested, and two tester compounds, * and **, which were randomly picked and were unrelated to compound 7 or 8 were utilized as negative controls as well. Potential energies for all compounds were calculated and listed in the tables.

Figure 4.7.

A

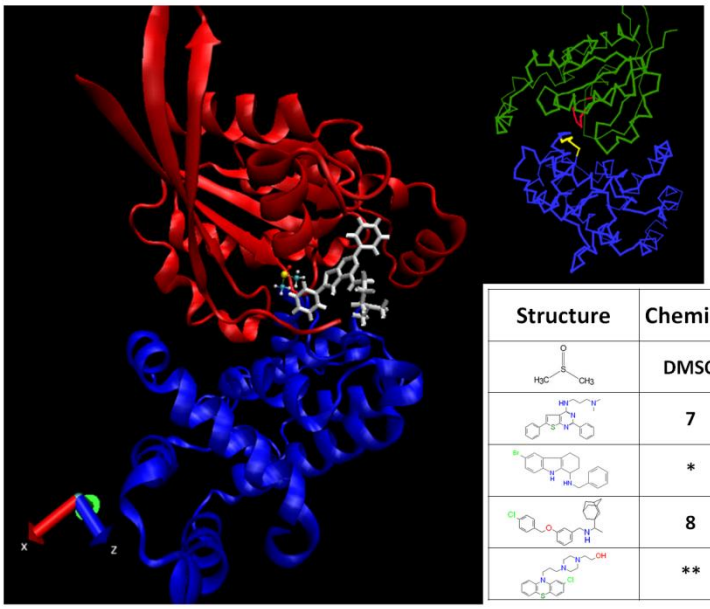

Structure	Chemical	Potential Energy
	DMSO	-15.1105
	7	-32.1582
	*	-26.4754
	8	-30.9710
	**	-30.4097

B

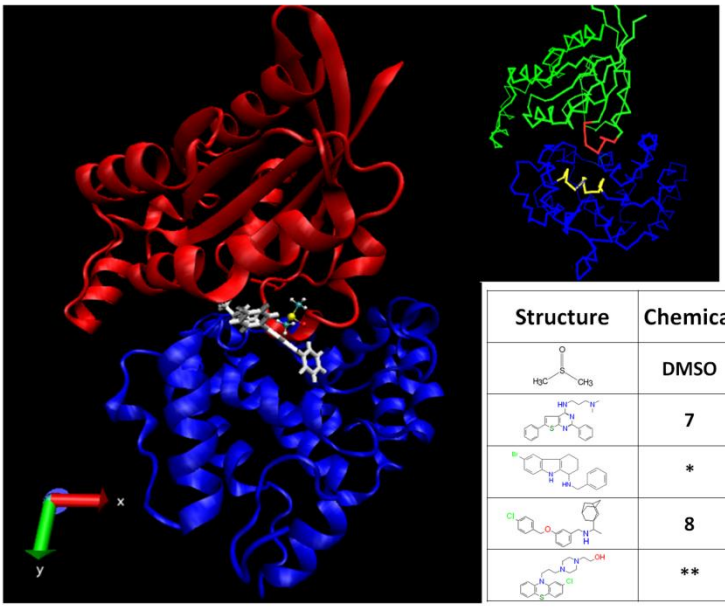

Structure	Chemical	Potential Energy
	DMSO	-11.3618
	7	-25.9469
	*	-22.2118
	8	-23.7095
	**	-24.3387

CONCLUSION

The regulation of pollen tube polarity involves complex and dynamic signaling networks including ROP1 pathway. ROP1 regulation of pollen tube growth and polarity involved downstream effectors which regulate tip F-actin dynamics, tip-localized cytosolic calcium, and exocytosis of secretory vesicles (Li et al., 1999; Lin and Yang, 1997; Yang and Watson, 1993; Fu et al., 2001; Gu et al., 2005; Gu et al., 2003; Li et al., 1999; Yan et al., 2009; Lee et al., 2008; Hwang et al., 2005). With the increasing understanding of the positive and negative feedback loops involved in ROP1 regulations, new questions arise regarding the links between the downstream components and ROP1 activity.

One important question which remains is the possible feedback relationships between ROP1 and tip-focused calcium. The promotion of tip-localized calcium gradient is positively regulated by a ROP1 effector protein, RIC3 (Li et al., 1999; Yan et al., 2009). In turn, the accumulation of tip high calcium antagonizes the tip F-actin assembly regulated by RIC4 which is involved in the positive feedback loop of ROP1 (Gu et al., 2005; Yan et al., 2009). Tip F-actin is also involved in exocytosis process by promoting the accumulation of exocytic vesicles to the tip region (Lee et al., 2008) and indirectly in the positive feedback loop since exocytic vesicles are likely to transport activated ROP1 from the cytosol to the apical PM and result in more downstream effectors recruited to the PM (Hwang et al., 2005; Yan et al., 2009). As a result, tip high calcium can also regulate the exocytic vesicles transport to the PM as evident in the observation that RIC3

OX resulted in the loss of apical YFP-RabA4d localization which labeled the inverted cone-shaped localization of exocytic vesicles within the apical clear zone (Lee et al., 2008). Thus high accumulation of tip-localized calcium gradient negatively regulates ROP1 activity through the regulation of F-actin dynamics and ROP1 exocytosis to the apical PM.

Recent evidence points to the possibility of calcium-mediated direct regulation of ROP1 pathway via ROP1 negative regulator, REN1GAP. The pollen tubes of weak *ren1* alelle, *ren1-3*, were mostly long and wavy with slight tip swelling when grown in optimal calcium media (2-5 mM Ca^{2+}) but became depolarized under low calcium media (0.5 mM Ca^{2+}) (Hwang et al., 2008) which suggested that REN1 activity can be affected by the tip calcium level generated by extracellular calcium influx. As such, the loss or significant reduction in REN1 activity in low calcium media, which would otherwise not the case in optimal calcium condition, was likely the cause of the loss of tip polarity due to enhanced ROP1 activity. Since REN1 does not interact with calcium, it is very likely that a calcium sensor such as CPK may have a role in calcium detection and calcium response.

CPKs involvements in a multitude of biological and cellular responses in protozoa and plants have been presented (Harper et al., 2004; Harper and Harmon, 2005; Klimecka and Muszynska, 2007; Kudla et al., 2010). The large family members of CPKs identified in multiple plant species such as Arabidopsis (Cheng et al., 2002), rice (Ye et al., 2009, Ray et al., 2007, Asano et al., 2005), and wheat (Li et al., 2008) suggested functional redundancy. CPK16 is one of the few CPKs expressed in mature pollen whose expression correlates highly with REN1 and is linked directly to REN1 in the coexpressed gene

network generated by ATTEDII gene expression database (http://atted.jp) (Obayashi et al., 2007; Obayashi et al., 2009; Obayashi et al., 2011). Thus CPK16 seem to be an exciting candidate for its potential involvement in REN1 regulation. We hypothesized that CPK16 detects tip-localized calcium gradient and decodes calcium signal by phosphorylating REN1 to regulate REN1 activity.

Our first line of evidence to support this hypothesis is the observation that CPK16 can phosphorylate REN1 in a calcium-dependent manner in *in vitro* phosphorylation assay. Interestingly, another pollen-expressed, CPK32 was also able to phosphorylate REN1; however its calcium dependency was not as clear as that of CPK16. The requirement of high calcium level for REN1 phosphorylation by CPK16 with relative EC_{50} value of 4.6 µM also seems to be physiologically relevant and consistent with our hypothesis if CPK16 indeed regulates REN1 activity at the apical PM of pollen tube tip, since high tip-calcium is known to negatively regulate ROP1 pathway.

In vitro phosphorylation studies have some limitations in uncovering important residues that are truly phosphorylated *in vivo*. Some of these limitations can be contributed to the facts that *in vitro* assays tend to use higher protein concentration which does not necessarily reflect that *in vivo*, lack the regulatory proteins which may otherwise be needed to suppress or enhance CPK activity, and ignore the cellular protein dynamics such as the spatial and temporal factors, protein half-life, and other factors. Nevertheless, *in vitro* studies can provide valuable information required for future functional studies. Analyses of REN1 phosphorylation sites by 2D-LC/MS/MS revealed that many sites can be phosphorylated *in vitro* especially at its C-terminal regions. Phosphorylation motifs

comparisons to the known CPK phosphorylation motifs indicated the presence of simple phosphorylation motif, Basic$_{-3}$-X$_{-2}$-X$_{-1}$-**S/T,** although some others displayed **S/T**-X$_{+1}$-Basic$_{+2}$-(or Basic$_{+3}$).

Due to the many potential REN1 phosphorylation sites, our main focus for functional studies was drawn toward the phosphorylation residues within two domains: the catalytic GAP domain at Ser$_{267}$ and the PM-localized phospholipid-binding, PH domain, at Ser$_{70}$ and Thr$_{151}$. GAP domain of RhoGAP proteins is known to be crucial for RhoGAPs activity (Ohta et al., 2006; Klahre and Kost, 2006; Lancaster et al., 1994) while PH domain is known to interact with phospholipids, such as PIP_2 or PIP_3, at the PM which allows for PH domain-containing proteins to be targeted to the membrane (Lemmon et al., 1995; Ma et al., 1997; Harlan et al., 1994; Salim et al., 1996; Yu et al., 2004); although, not all PH domain-containing proteins are membrane-targeted as well as interact strongly with phospholipids (Yu et al., 2004). As such, functional studies were done by generating two phosphorylation mutations in which Ser-to-Ala mutation mimics the nonphosphorylated state while Ser-to-Glu mimics the phosphomimic state (Witte et al., 2010; Choi et al., 2005). These analyses led us to the conclusion that phosphorylation at Ser$_{267}$ is important for REN1 activity since nonphosporylated mutant displayed reduced activity toward ROP1 and enhanced ROP1 activity. In contrast, phosphorylation at Ser$_{70,71}$ affected REN1 localization and subsequently reduced its activity and enhanced ROP1 activity.

The involvements of CPK16 in phosphorylating two distinct domains with contrasting effects in REN1 activity remain a question. In addressing the potential

mechanisms involved in these conflicting data, we proposed a model. In this model, we presented that *in vitro*, REN1 can be phosphorylated at many sites including the Ser_{267} and Ser_{70}. However, *in vivo*, it is likely that the membrane-bound Ser_{267} is phosphorylated but not Ser_{70} since PH domain interaction with the negatively-charged phospholipids may prevent phosphorylation. Future studies need to be conducted to investigate this possibility. In addition, it remains to be addressed how phosphorylation within the coiled coil regions affects REN1 activity. The functions of REN1 coiled coil regions has been assigned to promoting REN1 localization to the exocytic vesicles which was concluded from the observation that REN1 accumulated to the cytosol when the coiled coil regions were deleted (Hwang et al., 2008). Thus it will be interesting to see if REN1 phosphorylation at these regions may affect its localization to the exocytic vesicles as well.

Consistent with REN phosphorylation data and CPK16 potential involvement in regulating REN1, further analysis of *CPK16* loss-of-function mutant, *cpk16-3*, revealed that it is likely involved in calcium sensing and calcium response to regulate proper pollen tube germination and growth. Interestingly, when *cpk16-3* mutants were treated with BFA, which inhibits exocytosis, or LatB, which inhibits actin polymerization and tip-directed targeting of secretory vesicles, pollen tubes became depolarized as marked by tip swelling, increased pollen tube width, and shorter tubes which mimic similar phenotypes observed for the same treatments in partially complemented *ren1-1 Lat52::GFP-REN1* (Hwang et al., 2008). This further links CPK16 to ROP1 pathway which is known to regulate pollen tube growth and tip polarity. Furthermore, since

cpk16-3 mutant phenotype did not result in polarity defect and such depolarized growth can only be enhanced with BFA or LatB treatment, other CPKs may potentially play a role in compensating for the loss of CPK16. Although CPK18 is the closest homolog to CPK16, it does not seem to play a major role in regulating pollen tube growth even in the absence of CPK16. However, double mutant *cpk16-3cpk18-3* displayed slightly enhanced phenotypes with BFA or LatB treatment suggesting only partial redundancy. It remains to be investigated whether another CPK16 and CPK18 homolog, vegetative tissue-expressed CPK28 may be genetically redundant to CPK16. In addition, it is also possible that other CPKs may be involved in the feedback regulation of ROP1 pathway. Here, we presented the initial study of characterizing a potential regulator linking calcium signaling and ROP1 pathway. Our findings will provide future insights into the identifications of more CPKs which are likely involved in regulating pollen tube polarity via negative feedback regulation of ROP1 pathway.

Finally, in an attempt to dissect the spatial and temporal phase relationships between pollen tube growth oscillations, active ROP1, F-actin dynamics, and tip-focused calcium in a highly dynamic oscillatory system, we have screened for small molecules with the potential to disrupt ROP-GAP interactions. Our cell-based chemical screens using yeast two-hybrid assays combined with tobacco pollen tube phenotype screening and in vitro protein-protein interaction assays have led to the identification of compound #7. This compound induced slight tip swelling phenotype in WT pollen tubes and severely induced depolarized growth phenotype in *ROP1 OX* pollen tubes which suggested a functional interaction with ROP1 or other ROPs in affecting ROP-type

interactions. However, compound #7 also induced nonspecific effects such as pollen tube growth inhibition as well as yeast growth inhibition in the weaker interaction controls. Though several chemical analogs were tested in an attempt to identify more potent and specific compound(s), none of the limited analogs seemed to have activity in our assays. As such, further identification of more potent and specific compounds remains to be determined. Moreover, ligand-receptor docking analysis provided a model for the potential interactions between compound 7 and ROP interactions.

REFERENCES

Asano, T., Tanaka, N., Yang, G., Hayashi. N., and Komatsu, S. (2005) Genome-wide identification of the rice calcium-dependent protein kinase and its closely related kinase gene families: comprehensive analysis of the CDPKs gene family in rice. Plant Cell Physiol. **46(2)**: 356 – 366

Berg, T. (2003) Modulation of protein-protein interactions with small organic molecules. Angew. Chem. Int. Ed. **42**: 2462 – 2481

Cheng, S-H., Willmann, M. R., Chen, H-C., and Sheen, J. (2002) Calcium signaling through protein kinases. The *Arabidopsis* calcium-dependent protein kinase gene family. Plant Physiol. **129**: 469 – 485

Choi, H-I, Park, H-J., Park, J. H., Kim, S., Im, M-Y., Seo, H-H., Kim, Y-W., Hwang, I., and Kim, S. Y. (2005) Arabidopsis calcium-dependent protein kinase AtCPK32 interacts with ABF4, a transcriptional regulator of abscisic acid-responsive gene expression, and modulates its activity. Plant Physiol. **139**: 1750 – 1761

Fu, Y., Wu, G., and Yang, Z. (2001) Rop GTPase-dependent dynamics of tip-localized F-actin controls tip growth in pollen tubes. J Cell Biol. **152**: 1019-1032

Gu, Y., Vernoud, V., Fu, Y., and Yang, Z. (2003) ROP GTPase regulation of pollen tube growth through the dynamics of tip-localized F-actin. J. Exp. Bot. **54**: 93-101

Harlan, J. E., Hadjuk, P. J., Yoon, H. S., and Fesik, S. W. (1994) Pleckstrin homology domains bind to phosphatidylinositol-4,5-bisphosphate. Nature **371:** 168 – 170

Harper, J.F., Breton, G., and Harmon, A. (2004) Decoding Ca^{2+} signals through plant protein kinases. Annu. Rev. Plant Biol. **55**: 263-288

Harper, J. F. and Harmon, A. (2005) Plants, symbiosis and parasites: a calcium signaling connection. Nat. Rev. Mol. Cell Biol. **6**: 555 – 566

Hwang, J.U., Gu, Y., Lee, Y.J., and Yang, Z. (2005) Oscillatory ROP GTPase activation leads the oscillatory polarized growth of pollen tubes. Mol. Biol. Cell **16**: 5385-5399

Hwang, J.U., Vernoud, V., Szumlanski, A., Nielsen, E., and Yang, Z. (2008) A tip-localized RhoGAP controls cell polarity by globally inhibiting Rho GTPase at the cell apex. Curr. Biol. **18**: 1907-1916

Klahre, U., and Kost, B. (2006) Tobacco RhoGTPase ACTIVATING PROTEIN1 spatially restricts signaling of RAC/Rop to the apex of pollen tubes. Plant Cell **18**, 3033-3046

Klimecka, M. and Muszynska, G. (2007) Structure and functions of plant calcium-dependent protein kinases. Acta Biochim. Polonica **54(2)**: 219 – 233

Kudla, J., Batistic, O., and Hashimoto, K. (2010) Calcium signals: the lead currency of plant information processing. Plant Cell **22**: 541 – 563

Lancaster, C. A., Taylor-Harris, P.M., Self, A. J., Brill, S., van Erp, H. E., and Hall, A. (1994) Characterization of rhoGAP. J. Biol. Chem. **269(2)**: 1137 – 1142

Lee, Y.J., Szumlanski, A., Nielsen, E., and Yang, Z. (2008) Rho-GTPase-dependent filamentous actin dynamics coordinate vesicle targeting and exocytosis during tip growth. J. Cell Biol. **181**: 1155-1168

Lemmon, M. A., Ferguson, K. M., O'Brien, R., Sigler, P. B., and Schlessinger, J. (1995) Specific and high-affinity binding of inositol phosphates to an isolated pleckstrin homology domain. Proc. Natl. Acad. Sci. **92**: 10472 – 10476

Li, H., Lin, Y., Heath, R.M., Zhu, M.X., and Yang, Z. (1999) Control of pollen tube tip growth by a Rop GTPase-dependent pathway that leads to tip-localized calcium influx. Plant Cell **11**: 1731-1742

Li, A-L., Zhu, Y-F., Tan, X-M., Wang, X., Wei, B., Guo, H-Z., Zhang, Z-L., Chen, X-B., Zhao, G-Y., Kong, X-Y., Jia, J-Z., and Mao, L. (2008) Evolutionary and functional study of the CDPK gene family in wheat (*Triticum aestivum L.*). Plant Mol Biol **66**: 429 – 443

Lin, Y., and Yang, Z. (1997) Inhibition of pollen tube elongation by microinjected anti-Rop1Ps antibodies suggests a crucial role for Rho-type GTPases in the control of tip growth. Plant Cell **9**: 1647-1659

Ma, A. D., Brass, L. F., and Abrams, C. S. (1997) Pleckstrin associates with plasma membranes and induces the formation of membrane projections: requirements for phosphorylation and the NH_2-terminal PH domain. J. Cell Biol. **136(5)**: 1071 – 1079

Obayashi T, Hayashi S, Saeki M, Ohta H, Kinoshita K. (2009) ATTED-II provides coexpressed gene networks for Arabidopsis. Nucleic Acids Res. **37**: D987-D991

Obayashi T, Kinoshita K, Nakai K, Shibaoka M, Hayashi S, Saeki M, Shibata D, Saito K, Ohta H. (2007) ATTED-II: a database of co-expressed genes and cis elements for identifying co-regulated gene groups in Arabidopsis. Nucleic Acids Res. **35**: D863-D869

Obayashi T, Nishida K, Kasahara K, Kinoshita K. (2011) ATTED-II updates: condition-specific gene coexpression to extend coexpression analyses and applications to a broad range of flowering plants. Plant Cell Physiol. **52**: 213-219

Ohta, Y., Hartwig, J. H., and Stossel, T. P. (2006) FilGAP, a Rho- and ROCK-regulated GAP for Rac binds filamin A to control actin remodeling. Nat. Cell Biol. **8(8)**: 803 – 814

Salim, K., Bottomley, M. J., Querfurth, E., Zvelebil, M. J., Gout, I., Scaife, R., Margolis, R. L., Gigg, R., Smith, C. I. E., Driscoll, P. C., Waterfield, M. D., and Panayotou, G. (1996) Distinct specificity in the recognition of phosphoinositides by the pleckstrin homology domains of dynamin and Bruton's tyrosine kinase. EMBO J. **15(22)**: 6241 – 6250

Witte, C-P., Keinath, N., Dubiella, U., Demouliere, R., Seal, A., and Romeis, T. (2010) Tobacco calcium-dependent protein kinases are differentially phosphorylated *in vivo* as part of a kinase cascade that regulates stress response. J. Biol. Chem**. 285(13)**: 9740 – 9748

Wu, G., Li, H., and Yang, Z. (2000) Arabidopsis RopGAPs are a novel family of rho GTPase-activating proteins that require the Cdc42/Rac-interactive binding motif for rop-specific GTPase stimulation. Plant Physiol. **124**: 1625-1636

Yan, A., Xu, G., and Yang, Z.B. (2009) Calcium participates in feedback regulation of the oscillating ROP1 Rho GTPase in pollen tubes. Proc. Natl. Acad. Sci. **106**: 22002-22007

Yang, Z., and Watson, J.C. (1993) Molecular cloning and characterization of rho, a ras-related small GTP-binding protein from the garden pea. Proc. Natl. Acad. Sci. **90**: 8732-8736

Ye, S., Wang, L., Xie, W., Wan, B., Li, X., and Lin, Y. (2009) Expression profile of calcium-dependent protein kinase (CDPKs) genes during the whole lifespan and under phytohormone treatment conditions in rice (*Oryza sativa L. ssp. Indica*). Plant Mol. Biol. **70(3)**: 311 – 325

Yu, J. W., Mendrola, J. M., Audhya, A., Singh, S., Keleti, D., DeWald, D. B., Murray, D., Emr, S. D., and Lemmon, M. A. (2004) Genome-wide analysis of membrane targeting by *S. cerevisiae* pleckstrin homology domains. Mol. Cell **13:** 677 – 688